P O L I T E C H N I K A   P O Z N A Ń S K A

R O Z P R A W Y

Nr 352

MIECZYSŁAW SYLWESTER KUCZMA

# APPLICATION OF VARIATIONAL INEQUALITIES IN THE MECHANICS OF PLASTIC FLOW AND MARTENSITIC PHASE TRANSFORMATIONS

POZNAŃ 1999

Przewodniczący Komitetu Redakcyjnego
prof. dr hab. Jerzy Dembczyński

Recenzent
prof. dr hab. Bogdan Raniecki

Skład i łamanie tekstu
Mieczysław S. Kuczma

Wydano za zgodą
Rektora Politechniki Poznańskiej

*2132 publikacja WPP*



Reprodukowano z gotowych materiałów
dostarczonych przez Autora

Wydawnictwo Politechniki Poznańskiej
60-965 Poznań, pl. M. Skłodowskiej-Curie 2, tel. (061) 665 3516

Wydanie I

Druk wykonano w Zakładzie Graficznym Politechniki Poznańskiej

# Acknowledgements

The present work contains the fruits of my research within the last several years, which could not have been realized without the support of many people and institutions.

Especially I would like to thank Professor Erwin Stein who initiated my interest in plasticity and phase transformations. Part of my research was carried out at the Institut für Baumechanik und Numerische Mechanik (IBNM), University of Hannover, where my stays were supported by the DAAD and the European Communities. I am deeply grateful for his kind interest, valuable discussions and hospitality. I would also like to express my special gratitude to Professor John Whiteman for the cooperation and hospitality during my stay as a British Council fellow at the Brunel Institute of Computational Mathematics (BICOM), Brunel University. My warmest thanks I want to direct to Professor Valery Levitas for his useful suggestions, encouragement and friendship. Also I would like to express my appreciation to Professor Alexander Mielke for the cooperation and hospitality at the Institut für Angewandte Mathematik (IfAM), University of Hannover, where my stay was supported by the Volkswagen Stiftung. I wish to thank all my colleagues from IBNM, BICOM and IfAM for shaping the congenial atmosphere at the institutes and the fine excursions.

I am particularly indebted to Professor Jerzy Rakowski from my home Institute of Structural Engineering (IKB), for his helpful suggestions, opinions and continuous support. My attention to slackened systems I owe to Professor Andrzej Gawęcki from IKB who introduced me to this field. I greatly appreciate his stimulating discussions and continuous support. I am also grateful to Professor Andrzej Garstecki, Professor Oleg Kapliński and Professor Tomasz Łodygowski from IKB for their opinions and encouragement. I want to thank my colleagues from the Section of Structural Mechanics of IKB for the nice cooperation.

It is my great pleasure to acknowledge the valuable discussions, opinions and long-time support of Professor Gwidon Szefer of the Cracow University of Technology. I would like to express my sincere gratitude to Professor Bogdan Raniecki from IFTR PAS in Warsaw for the valuable and inspiring discussions.

The support of the DAAD, the European Communities, the British Council and the Volkswagen Stiftung, as well as the support of the Polish Committee of Scientific Research (KBN) through the grants in various forms (individual, DS, BW, DPB) are gratefully acknowledged. Part of the calculations were performed at the Poznań Supercomputing and Networking Centre.

I am thankful to the authors, too numerous to name here, who kindly sent me their papers.

Last but not least I thank my family for their love and patience.

pusta strona

# Contents

## Abstract

The work is concerned with the mathematical modelling and numerical solution of inequality problems for two classes of material behaviour: plastic flow and stress-induced thermoelastic martensitic phase transformations. The associated initial boundary value problems for these deformation processes with hysteresis are formulated in the unifying form of a variational inequality of evolution that encompasses both the conditions of static equilibrium and the criteria of loading/unloading and those of slackening, or the criteria of phase transformations. Under appropriate hypotheses, the existence and uniqueness of solutions to these global formulations are established. Two numerical algorithms are advised and several computer codes are developed. The algorithms have proved to be effective in determining the solution of complex, practical boundary value problems. The obtained results of numerical simulation with the proposed material models revealed interesting properties of viscoelastic-plastic structural systems, whereas those for the phase transformation process are unusual, but in good agreement with the results of laboratory observations.

**Key words:** variational inequalities, linear complementarity problems, finite element method, direct and iterative (SSORP plus PCG) numerical algorithms for LCP, viscoelastoplasticity, slackening, martensitic phase transformations, shape memory alloys.

# Notation

| | |
|---|---|
| $\mathcal{R}^n$ | set of ($n$ copies of) real numbers; |
| $Lin$ | set of all second-order tensors; |
| $Sym$ | set of all symmetric second-order tensors; |
| $LinLin$ | set of all fourth-order tensors; |
| $\boldsymbol{a}\cdot\boldsymbol{b} = a_i b_i$ | scalar product of vectors $\boldsymbol{a}, \boldsymbol{b} \in \mathcal{R}^n$; |
| $\boldsymbol{a} \otimes \boldsymbol{b}$ | tensor product of vectors $\boldsymbol{a}, \boldsymbol{b} \in \mathcal{R}^d$, $(\boldsymbol{a} \otimes \boldsymbol{b})_{ij} = a_i b_j$; |
| $\boldsymbol{A}\cdot\boldsymbol{B} = A_{ij}B_{ij}$ | scalar product of 2nd order tensors $\boldsymbol{A}, \boldsymbol{B}$; |
| $\mathbb{A} \in LinLin$ | tensor of elastic moduli, $\boldsymbol{C} = \mathbb{A}[\boldsymbol{B}]$, $\boldsymbol{B}, \boldsymbol{C} \in Lin$; |
| $\lvert\boldsymbol{a}\rvert,\ \lvert\boldsymbol{A}\rvert$ | Euclidean norm of vector $\boldsymbol{a}$ and tensor $\boldsymbol{A}$; |
| $\sigma,\ \varepsilon,\ E$ | stresses, strains, and Young's modulus (Section 4.1) |
| $\boldsymbol{T}, \boldsymbol{E} \in Sym$ | tensors of (Cauchy) stresses and (small) strains; |
| $\boldsymbol{D}_i \in Sym$ | transformation strain tensor (domain) of $i$-th phase; |
| $\boldsymbol{\sigma}, \boldsymbol{\epsilon} \in \mathcal{R}^n$ | vectors of generalized stresses and strains (Section 3.2); |
| $F$ | generic name for a functional (Section 2) ; |
| $F$ | force in a bar (Section 4.1); |
| $F,\ F^+,\ F_i^-$ | yield functions or phase transformation functions; |
| $\kappa,\ \kappa^+,\ \kappa_i^-$ | threshold functions of plastic flow or phase transformation; |
| $X$, $X_i$ | thermodynamic driving forces for phase transformations; |
| $c$, $c_i$ | volume fraction of martensite or $i$-th phase (variant); |
| $W_i(\cdot)$ | Helmholz free energy function of $i$-th phase; |
| $\widetilde{W}(\cdot)$ | Helmholz free energy function of mixture of phases; |
| $L^p(\Omega; \mathcal{R}^n)$ | space of vector-valued $p^{th}$-integrable functions; |
| $W^{m,p}(\Omega; \mathcal{R}^n)$ | Sobolev space of functions whose derivates of order $\lvert\boldsymbol{j}\rvert \le m$ are in $L^p(\Omega; \mathcal{R}^n)$; |
| $H^m(\Omega; \mathcal{R}^n)$ | Hilbert space, $H^m(\Omega; \mathcal{R}^n) = W^{m,2}(\Omega; \mathcal{R}^n)$; |
| $\Delta$ | finite increment operator; |
| $\nabla$ | gradient operator; |
| PT | Phase Transformation(s); |
| PTC | Phase Transformation Criterion(ia); |
| SMA | Shape Memory Alloy(s); |
| IBVP | Initial Boundary Value Problem(s); |
| VI | Variational Inequality(ies); |
| LCP | Linear Complementarity Problem(s); |
| SSORP | Symmetric Successive Overrelaxation method with Projection; |
| PCG | Preconditioned Conjugate Gradient method. |

# 1 Introduction

## 1.1 Motivation

THERE IS A WEALTH of phenomena and problems in science, technology and economy which are governed by laws expressed not exclusively in the form of equalities but inequalities (or differential inclusions) as well. The primary source of the inequality constraints are the laws of generally understood equilibrium, both of the physical and economic nature. The variational inequality and complementarity approach is not only a natural and mathematically unified description of such problems but it also constitutes the very useful basis for their numerical treatment.

In mathematical terms, the problems considered in this work are finally formulated in a weak form as the *variational inequality*:

Find a solution $u \in \mathcal{K}$ such that

$$\langle P(u),\, v - u \rangle \geq 0 \qquad \text{for all } v \in \mathcal{K}. \tag{1.1}$$

The symbol $\langle \cdot, \cdot \rangle$ stands for duality pairing between a space $\mathcal{V}$ and its dual space $\mathcal{V}^*$, i.e. $\langle \cdot, \cdot \rangle : \mathcal{V}^* \times \mathcal{V} \to \mathcal{R}$, with $\mathcal{R}$ denoting the reals. Further, $\mathcal{K}$ is a set of constraints imposed on the solution $u$. Usually, $\mathcal{K} \subset \mathcal{V}$ is a convex subset in a linear normed space $\mathcal{V}$, on which the operator $P : \mathcal{V} \to \mathcal{V}^*$ is defined. In the problems to be presented in the sequel, $\mathcal{V}$ and $\mathcal{K}$ are Cartesian products of some sets dictated by the variables involved in the underling process. It is worth noting that the processes under consideration are not monotone due to their history dependence and hysteretic effects.

The physical context of this work is the modelling of complex deformation processes in solid materials. We concentrate here upon two types of material behaviour: *plastic flow and stress-induced martensitic phase transformations*. Plastic flow is a characteristic of crystalline materials, mainly steels, however the concept of plastic flow is also useful in the mechanics of rocks, concrete and soils. Martensitic transformations are diffusionless solid-state changes occurring in metals, ceramics and polymers. It is now generally recognized that the shape memory effect, a unique property of certain alloys to regain after deformation their original shape by heating, is associated with a thermoelastic martensitic transformation. The alloys showing this property are called *shape memory alloys*, and the interesting point is that they manifest also another unique material behaviour called *pseudoelasticity* and, after a thermomechanical training, the two-way shape memory effect. Pseudoelasticity, which is of our concern in this work, is now understood as a mechanical kind of shape memory where the applied external stress is the agent to induce a reversible martensitic transformation.

In general, the mechanical response of a material element is quite a complicated issue which depends on many factors, including the micro-structure and chemical composition of the material, its initial state often characterized by impurities, defects and pre-deformation, and a thermomechanical loading program to which the material element will be subjected. As a result, a lot of mechanical and mathematical models were proposed and are still developing which are a compromise between the experimentally revealed complexity of the phenomena and the practical utility of the models. It is trite to remark that the criteria what is "purely theoretic" as opposite to "applicable" in engineering practice are not definitely set, as they are in fact the product of mutual interaction between the current achievements of science, demands of industry on new materials and mankind's desire to get a better understanding of the laws of physics (nature). Both martensitic transformations and plastic flow are deformation processes that take place on a microscopic (grain size) scale. Although they differ drastically in some respects, they have a lot in common. The significance of this observation is that the process of martensitic phase transformations and that of plastic flow have a similar mathematical structure which can be expressed in the form (1.1). Hence, our analysis of martensitic phase transformations is in many aspects parallel to the theory of plasticity. Moreover, as an extension of the classical theory of plasticity, we also consider deformation processes which exhibit plastic flow, viscous effects and unilateral contact conditions (locking). We have succeeded to frame all these phenomena in the unifying form of (1.1).

This work thus straddles the territory between mechanics of solids and applied and computational mathematics. We have taken the vantagepoint that although the deformation process considered involves rearrangements at a fine microscopic scale, the quantity of most practical interest is the resultant macroscopic material behaviour. So, our principle goal is to arrive at macroscopic (phenomenological) models of material behaviour which could be effectively applied for solving boundary value problems of engineering importance. To achieve this we have adapted some results of homogenization procedures and of the thermodynamics of irreversible processes. The present work is based on the author's research that he has done during the last years into the problems of plasticity, unilateral contact and phase transformations [45, 80, 81, 82, 83, 84, 85, 86, 87, 89, 90, 168].

## 1.2 Brief review of the literature

The subject matter of this work is a cross-point of several different disciplines, including metallurgy, crystallography, continuum mechanics and mathematics. Although the general objective is the same, each of the sciences concentrates on characteristic but specialized aspects of the problem, using own language and methodology. Due to the different languages used and the assumptions taken the 'transformation' of achievements from one research field to another is not easy. As the bulk of related literature is too large to be reviewed here, let us mention only some (available) of the representative works in the fields and the accounts that directly motivated our considerations.

Theory of plasticity is now a well-established science whose methods and predictions are instrumental in manufacturing processes and the designing of engineering structures, as demonstrated in many monographs, for example: HILL [56], OLSZAK, PERZYNA & SAWCZUK [135], KACHANOV [67], ŻYCZKOWSKI [198], LUBLINER [103]. The rate-independent plastic behaviour is a classical, conventional idealization which leads to acceptable estimations for the real response of a wide class of materials working at certain ranges of thermomechanical loadings. Viscous effects appear to be important for metals working at elevated temperatures or soil-like and rock-like materials. In such cases the material behaviour is described by models of greater complexity, accounting for both permanent and temporal (and temperature) properties in the framework of viscoelasticity and plasticity, or some combinations thereof (viscoelasto-plasticity, elasto-viscoplasticity or unified modells): PERZYNA [142], NAGHDI & MURCH [124], PONTER & LECKIE [145], RICE [155], MRÓZ & RANIECKI [119].

Although the understanding of physics of plastic deformation and the mechanical models of plastic flow have achieved already a high level of maturity, the corresponding boundary value problems are still a challenge facing today's applied and computational mathematics. The crucial question of uniqueness of a solution to the rate-boundary value problem in plasticity was studied by HILL who in a series of papers, see e.g. [57], derived uniqueness criteria for a general elastoplastic continuum, starting from the potential expressed in rates of stress or strain. DRUCKER, e.g. [26], has formulated the fundamental postulate, extended later to the work condition by ILYUSHIN [62]. KOITER [76] has initiated the uniqueness analysis of non-smooth multi-surface plasticity, further studied by MANDEL [106] and others. The important results in non-associated plasticity in the context of small deformations were obtained by MRÓZ, see e.g. [118], and then for dry contact friction by MICHAŁOWSKI & MRÓZ [111]. TELEGA [181] derived variational settings for a number of models of non-associated plasticity, applying the method of adjoint operator. The sufficient conditions of uniqueness for the rate problem of non-associated plastic flow have been established by RANIECKI [147] and RANIECKI & BRUHNS [149], who introduced the well-known concept of a *linear comparison solid*.

A powerful mathematical tool in the treatment of boundary value problems in mechanics (plasticity, unilateral contact and friction) are the methods of convex analysis and variational inequalities. MOREAU [116, 117] has provided the unified formulation and qualitative analysis for non-differentiable problems in plasticity. DUVAUT & LIONS [27] have studied a variety of problems using regularization techniques and variational inequalities. Modern methods have been also applied by NEČAS & HLAVÁČEK [128]. Further existence results for plasticity problems were obtained by JOHNSON [66], MATTHIES [109], SUQUET [174], JIANG [65], TEMAM [183], and REDDY [153]. HALPHEN & NGUYEN [52] have introduced a wide class of dissipative materials, later extended to the case of non-convex potentials by KIM & ODEN [71], and in terms of *hemivariational inequalities* due to NANIEWICZ & PANAGIOTOPOULOS [126]. A general theory of constraints in mechanics has been studied by WOŹNIAK [192]. The present writer contributed to the variational inequality setting of plasticity problems presented in the joint papers with STEIN [89] and WHITEMAN [90].

As is well-known the strain problem for (elastic-) perfect plastic bodies is more difficult than the corresponding stress problem due to the drastically different regularity of their solutions. The reason is that the plastic strains should be rather described by (bounded) measures. Thus an appropriate mathematical setting of the strain problem of perfect plasticity is the non-reflexive space of bounded deformations $BD(\Omega)$, cf. [172, 174]. This class of measures allows for the possibility of discontinuous displacement fields inside the bulk material where the strains accumulate in thin bands (the localization phenomenon), treated as surfaces (lines, hinges) of jump discontinuities [175, 143]. Usually the localization problem is regularized by applying higher order theories [120, 170, 14], or by the viscoplastic regularization model of Perzyna, a recent application of which is presented by LODYGOWSKI & PERZYNA [102]. Another issue which deserves mentioning here is shakedown analysis as discussed e.g. in STEIN, ZHANG & MAHNKEN [169].

The distinctive feature of plastic flow are the loading/unloading conditions that take the form of the following complementarity relations:

$$-F \geq 0 \qquad \dot{\lambda} \geq 0 \qquad F \cdot \dot{\lambda} = 0 \tag{1.2}$$

where $\dot{\lambda} = \dot{\lambda}(\boldsymbol{x}, t)$ is the so-called *plastic multiplier*, a scalar function of position $\boldsymbol{x}$ and (process) time $t$. The scalar function $F = F(\dot{\lambda})$ represents the so-called *yield condition* which additionally depends, of course, upon some state and internal (hidden) variables of the deformation process. In optimization theory, (1.2) are also known as the Karush-Kuhn-Tucker (KKT) conditions. In the particular case where F is an affine function of $\dot{\lambda}$, conditions (1.2) are called a *linear complementarity problem*. In this work we make use of the observation, which is critical in our approach, that conditions (1.2) are equivalent to a variational inequality of type (1.1).

Numerical methods for plasticity problems are based mainly on the spatial finite element approximation, of which the comprehensive expositions are Zienkiewicz & Taylor [196], Kleiber [73], Simo & Hughes [162]. In the theory of plastic flow the main difficulty is because of the different constitutive relations in the elastic and plastic domains, wherein the division into the two regions is not known *a priori* but constitutes the additional unknown of the problem, being governed by the loading/unloading conditions (1.2). Due to this property one speaks about the *catching-up* or *sweeping process*, the notion coined by Moreau [117]. When looked at from the other side, or in terms of an iterative numerical algorithm, the requirement $(1.2)_1$ amounts to the projection of the current (trial, exterior to $F$) state of material point onto the yield surface $F$. A numerical scheme based on the Moreau formulation has been discussed by Nguyen [129]. This is also the underlying idea of the *return mapping* and *closest-point projection* algorithms. Ortiz & Popov [138] have discussed generalized integration schemes that include the radial return and midpoint rules. Accounting for the properties of numerical projection step in the equilibrium step leads to the modified elastoplastic tangent operator, the so-called consistent *algorithmic* moduli, that helps in improving the rate of convergence, as shown in Simo & Taylor [163]. While being initially developed in the format of $J_2$ flow theory, the projection techniques were extended to large deformation regimes and coupled problems [162, 193, 112].

Numerical methods of structural plasticity may be regarded as the precursor of the continuum mechanics ones, where the numerical implementation of the abstract notions of convex analysis and variational inequalities is more transparent. Maier in a series of papers, see e.g. [104, 105, 48] have implemented mathematical programming methods in solving of practical problems. A comprehensive exposition of this approach is Borkowski [13]. The concept of *piecewise linearization* has been used by Gawęcki who developed the theory of elastic-plastic *slackened* systems [41, 42, 43]. The concept of *locking materials* was introduced by Prager [146]. Corradi & Maier [22] have considered the case of elastic-locking structures. A mathematical study of locking materials is given by Demengel & Suquet [24]. The point here is that the locking conditions have the form of (1.2), with $F$ representing now the locking (or clearance) function. The present author's contribution to such problems of structural mechanics is contained in the papers [45, 46, 81].

Passing to the second type of material behaviour, by way of motivation we wish to remark that the shape memory alloys have become recently the subject of very intensive research for they represent a new class of materials, the so-called *smart materials*. Although discovered about half a century ago, the shape memory effects still remain a mystery in many respects. A comprehensive picture of the related metallurgical aspects and diverse applications of shape memory alloys can be found in [12, 36, 131, 134, 141, 148, 171]. Shape-memory alloys are applied in adaptive structures as devices for control of stiffness and damping (electrical connectors, sensors and actuators) and in medicine as various medical tools, to mention a few.

Martensitic transformations can be defined as shear-dominant, diffusionless first-order transformations occurring by nucleation and growth. A martensitic transformation proceeds by a displacive process in which atoms are rearranged by cooperative movements into a new more stable crystal structure, without changing the chemical properties of the matrix. As a result the product phase, conventionally called *martensite*, inherits the composition and atomic order of the parent phase, conventionally called *austenite*. It is crystallographically instructive to decompose the transformation from austenite to martensite in two parts: the Bain strain and the lattice-invariant shear. The Bain strain encompasses all the atomic movements needed to produce the new structure from the old. The lattice-invariant shear is an accommodation step in which the new structure and the surrounding material must be changed to fit with each other. There are two mechanisms of accommodation: *slip* which is a permanent change, and *twinning*, which can accommodate shape changes in a reversible way. Thus, on the contrary to plastic flow, the characteristic feature of a thermoelastic martensitic transformation is its crystallographic reversibility which is the result of the essentially elastic accommodation of martensite domains, with the coherent interface capable of backwards movement. Yet, during a nonthermoelastic phase transformation the austenite and martensite may be somewhat damaged by accompanying plastic deformation, which inhibits then the complete crystallographic reversibility of this transformation; the phenomenon known as *transformation induced plasticity* (TRIP). Also in the case of stress-induced martensite if a critical stress is reached, permanent deformations appear that tend to restrict the reversal process upon removing stresses and result in an incomplete shape memory. The important experimental and modelling results on plastic effects under the phase transformation process are presented in OLSON & COHEN [133], LEBLOND, DEVAUX & DEVAUX [92, 91], PATOR, EBERHARD & BERVEILLER [140], LEVITAS [97], SPIELFELD & HORNBOGEN [166], and FISCHER [35]. However, it should be mentioned that the mutual interaction of martensitic transformations and plastic flow is still not totally understood and awaits further investigations. Another characteristic of a martensitic transformation is that applied stresses help the transformation; PATEL & COHEN [139] have stated: "*The transformation is aided by shear stresses, but may be aided or opposed by the normal stress component depending on whether the latter is tensile or compressive*".

Finally, on the side of common features, we observe that both plastic flow and martensitic transformations are controlled by some resistance phenomena of the dry friction type, in a manner that does not depend on the scale of time under idealized isothermal and quasi-static conditions.

The sketched above characteristics of martensitic transformations result in the unusual hysteretic behaviour observed in the force-displacement space as revealed in many laboratory tests, e.g. SCHROEDER & WAYMAN [159] and HUO & I. MÜLLER [59], cf. Fig. 6, and ICHINOSE, FUNATSU & OTSUKA [61], see Fig. 27. There have been devised a number of constitutive models for thermoelastic martensitic phase transformations derived on a micromechanical or phenomenological basis; some of them will be outlined. FALK has developed a model based on the Ginzburg-Landau theory in a number of papers, cf. e.g. [33]. Using the concepts of statistical mechanics and that of irreversible thermodynamics, I. MÜLLER and his co-workers have developed in a series of papers a model which describes their experimental findings, for reviews see [122, 59], and the discussion of WILMAŃSKI [190]. Müller's model was extended to the 3D case by RANIECKI *et al.* [151, 150], who introduced two types of models: the so-called $R$-model that is based on the notion of Maxwell's stress and excludes energy dissipation, and the $R_L$-model which accounts for dissipation effects. In order to account for the hysteresis loops displayed in [59], BRANDON & ROGERS [16] have employed a switching function that differentiates between the 'elastic and plastic modes'. The response of Müller's model was examined by the present author and MIELKE [84, 85] who observed a fundamental difference between the local and global behaviour in a non-homogeneous case. FREMOND has considered the austenite/martensite mixture as a three-phase system and posed his model in the framework of convex analysis, for a summary account see [38]. In deriving the averaged constitutive relations BERVEILLER *et al.* [8, 140] have used a self-consistent procedure for the micro-macro transition. LEVITAS [96, 97] and LEVITAS & STEIN [99, 98] have approached the phase transformation process by making use of the postulate of realizability. FISCHER *et al.* [36] have discussed the phase transformation conditions useful on the level of continuum mechanics description. Accounting for both phase transformation and reorientation (detwinning) effects of martensite variants is demonstrated by SUN & HWANG [173]. A detailed discussion of two and multiphase systems is provided by BOYD & LAGOUDAS [15]. Interesting results in numerical simulations of phase transformations are presented by MARKETZ & FISCHER [107] and LEVITAS, IDESMAN & STEIN [95].

Thermoelastic martensitic phase transformations are a result of the exchange of stability that is manifested by discontinuous changes in the crystal lattice of the high temperature phase (austenite), which possesses a greater symmetry, and that of the low temperature phase (martensite), which may exist in many variants. The new crystal structure replaces the parent material in the area where phase transformation has taken place. In terms of the free energy function this amounts to a potential with multiple local minima (energy wells). Analysis of the so-called *non-elliptic* elastic solids appears to be initiated by KNOWLES and co-authors, in particular KNOWLES AND ABEYARATNE [2] have shown that in quasi-static, maximally dissipative motions their response coincides with that of a rate-independent elastic-perfectly plastic solid. The seminal contribution for such materials is due to ERICKSEN [31], see also [32]. JAMES [64] has established the necessary and sufficient conditions that some piecewise homogeneous deformations in phase transformations are stable under dead loads. BALL & JAMES [6, 7] have shown that the failure of semicontinuity of the free energy functionals in non-elliptic materials is the reason for fineness of microstructures observed in martensitic transformations. The illuminating analyses of microstructure by Ball and James and many others, e.g. CHIPOT & KINDERLEHRER [19], FONSECA & S. MÜLLER [37], reveal that the precise modelling of that complex material behaviour must accounts for very fine properties of underlying functions, what requires some deep mathematical concepts (e.g. Y-measure, H-measure) even though the mathematical models are designed for idealized situations at the time.

With more inclination towards the metallurgical literature, KOHN has exploited the techniques of homogenization, see paper [74] and its extended version [75], to mathematically substantiate and generalize the results of averaging procedures commonly used in continuum mechanics (KHACHATURYAN [69] and others). In deriving the model, he assigns each phase (variant) of the austenite/martensite mixture a quadratic free energy function. The weighting coefficients in the resulting expression for the effective energy of the multiphase system correspond to volume fractions of the phases, playing the role of internal variables in continuum mechanics. For a two-component case, using another method PIPKIN [144] obtained a result similar to Kohn's. With a piecewise quadratic approximation of the strain energy function, otherwise it is difficult to explicitly compute that function in the large strain range, FRIED & GURTIN [39] have analyzed the equilibrium problem of multi-phase systems. MIELKE *et al.* [114] have investigated the time-dependent process of phase transformation using an extremum principle. The present author *et al.* [84, 86, 80] have developed a variational inequality formulation for the martensitic deformation process that accounts for hysteretic effects and leads to useful numerical algorithms for associated initial boundary value problems.

Closing this section, we wish to underline the crucial rôle that is played in the dissipative deformation processes by thermodynamics, although there are some reservations among the researches as for the form(s) of the *Second Principle of Thermodynamics*, as evidenced in a number of the above cited works and the following: Truesdell [184], Coleman & Gurtin [21], I. Müller [121], Kestin & Rice [68], Edelen [29], Hutter [60], Germain, Nguyen & Suquet [47], Muschik [123], Wollants, Roos & Delaey [191] and others. The *Clausius-Duhem inequality* imposes restrictions on constitutive relations and a restriction on motions, the latter pertains to the direction in which the process occurs in nature. The significant fact is that this inequality may be treated as a criterion of stability (entropy rate admissibility), which helps one to single out a single solution.

## 1.3 Aims, scope and main assumptions

This work focuses on the analysis of equilibrium problems for solids which are subject to unilateral constraints. The source of such constraints are the constitutive laws of materials – plasticity, locking and phase transformations – which are expressed in the form of complementarity conditions. In the previous section we have looked at the problems in wide perspective, by recalling the instances where these conditions operate. In order to bring the central idea of our approach into sharp focus, we have adopted some assumptions, with emphasis being placed on the structure and practical usefulness of the models. For simplicity and without loss of generality for our purposes, infinitesimal deformations and initially homogeneous materials are assumed. Slow isothermal deformation processes are considered and inertial effects are neglected. Only in Section 4.1.4 a strain-temperature coupling due to the *latent heat* of transformation is taken into account. We are concerned with *coherent* martensitic transformations, that is the displacement vector in a body is continuous and its gradient can be piecewise continuous. Although we make use of geometrically linear theories, the underlying problems are nonlinear due to their intrinsic complexity. In the majority of the aforementioned works the authors are concerned with stable configurations of shape memory materials. Our interest is in the process of evolution, so we account for the dissipation effects, eventually tracing the process as a sequence of equilibrium states (discrete-in-time problem). The approach we use is based on the theory of elliptic operator equations which for the *free-boundary problems* studied in this work take the form of variational inequalities. Here the free boundary is a boundary between the elastic and the plastic region, or it is the front of a forward and reverse martensitic phase transformation or, in the case of locking, it is the boundary of a contact area.

In brief terms, we have tried to investigate the deformation process of a solid body by resolving the four interacting tasks:

- to derive a mathematical formulation (model) of the process,
- to establish the conditions of existence and uniqueness of a solution to the associated initial boundary value problem,
- to develop robust numerical algorithms and computer programs based directly on the proposed mathematical model, and
- to compare the model predictions with published experimental results.

In the case of plastic behaviour we are concerned with materials that exhibit positive (isotropic) hardening, which allows us to set the related variational boundary value problem in the framework of Sobolev spaces. In Section 3.2 we have relaxed this assumption by permitting the case of localized (lumped) plastic hinges in the mechanism of perfect plastic flow, which corresponds to Dirac delta shape functions in the sense of finite element method. We have made some efforts to complete the proposed variational inequality formulations by an analysis on existence and uniqueness. Clearly, existence theorems allow one to prove, independently of any physical and experimental evidence, the consistency of the constitutive assumptions and, in particular, the wellposedness of the corresponding initial boundary value problem (IBVP). The issue of regularity of a weak solution is behind the scope of this work. We merely remark that no matter how smooth the data, the solution of the variational inequality problem cannot be "too regular", i.e. even under very strong regularity assumption on the data, the existence of a smooth solution cannot be expected in general.

Of great practical importance is the computational algorithm implied by a mathematical formulation of IBVP. The mechanical problems considered in this work are finally solved as a sequence of certain forms of the linear complementarity problem (LCP). Specifically, for the numerical solution of the IBVP we elaborated numerical algorithms suitable for our LCP and written a number of computer codes that are based essentially on the following items:

- an implicit one-step time integration scheme,
- the finite element method,
- two methods for the LCP: (i) a direct elimination algorithm using the idea of pivoting, and (ii) a two-step iterative algorithm.

Let us remark in passing here that the developed numerical LCP-algorithms are quite general and may be used for solving similar problems in economy, game theory, traffic planning, etc.

The layout of the presentation is as follows. In the next chapter we recall some definitions and theorems related to the complementarity problem and variational inequalities. In particular, the equivalence lemma of the complementarity and variational inequality problems is proved, and the the fundamental existence and uniqueness theorem in the theory of variational inequalities is recorded. Computational aspects of solving the linear complementarity problems resulting from our material models are also discussed. Chapter 3 is devoted to plasticity problems. First we consider rather in detail a model problem of plastic flow. We formulate the corresponding IBVP of the displacement driven process as a variational inequality, and for its incremental version we prove the existence of a unique solution. Next, a new mathematical model for the slackened-viscoelastic-plastic response of skeletal structural systems is presented. Here also the question of existence and uniqueness is addressed. We include the results of some numerical experiments for typical engineering test problems. In Chapter 4 we deal with the other type of material behaviour — martensitic phase transformations. The characteristic features of the PT deformation process are investigated first by means of a one-dimensional model describing a series of laboratory tests on SMA wires. Subsequently this two-phase 1D model is generalized to the 3D case and defined in the variational inequality format. This allows us to prove existence and uniqueness, following actually the lines of reasoning in the model problem of plastic flow. By a next extension of this model we arrive at a multi-well problem, for which we again establish the existence and uniqueness result. We are aware that there is some repetition in the proofs of the uniqueness theorems, but they are given for each problem considered for the sake of self-containness and clarity of the different mechanical problems, although many intermediate steps are skipped. The included numerical results of the uniaxial tension test on two-phase strips illustrate the intriguing properties of martensitic phase transformations. The obtained results and gained observations not explicitly commented in the course of derivations are summarized in the last chapter, where also certain directions for further work are indicated.

Throughout this work we adopt the natural assumption that the initial state of the material is regular, i.e., the data needed satisfy all the relations defining the associated IBVP.

Finally, a word about the notation used. We have tried to find a compromise between the symbols traditionally used in mechanics and mathematics, the solution of which is, unfortunately, not unique as the Notation shows. Roughly, Gurtin [51] is used as a guide in mechanical aspects and Oden [132] in the mathematical ones. The end of some logical items (definition, theorem, remark) is marked by the symbol ❑ .

# 2 The minimization problem and variational inequalities

In this section we wish to present some mathematical preliminaries to be used in the next sections devoted to the mechanical problem. These are concepts of optimization theory and functional analysis which may be found in many sources, our favorite general references are COTTLE *et al.* [23], GLOWINSKI *et al.* [49], EKELAND & TEMAN [30], ODEN [132], ROCKAFELLAR [157] and ZEIDLER [195]. Such a mathematical framework was used by the present author in [79], in the context of unilateral contact problems. First we motivate variational inequalities from the standpoint of optimization theory, and introduce standard mathematical notations. Then the equivalence lemma between the variational inequality and the complementarity problem is established. Finally two numerical algorithms for the linear complementarity problem are discussed.

## 2.1 Statement of the problem

Formally, the minimization problem can be formulated as follows: Among all the functions satisfying some prescribed conditions, as defined via a set $\mathcal{K}$, find the function(s) which minimizes a given functional $F : \mathcal{K} \to \mathcal{R}$,

$$\text{Find } u \in \mathcal{K} \quad \text{such that} \quad F(u) = \inf_{v \in \mathcal{K}} F(v) \tag{2.1}$$

The constraint set $\mathcal{K} \subset \mathcal{V}$ is a subset of a space of functions $\mathcal{V}$ in which the problem can 'reasonably' be posed; usually, a reflexive Banach space. Of course, the question of existence and uniqueness of solution(s) to (2.1) depend upon both the properties of the functional $F$ and the constraint set $\mathcal{K}$. In order that the minimization problem be meaningful, $F$ must be bounded below on $\mathcal{K}$, i.e. $\min\{F(u) \mid u \in \mathcal{K}\} > -\infty$.

The qualitative analysis of (2.1) is the subject of the direct methods of the calculus of variations. Their aim is to establish conditions on $F$ and $\mathcal{K}$ under which the minimization problem possesses one or more solutions and to characterize them. For simplicity, presume that $F$ is Gateaux differentiable and $\mathcal{K}$ a closed convex subset of $\mathcal{V}$. Then, a minimizer $u$ of (2.1) is also a solution of the *variational inequality*:

$$\text{Find } u \in \mathcal{K} \quad \text{such that} \quad \langle DF(u),\, v - u \rangle \geq 0 \quad \text{for all } u \in \mathcal{K} \tag{2.2}$$

where $\langle \cdot, \cdot \rangle : \mathcal{V}^\star \times \mathcal{V} \to \mathcal{R}$ is duality pairing between the linear space $\mathcal{V}$ and its dual $\mathcal{V}^\star$. If furthermore $F$ is convex, then the problems (2.1) and (2.2) are equivalent. Actually, (2.2) is a weak form of the *Euler-Lagrange inequality* for the problem (2.1), and it reduces to an equality (Euler's equation) if the set $\mathcal{K}$ is a linear space. The role of variational methods in mechanics is clearly shown in the review by SZEFER [177], where various expressions for the potential $F$ are given. In the analysis of problems (2.1) and (2.2) very fine properties of the functional $F$ and the constraints set $\mathcal{K}$ must be taken into account.

Due to the constraint $\mathcal{K}$, it is sometimes convenient to reformulate (2.1) as the following minimization problem defined on the whole set $\mathcal{V}$

$$\bar{F}(u) = \inf_{v \in \mathcal{V}} \{F(v) + \chi_{\mathcal{K}}(v)\} \tag{2.3}$$

in which $\bar{F} : \mathcal{V} \to \mathcal{R} \cup \{+\infty\}$ is an extended real-valued functional and $\chi_{\mathcal{K}}$ is the indicator function of the set $\mathcal{K}$

$$\chi_{\mathcal{K}}(v) = \begin{cases} 0 & \text{if } v \in \mathcal{K}, \\ +\infty & \text{if } v \notin \mathcal{K}. \end{cases} \tag{2.4}$$

Notice that the use of the device (2.4) does not remove the necessity of taking into account inherent features of the constraint $\mathcal{K}$, because the actual minimizer of $\bar{F}$ is still an element in $\mathcal{K}$. We remark here that extended real-valued functionals are not only the matter of convenience, for they can be also arrived at from physical grounds, e.g. the case of the strain energy function in finite elasticity.

In order to introduce the terminology and notation we recall the definitions of some classes of functions which are an indispensable tool for the study of (weak) solutions of partial differential equations and problems in the calculus of variations. With $\Omega$ being a domain in $\mathcal{R}^d$, $d$ a positive integer and $1 \leq p \leq \infty$ an extended number, we denote by $L^p(\Omega)$ the set of (equivalent classes of) measurable functions that are $p^{th}$-power integrable on $\Omega$. The norm on $L^p(\Omega)$ is given by

$$\begin{aligned} \|u\|_{L^p(\Omega)} &= \left( \int_\Omega |u|^p \, \mathrm{d}x \right)^{1/p} && \text{if} \quad 1 \leq p < \infty, \\ \|u\|_{L^\infty(\Omega)} &= \operatorname*{ess\,sup}_{\boldsymbol{x} \in \Omega} |u(\boldsymbol{x})| && \text{if} \quad p = \infty, \end{aligned}$$

wherein the integration is with respect to Lebesgue measure $\mathrm{d}x$.

Let $m \geq 0$ be an integer and $1 \leq p \leq \infty$ a real number. The Sobolev space $W^{m,p}(\Omega)$ consists of those functions $u \in L^p(\Omega)$ whose all weak partial derivatives of order $|\boldsymbol{j}| \leq m$ are also in $L^p(\Omega)$, i.e.

$$W^{m,p}(\Omega) = \left\{ u \in L^p(\Omega) \mid D^{\boldsymbol{j}} u \in L^p(\Omega), \, |\boldsymbol{j}| \leq m \right\},$$

where multi-index notation, $D^{\boldsymbol{j}}$, is used with $\boldsymbol{j} = (j_1, j_2, \dots, j_d)$ being a $d$-tuple of nonnegative integers,

$$D^{\boldsymbol{j}} = \frac{\partial^{|\boldsymbol{j}|}}{\partial x_1^{j_1} \dots \partial x_d^{j_d}}, \qquad |\boldsymbol{j}| = j_1 + j_2 + \dots + j_d.$$

The space $W^{m,p}(\Omega)$ is equipped with the norm

$$\begin{aligned} \|u\|_{W^{m,p}(\Omega)} &= \left( \int_\Omega \sum_{|\boldsymbol{j}| \le m} |D^{\boldsymbol{j}} u|^p \, \mathrm{d}x \right)^{1/p} && \text{if} \quad 1 \le p < \infty, \\ \|u\|_{W^{m,\infty}(\Omega)} &= \max_{|j| \le m} \left\| D^{\boldsymbol{j}} u \right\|_{L^\infty(\Omega)} && \text{if} \quad p = \infty. \end{aligned}$$

The Sobolev space $W^{m,p}(\Omega)$ is a Banach space, which is reflexive if $1 < p < \infty$. In the particular case of $p = 2$, $W^{m,2}(\Omega)$ is a Hilbert space $H^m(\Omega) \equiv W^{m,2}(\Omega)$. Denoting by $W_0^{m,p}(\Omega)$ the closure (in the norm of $W^{m,p}(\Omega)$) of infinitely differentiable functions with compact support, $C_0^\infty(\Omega)$, we obtain in particular a Hilbert space $H_0^m(\Omega) \equiv W_0^{m,2}(\Omega)$. For the vector-valued functions $\boldsymbol{u} = (u_1, u_2, \dots, u_d)$ with $u_i \in L^p(\Omega)$ or $u_i \in H^m(\Omega)\, (i = 1, 2, \dots, d)$ we will use the notation $L^p(\Omega; \mathcal{R}^d)$ and $H^m(\Omega; \mathcal{R}^d)$, respectively. The space of functions with bounded deformation $BD(\Omega)$, which is a proper function space for problems of perfect plasticity, is defined by

$$BD(\Omega) = \left\{ \boldsymbol{u} \in L^1(\Omega; \mathcal{R}^d) \mid E_{ij} \in M^1(\Omega),\ 1 \le i, j \le d \right\}$$

where $E_{ij} = (u_{i,j} + u_{j,i})/2$ are components of the tensor of small strains, $\boldsymbol{E}$, and $M^1(\Omega)$ is the space of bounded measures on $\Omega$.

Finally, it should be mentioned that the indicated connection of minimization problems and variational inequalities is not the only source of the latter, they can also arise independently as a direct description in weak form of real phenomena.

## 2.2 Variational inequalities and complementarity problems

We begin with a variational inequality associated to a bilinear form $a$ defined on $\mathcal{V}$, a real Hilbert space endowed with norm $\|\cdot\|_{\mathcal{V}}$.

**Definition 2.1.** Let $a : \mathcal{V} \times \mathcal{V} \to \mathcal{R}$ be a bilinear form on $\mathcal{V}$. It is said that:
i) $a$ is *continuous* on $\mathcal{V}$ if there is a positive constant $C$ such that

$$|a(u, v)| \le C \, \|u\|_{\mathcal{V}} \, \|v\|_{\mathcal{V}} \qquad \text{for all} \quad u, v \in \mathcal{V};$$

ii) $a$ is *coercive* on $\mathcal{V}$ if there is a positive constant $\alpha$ such that

$$a(v,\, v) \geq \alpha\, \|v\|_{\mathcal{V}}^2 \qquad \text{for all} \quad v \in \mathcal{V};$$

iii) $a$ is *symmetric* on $\mathcal{V}$ if

$$a(u,\, v) = a(v,\, u) \qquad \text{for all} \quad u, v \in \mathcal{V}.$$

❑

Let $l$ be an element of the dual space $\mathcal{V}^*$, i.e. $l \in \mathcal{V}^*$, and $\mathcal{K}$ a convex set in $\mathcal{V}$. Consider the following problem (variational inequality):

Find $u \in \mathcal{K}$ such that

$$a(u,\, v-u) \geq \langle\, l,\, v-u\,\rangle \qquad \text{for all} \quad v \in \mathcal{K}. \tag{2.5}$$

Formula (2.5) is a generalization of the variational formulation of boundary value problems for linear elliptic equations. In the special case that $\mathcal{K} \subset \mathcal{V}$ is a subspace of $\mathcal{V}$, (2.5) reduces to a variational equality.

The following theorem is the fundamental result in the theory of variational inequalities.

**Theorem 2.2.** *Let $a(\cdot,\cdot)$ be a continuous and coercive bilinear form on $\mathcal{V}$, and let $\mathcal{K} \subset \mathcal{V}$ be a nonempty closed and convex subset. There exists a unique solution to the problem (2.5). The mapping $l \to u$ is Lipschitz continuous from $\mathcal{V}^*$ into $\mathcal{V}$.*

**Proof.** See Lions & Stampacchia [101], Kinderlehrer & Stampacchia [72]. ❑

Observe that a linear and continuous mapping $A : \mathcal{V} \to \mathcal{V}^*$ determines a bilinear form $a$ by the relationship

$$a(u,\, v) = \langle\, Au,\, v\,\rangle\,, \tag{2.6}$$

and vice verse, given a bilinear form $a$, the linear transformation

$$v \to a(u,\, v) \qquad \text{for all} \quad v \in \mathcal{V} \tag{2.7}$$

assigns a continuous linear operator $A : \mathcal{V} \to \mathcal{V}^*$ that satisfies (2.6).

Letting $P : \mathcal{V} \to \mathcal{V}^*$ be a continuous (not necessarily linear) operator, we can generalize the variational inequality (2.5) as follows.

Find $u$ such that

$$u \in \mathcal{K}, \quad \langle\, P(u),\, v-u\,\rangle \geq 0 \qquad \text{for all} \quad v \in \mathcal{K}. \tag{2.8}$$

Closely related to (2.8) is the complementarity problem which is posed on $\mathcal{K}^* \times \mathcal{K} \subset \mathcal{V}^* \times \mathcal{V}$, where $\mathcal{K}$ is a nonempty positive closed cone in $\mathcal{V}$ and $\mathcal{K}^*$ is its dual cone, that is

$$\mathcal{K}^* = \{ w \in \mathcal{V}^* \mid \langle w, v \rangle \geq 0 \text{ for all } v \in \mathcal{K} \} . \tag{2.9}$$

Recall that a subset $\mathcal{K} \subset \mathcal{V}$ is a cone in $\mathcal{V}$ (a convex cone with its vertex at the origin) iff for any $u, v \in \mathcal{K}$ the element $u + v \in \mathcal{K}$ and for any $u \in \mathcal{K}$ the element $\lambda u \in \mathcal{K}$ for all $\lambda \geq 0$.

The generalized complementarity problem is defined as follows.

Find $u$ such that

$$u \in \mathcal{K}, \quad P(u) \in \mathcal{K}^*, \quad \langle P(u), u \rangle = 0. \tag{2.10}$$

The following lemma, used in [79, 89, 90], has proved quite useful in our modelling of mechanical problems.

**Lemma 2.3.** *The complementarity problem* (2.10) *and the variational inequality (2.8), both defined on the same cone $\mathcal{K}$, are equivalent.*

**Proof.** First we show that variational inequality (2.8) implies complementarity problem (2.10). If $\mathcal{K}$ is a convex cone (with vertex at the origin), then $\eta u \in \mathcal{K}$ and $u + w \in \mathcal{K}$ for any $u, w \in \mathcal{K}$, $\eta \in [0, \infty)$. By setting $v = 0$ and $v = 2u$ in (2.8), we obtain respectively

$$\langle P(u), -u \rangle \geq 0 \quad \text{and} \quad \langle P(u), u \rangle \geq 0$$

thus, for $u \in \mathcal{K}$,

$$\langle P(u), u \rangle = 0.$$

Next, by taking $v = u + w$ in (2.8), we reduce the latter to

$$\langle P(u), w \rangle \geq 0 \qquad \text{for all} \quad w \in \mathcal{K}$$

which means that $P(u) \in \mathcal{K}^*$.

The inverse implication follows easily from the definition of the dual cone. Let $u \in \mathcal{K}$ and $P(u) \in \mathcal{K}^*$, then by subtracting $\langle P(u), u \rangle = 0$ from the inequality of (2.9), we arrive at (2.8), which completes the proof. ❑

The property of monotonicity is instrumental in the question of existence and uniqueness of a solution to operator equations.

**Definition 2.4.** Let $P : \mathcal{V} \to \mathcal{V}^*$ be an operator mapping a real reflexive Banach space $\mathcal{V}$ into its dual $\mathcal{V}^*$. It is said that:
(i) $P$ is *monotone* on $\mathcal{V}$ iff

$$\langle\, P(u) - P(v),\, u - v \,\rangle \geq 0 \qquad \text{for all} \quad u, v \in \mathcal{V},$$

(ii) $P$ is *strictly monotone* on $\mathcal{V}$ if and only if $P$ is monotone and $\langle\, P(u) - P(v),\, u - v \,\rangle = 0$ implies $u = v$.

(iii) $P$ is *strongly monotone* on $\mathcal{V}$ iff there exists a constant $\alpha > 0$ such that

$$\langle\, P(u) - P(v),\, u - v \,\rangle \geq \alpha\, \|u - v\|_{\mathcal{V}}^2 \qquad \text{for all} \quad u, v \in \mathcal{V};$$

(iv) $P$ is *coercive* on $\mathcal{V}$ iff

$$\lim_{\|u\|_{\mathcal{V}} \to \infty} \frac{\langle\, P(u),\, u \,\rangle}{\|u\|_{\mathcal{V}}} = +\infty;$$

v) $P$ is *hemicontinuous* at $u \in \mathcal{V}$ if

$$h(\xi) \equiv \langle\, P(u + \xi v),\, w \,\rangle \qquad \xi \in [0, 1]$$

is a continuous function of $\xi$ for every $v, w \in \mathcal{V}$. ❑

We also record the definition of stable operators on Banach spaces.

**Definition 2.5.** Let $X$ and $Y$ be real Banach spaces. The operator $P : X \to Y$ is said to be *stable* iff

$$\|P(u) - P(v)\|_Y \geq \alpha\, (\|u - v\|_X) \qquad \text{for all} \quad u, v \in X,$$

where $\alpha : \mathcal{R}_+ \to \mathcal{R}_+$ is continuous, strongly monotone increasing function with $\alpha(0) = 0$ and $\alpha(\xi) \to \infty$ as $\xi \to \infty$. ❑

The following statement follows directly from the above definitions.

**Proposition 2.6.** *Let $P : \mathcal{V} \to \mathcal{V}^*$ be a strongly monotone operator. Then $P$ is coercive and stable.* ❑

Let us introduce another class of operators.

**Definition 2.7.** An operator $P : \mathcal{V} \to \mathcal{V}^*$ is said to be *pseudomonotone* iff, for each $u \in \mathcal{V}$ and each sequence $\{u_n\}$ in $\mathcal{V}$

$$u_n \rightharpoonup u \quad \text{as } n \to \infty \qquad \text{and} \qquad \limsup_{n \to \infty} \langle\, P(u_n),\, u_n - u \,\rangle \leq 0$$

it follows that

$$\liminf_{n \to \infty} \langle\, P(u_n),\, u_n - v \,\rangle \geq \langle\, P(u),\, u - v \,\rangle \qquad \text{for all} \quad v \in \mathcal{V}.$$

❑

In a sense, pseudomonotone operators generalize the class of monotone operators.

**Proposition 2.8.** *Let $\mathcal{V}$ be a reflexive Banach space and $P : \mathcal{V} \to \mathcal{V}^*$ be strongly monotone and hemicontinuous. Then $P$ is pseudomonotone.* ❏

The following theorem expresses some general existence result for pseudomonotone variational inequalities.

**Theorem 2.9.** *Let $\mathcal{V}$ be a separable reflexive Banach space, $\mathcal{V}^*$ its topological dual and let $\mathcal{K} \subset \mathcal{V}$ be a nonempty closed convex unbounded subset of $\mathcal{V}$. Let an operator $P : \mathcal{K} \to \mathcal{V}^*$ be bounded and pseudomonotone. Furthermore, let $P$ be coercive in the following sense: There exists a $v_0 \in \mathcal{K}$ such that*

$$\frac{\langle\, P(v),\, v - v_0 \,\rangle}{\|v\|_{\mathcal{V}}} \to +\infty \quad \textit{as} \quad \|v\|_{\mathcal{V}} \to +\infty \quad \textit{for all} \quad v \in \mathcal{K}.$$

*Then there exists at least one solution $u \in \mathcal{K}$ to the variational inequality*

$$\langle\, P(u),\, v - u \,\rangle \geq 0 \qquad \textit{for all} \quad v \in \mathcal{K}.$$

**Proof.** See ODEN [132]. ❏

In the special case of great practical importance in which P is an affine mapping, i.e. $P(u) \equiv Au + b$, where $A : \mathcal{V} \to \mathcal{V}^*$ is a linear operator and $b \in \mathcal{V}^*$, problem (2.10) is called a *linear complementarity problem* (LCP),

$$u \in \mathcal{K}, \quad Au + b \in \mathcal{K}^*, \quad \langle\, Au + b,\, u \,\rangle = 0. \tag{2.11}$$

The numerical treatment of the LCP defined in $\mathcal{R}^n$ is briefly discussed next.

## 2.3 Numerical methods for the LCP

The complementarity problems first appeared in optimization theory and mathematical programming as the necessary conditions of optimality (Karush-Kuhn-Tucker conditions), and usually were formulated in the finite dimensional context, i.e. $\mathcal{V} \equiv \mathcal{R}^n$, where $\mathcal{R}^n$ stands for the Euclidean space of real ordered n-tuples. In particular, any quadratic programming problem may be solved as a linear complementarity problem. Restricting our further consideration to the finite dimensional case we let $P$ be now an affine mapping of the form $P(\boldsymbol{x}) \equiv \boldsymbol{A}\boldsymbol{x}+\boldsymbol{b}$, where $\boldsymbol{A} \in \mathcal{R}^{n\times n}$ is a square matrix and $\boldsymbol{x} \in \mathcal{R}^n$, $\boldsymbol{b} \in \mathcal{R}^n$

are $n$-dimensional vectors. Now, the linear complementarity problem (LCP) is to find the vector $\boldsymbol{x} \in \mathcal{R}^n$ such that

$$\begin{aligned} \boldsymbol{x} &\geq \mathbf{0}, \\ \boldsymbol{A}\boldsymbol{x} + \boldsymbol{b} &\geq \mathbf{0}, \\ \boldsymbol{x} \cdot (\boldsymbol{A}\boldsymbol{x} + \boldsymbol{b}) &= 0. \end{aligned} \tag{2.12}$$

By introducing a slack variable $\boldsymbol{y} \equiv \boldsymbol{A}\boldsymbol{x} + \boldsymbol{b}$ we can rewrite the system (2.12) in the following standard form which is convenient when solving the problem by a direct method:

$$\begin{gathered} \bar{\boldsymbol{A}}\boldsymbol{x} + \boldsymbol{y} = \boldsymbol{b}, \\ \boldsymbol{x} \geq \mathbf{0}, \quad \boldsymbol{y} \geq \mathbf{0}, \quad \boldsymbol{x} \cdot \boldsymbol{y} = 0, \end{gathered} \tag{2.13}$$

wherein $\bar{\boldsymbol{A}} = -\boldsymbol{A}$. When matrix $\boldsymbol{A}$ is symmetric, the problems (2.12) and (2.13) are called *symmetric*, otherwise *nonsymmetric*.

In the problems we consider in Section 3.2 the unknown vector consists of three subvectors, $\boldsymbol{x} = \mathrm{col}\,(\boldsymbol{x}_1, \boldsymbol{x}_2, \boldsymbol{x}_3)$, and the matrix $\bar{\boldsymbol{A}}$ has the structure,

$$\bar{\boldsymbol{A}} = \begin{bmatrix} \bar{\boldsymbol{A}}_{11} & \bar{\boldsymbol{A}}_{12} & \bar{\boldsymbol{A}}_{13} \\ \bar{\boldsymbol{A}}_{21} & \bar{\boldsymbol{A}}_{22} & \bar{\boldsymbol{A}}_{23} \\ \bar{\boldsymbol{A}}_{31} & \bar{\boldsymbol{A}}_{32} & \bar{\boldsymbol{A}}_{33} \end{bmatrix} \tag{2.14}$$

where the submatrices $\bar{\boldsymbol{A}}_{ij} \in \mathcal{R}^{n_i \times n_j}$, with $i, j = 1, 2, 3$ and $n_i, n_j \in \mathcal{N}$ being a positive integers, cf. (3.90), (3.92). The critical property of those LCP is that their first unknown component vector $\boldsymbol{x}_1$ is unrestricted in sign. Accounting for this we arrive at the form of LCP which we call a *nested linear complementarity problem* (nLCP):

$$\begin{gathered} \bar{\boldsymbol{A}}\boldsymbol{x} + \boldsymbol{y} = \boldsymbol{b}, \\ \boldsymbol{x}_2 \geq \mathbf{0}, \quad \boldsymbol{x}_3 \geq \mathbf{0}, \quad \boldsymbol{y}_1 = \mathbf{0}, \quad \boldsymbol{y}_2 \geq \mathbf{0}, \quad \boldsymbol{y}_3 \geq \mathbf{0}, \quad \boldsymbol{x} \cdot \boldsymbol{y} = 0. \end{gathered} \tag{2.15}$$

Another characteristic feature of the systems (3.90), (3.92) is that $\bar{\boldsymbol{A}}$ is *bisymmetric*, i.e. its components satisfy the conditions: $\bar{\boldsymbol{A}}_{ii}$ $(i = 1, 2, 3)$ are symmetric, and $\bar{\boldsymbol{A}}_{ij} = -\bar{\boldsymbol{A}}_{ji}^{\mathrm{T}}$, with $i, j = 1, 2, 3$, $i \neq j$. A similar modification is pertinent to the nLCP expressed via matrix $\boldsymbol{A}$, so we have

$$\begin{gathered} \boldsymbol{A}\boldsymbol{x} + \boldsymbol{b} \geq \mathbf{0}, \\ \boldsymbol{x}_2 \geq \mathbf{0}, \quad \boldsymbol{x}_3 \geq \mathbf{0}, \quad \boldsymbol{x} \cdot (\boldsymbol{A}\boldsymbol{x} + \boldsymbol{b}) = 0. \end{gathered} \tag{2.16}$$

The question of existence and uniqueness of a solution to the linear complementarity problem is dealt with in the following theorem proved in Cottle *et al.* [23]. We formulate the theorem in terms of the properties of matrix $\boldsymbol{A}$.

**Theorem 2.10.** *(i) Let $\boldsymbol{A} \in \mathcal{R}^{n\times n}$ be positive definite, then the linear complementarity problem* (2.12) *and* (2.15) *has a unique solution for any $\boldsymbol{b} \in \mathcal{R}^n$.*
*(ii) Let $\boldsymbol{A} \in \mathcal{R}^{n\times n}$ be positive semi-definite and $\boldsymbol{b} \in \mathcal{R}^n$. Let $\boldsymbol{x}^\diamond$ be a solution of the linear complementarity problem* (2.12) *or* (2.15). *If $\boldsymbol{x}^\diamond$ is not degenerate (i.e. there is no index $0 \le i \le n$ that both $x_i^\diamond$ and $y_i^\diamond$ are equal to zero) and the corresponding matrix $\boldsymbol{A}^\diamond \subset \boldsymbol{A}$ ($\boldsymbol{A}^\diamond$ is composed of these rows $A_{k.}$ and columns $A_{.k}$ for which $x_k^\diamond > 0$) is nonsingular, then $\boldsymbol{x}^\diamond$ is the unique solution of the problem.* ❑

Finally we want to observe that also the LCP (4.59) in Section 4.2.4 can be written in the form of (2.15), but now with the LCP-matrix $\boldsymbol{A}^\star$

$$\boldsymbol{A}^\star = \begin{bmatrix} \bar{\boldsymbol{A}} & -\hat{\boldsymbol{I}}^{\mathrm{T}} \\ \hat{\boldsymbol{I}} & \boldsymbol{0} \end{bmatrix} \qquad \text{with} \quad \hat{\boldsymbol{I}} = \begin{bmatrix} \boldsymbol{0} & \boldsymbol{I} & \boldsymbol{0} \\ \boldsymbol{0} & \boldsymbol{0} & \boldsymbol{I} \end{bmatrix}. \tag{2.17}$$

For solving the inequality problems one has to resort to numerical techniques. There are basically two classes of algorithms for the linear complementarity problem: direct methods and iterative methods. The direct methods are based on the process of pivoting on the elements of the underlying matrix. This amounts, in simple terms, to successive exchanges of a selected basis variable with its complementary variable. The principle advantage of direct methods is their robustness and finite character. The latter means that they terminate after a finite number of computations, determining the solution if it exists or, providing the answer that no solution to the underlying LCP exists. On the other hand, the first class of algorithms require large storage memory, which makes them impractical for large problems (more then three thousands of unknowns, say). In the context of finite element method, free from this shortcoming are iterative methods, which are additionally insensitive to round-off-errors. Hence, they are well suited for large scale problems, but there is the price to pay: to assure their convergence and effectiveness one has to properly predict some algorithmic parameters, which in the case of inequality constraints is not straightforward.

We have developed two algorithms. The first algorithm is an enhancement of the direct method elaborated in Van de Panne [185]. The main steps of the algorithm are presented in Kuczma [81], and we refrain from discussing it here. The second scheme is an adaptation of the two-step iterative algorithm devised by Kočvara & Zowe [77]. Within the first step the *symmetric successive overrelaxation method with projection* (SSORP) is used, while within the second step the *preconditioned conjugate gradient method* (PCG) solves the system of equations for the active variables as determined by the SSORP. In simple terms, this scheme combines the SSORP method and the PCG method, with *preconditioning* by *modified incomplete factorization* ($MIC(0)^*$). Details of the two-step algorithm are presented in [77], and will not be recalled here, but two things should be mentioned. First, that algorithm is designed for the LCP with positive definite matrix, so it cannot be applied to the problems in Section 3.2. Second, on a part of the vector of unknowns in our LCP for martensitic phase transformations in Section 4, the box constraints are imposed, so some modifications of the original version [77] were needed. Furthermore, our LCP-matrix is generated by two mechanically different sources: equilibrium conditions and phase transformations rules. We observe that the convergence rate can further be improved if we have additionally scaled the LCP-matrix $\boldsymbol{A}^\star$. The very important issue of the properties and quality of finite element approximations is not one of our purposes in this work. However it is worthwhile to mention that in the numerical calculations we have, on principle, used compatible finite elements with polynomial basis functions (shape functions) that assure the internal approximation of the constraint set $\mathcal{K}$.

# 3 Problems in viscoelastoplasticity

The first part of this chapter concerns a model problem of plastic flow. With emphasis being laid on the structure, we confine ourselves to a fundamental case in the theory of plastic flow — the Huber-von Mises yield criterion with isotropic hardening. Following the paper [90][1] we present a detailed derivation of the associated initial boundary value problem (IBVP) for a three dimensional body in the form of a variational inequality (VI). The results of numerical experiments for a test problem are provided in [90] and will not be recalled here. Instead, we strengthen here the previous result by establishing the conditions of existence and uniqueness of solutions to the incremental boundary value problem.

In the second part we develop a model of slackened-viscoelastic-plastic media. Although we have formulated the model in the context of skeletal structural systems, the derived matrix relations are of general importance, in the sense that they may be regarded as a discrete description of two- or three-dimensional bodies made from materials with such properties, provided that due care will be taken in generating the finite dimensional approximations. Such approximations are rather straightforward in the one-dimensional case [13]. We cast the matrix relations in the format of a linear complementarity problem which, of course, by virtue of Lemma 2.3 can be expressed in a VI form. The qualitative questions for this problem are also addressed, yet, they are quite delicate in a general case.

To motivate our derivations let us emphasize that the VI approach to problems of elastoplasticity and locking is most natural since it reflects directly the intrinsic features of these kinds of material behaviour. Notice the the variational inequalities (or complementarity problems) derived for the problems in this chapter need not to be associated with potential operators, cf. Chapter 2 for a discussion on this. In more precise terms, the obtained variational inequalities are a week form of the loading/unloading conditions, slackening (locking, unilateral contact) constraints and equilibrium equations. The remarkable advantage is that the VI description automatically covers both the case of plastic loading and that of elastic unloading, whereas the boundary between the plastic and elastic regions is a 'by-product' of solving the variational inequality. Analogously for the locking response, in which case we utilize a locking criterion which is to 'signal' the presence of resistance of the material.

Some conclusions close the chapter.

[1]The paper was presented on the Eighth Conference MAFELAP, Uxbridge, 27-30 April 1993.

## 3.1 The model problem of plastic flow

In this section we develop the VI formulation for the model problem of plasticity. We consider the quasi-static deformation process of an elastic-plastic body, modelled according to infinitesimal theory of plastic flow with isotropic hardening. In this case the total infinitesimal strain tensor can be split additively into an elastic part and a plastic part. Moreover, we restrict our attention to initially homogeneous and isotropic materials. Let us also remark that for the Huber-von Mises yield criterion, which is under consideration, the notions of work-hardening and of strain-hardening are equivalent. We formulate the problem in **strain space**, following the idea due to NAGHDI & TRAPP, see e.g. [125], used also in a VI formulation by HLAVÁČEK *et al.* [58]. The proposed variational formulation consists of (a) a variational equation which is the weak form of the equilibrium conditions, and (b) a variational inequality that accounts for the irreversibility of the plastic deformation, controlled here by a rate of plastic multiplier $\dot{\lambda}$. The independent variables of the formulation are the fields of displacements $\boldsymbol{u} = \boldsymbol{u}(\boldsymbol{x}, t)$ and of plastic multiplier $\dot{\lambda} = \dot{\lambda}(\boldsymbol{x}, t)$, where $\boldsymbol{x}$ is a vector of the space coordinates of a material point and $t$ stands for time.

We begin with recalling the constitutive relations for the elastic-plastic material, and setting the relevant notations. Then, the variational formulation of the related IBVP is given and a time-step $t_{n-1} \to t_n$ problem is defined. Finally, under appropriate conditions, the existence and uniqueness of solutions to the incremental problem is established.

### 3.1.1 Fundamental constitutive relations

We are concerned with the elastic-plastic, quasi-static deformation process of a solid body. The body, in its undeformed state, corresponds to an open bounded domain $\Omega \subset \mathcal{R}^d$ $(d \leq 3)$ with sufficiently smooth boundary $\Gamma$ which consists of two mutually disjoint parts $\Gamma_u$ and $\Gamma_\sigma$, i. e. $\Gamma = \overline{\Gamma}_u \bigcup \overline{\Gamma}_\sigma$ and $\Gamma_u \bigcap \Gamma_\sigma = \emptyset$. We will consider the case that the body is supported on a set $\Gamma_u$ with positive measure, i.e. $\operatorname{meas} \Gamma_u > 0$. Let $\boldsymbol{u} = (u_1(\boldsymbol{x}), \ldots, u_d(\boldsymbol{x}))$, $\boldsymbol{T} = \boldsymbol{T}(\boldsymbol{x})$ and $\boldsymbol{E} = \boldsymbol{E}(\boldsymbol{x})$ denote the displacement vector, (Cauchy) stress and (small) strain tensors, respectively, at a material point $\boldsymbol{x} \in \bar{\Omega} = \Omega \bigcup \Gamma$.

The system of the local equilibrium equations of the body, subjected to a volumic force vector $\boldsymbol{f}$, reads

$$\operatorname{div} \boldsymbol{T} + \boldsymbol{f} = \boldsymbol{0} \quad \text{in} \quad \Omega. \tag{3.1}$$

Let the following conditions be prescribed on the boundary $\Gamma$

$$\boldsymbol{u} = \boldsymbol{0} \quad \text{on} \quad \Gamma_u, \tag{3.2}$$

$$\boldsymbol{T}\boldsymbol{n} = \boldsymbol{t} \quad \text{on} \quad \Gamma_\sigma, \tag{3.3}$$

where $\boldsymbol{t}$ and $\boldsymbol{n}$ are the given traction vector and outward unit normal to $\Gamma$.

Under the assumption of small strain we have

$$\boldsymbol{E} = \boldsymbol{E}(\boldsymbol{u}) = \frac{1}{2}\left[\nabla\boldsymbol{u} + (\nabla\boldsymbol{u})^{\mathrm{T}}\right]. \tag{3.4}$$

Moreover, for a linear elastic material the constitutive equations take the form of Hooke's law

$$\boldsymbol{T} = \mathbb{A}[\boldsymbol{E}], \tag{3.5}$$

where the elasticity tensor $\mathbb{A}$ possesses the usual properties of symmetry

$$A_{ijkl} = A_{jikl} = A_{ijlk} = A_{klij} \qquad 1 \leq i,j,k,l \leq 3\ ,$$

and $\mathbb{A}$ is uniformly pointwise stable with bounded entries [108], that is, there exist constants $k_A > 0$ and $k'_A < \infty$ such that

$$\begin{aligned} \boldsymbol{S}\cdot\mathbb{A}[\boldsymbol{S}] &\geq k_A\,|\boldsymbol{S}|^2, \qquad \forall\boldsymbol{S}\in Sym \\ \max_{i,j,k,l}\|A_{ijkl}\|_\infty &< k'_A. \end{aligned} \tag{3.6}$$

For a linear isotropic elastic material

$$\mathbb{A} = 2\mu\mathbb{I} + \xi\boldsymbol{I}\otimes\boldsymbol{I} \tag{3.7}$$

and equation (3.5) simplifies to

$$\boldsymbol{T} = 2\mu\boldsymbol{E} + \xi(\operatorname{tr}\boldsymbol{E})\boldsymbol{I} \tag{3.8}$$

where $\mu$ and $\xi$ are Lame's constants of the material, and $\mathbb{I}$ and $\boldsymbol{I}$ denote the unit tensors of fourth and second order, with the components $(\mathbb{I})_{ijkl} = (\delta_{ik}\delta_{jl} + \delta_{il}\delta_{jk})/2$ and $(\boldsymbol{I})_{ij} = \delta_{ij}$ (Kronecker's delta).

Confining ourselves to small deformations we may split the total strain tensor into an elastic $\boldsymbol{E}^e$ and a plastic $\boldsymbol{E}^p$ part so that

$$\boldsymbol{E} = \boldsymbol{E}^e + \boldsymbol{E}^p. \tag{3.9}$$

In the case under consideration the elastic part of the total strain tensor is related to the stress tensor by Hooke's law,

$$\boldsymbol{T} = \mathbb{A}[\boldsymbol{E} - \boldsymbol{E}^p] \tag{3.10}$$

whereas the plastic part is

$$\boldsymbol{E}^p = \boldsymbol{E}^p(t) \equiv \int_0^t \dot{\boldsymbol{E}}^p(\tau)\ \mathrm{d}\tau \tag{3.11}$$

in which $\dot{\boldsymbol{E}}^p$ is governed by an incremental flow rule.

In the theory of plastic flow it is expedient to use the concept of the *yield function* $F$ depending on the stress $\boldsymbol{T}$ and a family of internal variables $\boldsymbol{\kappa}$ by which the structural rearrangements in the course of the deformation process are accounted for,

$$F = F(\boldsymbol{T}, \boldsymbol{\kappa}),$$

with $F$ specifying a region $\mathcal{E}_\sigma$ in stress space

$$\mathcal{E}_\sigma = \{\, (\boldsymbol{T}, \boldsymbol{\kappa}) \in Sym \times \Upsilon \mid F(\boldsymbol{T}, \boldsymbol{\kappa}) \le 0 \,\}. \tag{3.12}$$

The interior of $\mathcal{E}_\sigma$ defined by the strict inequality is called the *elastic region*, whilst plastic flow is stipulated to occur only on the *yield surface* that is the boundary of $\mathcal{E}_\sigma$ defined by $F = 0$.

The appearance of plastic strains renders the analysis of an elastic-plastic body nonlinear, even under the assumption of linear kinematical relations. Hence, also in the quasi-static case, the state of the body is a function not only of place $\boldsymbol{x} \in \bar{\Omega}$ but also of a time-like parameter $t \in [0, T], (T < \infty)$, which we call a *process time*. The process time records the sequence of events in the deformation process and thereby hysteresis effects (dissipation).

The flow rule relates the rate of change of plastic strain to the rate of change of stress, and in the case of associative plasticity it may be assumed in the form

$$\dot{\boldsymbol{E}}^p = \dot{\lambda} \frac{\partial F}{\partial \boldsymbol{T}} \tag{3.13}$$

where $\dot{\lambda}$ is the rate of an unspecified scalar function which cannot be negative in order to take account of the irreversible character of the plastic deformation.

At any time $t$ in every material point $\boldsymbol{x} \in \bar{\Omega}$ the following possibilities may be distinguished:

$$\boxed{\begin{array}{llll} F < 0 & \text{then} & \dot{\lambda} = 0 & \text{— elastic state} \\ F = 0 & \text{and} & \dot{\lambda} = 0 & \text{— plastic state: neutral loading} \\ F = 0 & \text{and} & \dot{\lambda} > 0 & \text{— plastic state: plastic loading} \end{array}} \tag{3.14}$$

Thus, the process (or loading) is termed *plastic*, if it is accompanied by an increment of plastic strain, otherwise it is *elastic*.

As can easily be seen, the relations (3.14) can be written equivalently as the complementarity conditions

$$F \leq 0 \quad \text{and} \quad \dot{\lambda} \geq 0 \quad \text{and} \quad F\,\dot{\lambda} = 0, \tag{3.15}$$

which in conjunction with equation (3.13) constitute the very characteristic loading/unloading criteria of the theory of plastic flow.

Many researches supplement (3.15) by the so-called *consistency condition*

$$\dot{F}\,\dot{\lambda} = 0. \tag{3.16}$$

which is *de facto* redundant because the following statement holds.

**Proposition 3.1.** *The loading/unloading conditions (3.15) imply the consistency condition (3.16).*

**Proof.** Let $F(t) < 0$ at given time $t$, then $\dot{F}(t)$ is not restricted but by $(3.15)_3$ we have $\dot{\lambda} = 0$, so (3.16) is satisfied. If $F(t) = 0$, there are two cases: (i) $\dot{F}(t) = 0$, so (3.16) follows trivially and, (ii) $\dot{F}(t) < 0$ which leads to $F(t + \mathrm{d}t) = F(t) + \dot{F}(t)\;\mathrm{d}t < 0$, so again by $(3.15)_3$ we arrive at (3.16). ❑

The above observation shows that the loading/unloading conditions (3.15) completely control the plastic flow process of an elastic-plastic material. We use (3.15) as our point of departure for the VI formulation to be given below.

The precise way in which the yield function changes during the deformation process is a complex issue. For this model problem we adopt the Huber–von Mises yield criterion with isotropic hardening

$$F = F(\boldsymbol{T}, \boldsymbol{\kappa}) \equiv F(\boldsymbol{T}, \boldsymbol{E}^p) = f(\boldsymbol{T}) - \kappa(\epsilon^p) \tag{3.17}$$

where

$$f(\boldsymbol{T}) = \sqrt{3J_2(\operatorname{dev}\boldsymbol{T})} = \sqrt{\frac{3}{2}}\;|\operatorname{dev}\boldsymbol{T}|, \tag{3.18}$$

$$\kappa(\epsilon^p(t)) = \kappa\left(\int_0^t \dot{\epsilon}^p(\tau)\;\mathrm{d}\tau\right), \tag{3.19}$$

with $\operatorname{dev}\boldsymbol{T} = \boldsymbol{T} - \frac{1}{3}(\operatorname{tr}\boldsymbol{T})\boldsymbol{I}$ being the deviatoric part of the stress tensor, and $\dot{\epsilon}^p$ denoting the rate of effective plastic strain

$$\dot{\epsilon}^p = \sqrt{\frac{2}{3}}\;|\dot{\boldsymbol{E}}^p|\,. \tag{3.20}$$

Making use of the flow rule (3.13) and definition (3.20) we obtain

$$\dot{\epsilon}^p = \dot{\lambda}\,. \tag{3.21}$$

Hence the function $\kappa$ can be expressed as a function of the plastic multiplier, $\kappa \equiv \kappa(\lambda(t))$, and we impose on it the following conditions

$$\kappa(0) \equiv \sigma_Y, \qquad \kappa' \equiv \frac{\partial \kappa(\lambda)}{\partial \lambda} \geq 0, \tag{3.22}$$

where $\sigma_Y > 0$ is the initial yield stress taken from a uniaxial tension test.

Upon substituting $\boldsymbol{T}$ according to equation (3.10) into equation (3.17) we can obtain the yield condition, hereafter denoted by G, expressed in the strains $\boldsymbol{E}$ and $\boldsymbol{E}^p$,

$$F\left(\mathbb{A}[\boldsymbol{E} - \boldsymbol{E}^p], \boldsymbol{E}^p\right) \equiv G(\boldsymbol{E}, \boldsymbol{E}^p) = g(\boldsymbol{E}, \boldsymbol{E}^p) - \kappa(\epsilon^p) \tag{3.23}$$

with

$$g(\boldsymbol{E}, \boldsymbol{E}^p) \equiv f\left(\mathbb{A}[\boldsymbol{E} - \boldsymbol{E}^p]\right). \tag{3.24}$$

Let $\boldsymbol{M}$, $\boldsymbol{N} \in \mathit{Sym}$ denote the 'normals' to the surfaces defined by the functions $g$ and $f$, respectively,

$$\boldsymbol{M} \equiv \frac{\partial g}{\partial \boldsymbol{E}}, \qquad \boldsymbol{N} \equiv \frac{\partial f}{\partial \boldsymbol{T}}, \tag{3.25}$$

then by (3.24)

$$\boldsymbol{N} = \mathbb{A}^{-1}[\boldsymbol{M}], \tag{3.26}$$

where $\mathbb{A}^{-1}$ is the inverse of the elasticity tensor $\mathbb{A} \in \mathit{LinLin}$. In particular, for the isotropic material and the Huber–von Mises yield function we have

$$\boldsymbol{M} = \sqrt{6}\mu \, \frac{\operatorname{dev} \boldsymbol{E}^e}{|\operatorname{dev} \boldsymbol{E}^e|}. \tag{3.27}$$

In the sequel we shall need the following inequality

$$\boldsymbol{M} \cdot \mathbb{A}^{-1}[\boldsymbol{M}] \leq k_M, \qquad 0 < k_M < \infty, \tag{3.28}$$

which is satisfied in view of (3.6) and (3.27).

Finally the flow rule (3.13) and the conditions (3.15) can be rewritten as

$$\dot{\boldsymbol{E}}^p = \dot{\lambda}\, \boldsymbol{N} = \dot{\lambda}\, \mathbb{A}^{-1}[\boldsymbol{M}], \tag{3.29}$$

$$G \leq 0 \qquad \dot{\lambda} \geq 0 \qquad G \cdot \dot{\lambda} = 0. \tag{3.30}$$

Summing up, we emphasize that the relations presented above describe the response at the level of a generic material point of an elastic-plastic continuum. These requirements will be formulated for the body as a whole in the next section.

### 3.1.2 Variational inequality formulation

In this section our aim is to develop a weak formulation of the elastic-plastic boundary value problem, as defined by the equilibrium conditions (3.1) and the plastic flow conditions (3.30). The crucial point in our further consideration is the equivalence which exists between a complementarity problem and a class of variational inequalities which is formulated as Lemma 2.3.

We begin with a weak form of the equilibrium conditions. Let $V$ be the set of all kinematically admissible displacements of the body,

$$V = \Big\{ \boldsymbol{v} \in H^1(\Omega, \mathcal{R}^d) \mid \ \boldsymbol{v}|_{\Gamma_u} = \boldsymbol{0} \text{ in the sense of traces} \Big\} \tag{3.31}$$

where $H^1(\Omega, \mathcal{R}^d)$ is the usual Sobolev space. We remark that the homogeneous conditions for the displacement vector on the boundary are taken for convenience, this is commonly used cf. [20, 167].

The weak formulation of the equilibrium condition (3.1) for the case of linear elasticity, i.e. $\boldsymbol{E} \equiv \boldsymbol{E}^e$, may be formulated as follows:

Find $\boldsymbol{u} \in V$ such that

$$a(\boldsymbol{u}, \boldsymbol{v}) = f(\boldsymbol{v}) \quad \text{for all} \quad \boldsymbol{v} \in V. \tag{3.32}$$

The bilinear form $a : V \times V \to \mathcal{R}$ and the linear form $f \in V^*$, i.e. $f : V \to \mathcal{R}$, are defined by

$$a(\boldsymbol{u}, \boldsymbol{v}) = \int_\Omega \boldsymbol{E}(\boldsymbol{v}) \cdot \mathbb{A}[\boldsymbol{E}(\boldsymbol{u})] \ \mathrm{d}x \ = \int_\Omega \nabla \boldsymbol{v} \cdot \mathbb{A}[\nabla \boldsymbol{u}] \ \mathrm{d}x, \tag{3.33}$$

$$f(\boldsymbol{v}) = \int_\Omega \boldsymbol{f} \cdot \boldsymbol{v} \ \mathrm{d}x + \int_{\Gamma_\sigma} \boldsymbol{f}_\Gamma \cdot \boldsymbol{v} \ \mathrm{d}s. \tag{3.34}$$

By making use of the split (3.9), we can express the weak form of the equilibrium condition (3.1) as

$$a(\boldsymbol{u}, \boldsymbol{v}) - p(\boldsymbol{E}^p, \boldsymbol{v}) = f(\boldsymbol{v}) \quad \text{for all} \quad \boldsymbol{v} \in V \tag{3.35}$$

where

$$p(\boldsymbol{E}^p, \boldsymbol{v}) = \int_\Omega \boldsymbol{E}(\boldsymbol{v}) \cdot \mathbb{A}[\boldsymbol{E}^p] \ \mathrm{d}x. \tag{3.36}$$

Let $K$ stand for the closed convex positive cone in $L^2(\Omega)$, i.e.

$$K = \left\{ u \in L^2(\Omega) | \ \langle u, v \rangle \geq 0 \ \forall v \geq 0 \text{ in } L^2(\Omega) \right\}, \tag{3.37}$$

where $\langle \cdot, \cdot \rangle$ denotes the inner product in $L^2(\Omega)$, i.e. for $u, v \in L^2(\Omega)$

$$\langle u, v \rangle = \int_\Omega u(\boldsymbol{x}) \, v(\boldsymbol{x}) \ \mathrm{d}x.$$

Now, by virtue of Lemma 2.3, we can write the complementarity conditions (3.30) in the weak form as the following variational inequality

$$\dot{\lambda} \in K \qquad \left\langle -G\left(\boldsymbol{E}(\boldsymbol{u}), \boldsymbol{E}^p(\boldsymbol{u}, \dot{\lambda}\right), \gamma - \dot{\lambda} \right\rangle \geq 0 \quad \text{for all} \quad \gamma \in K. \tag{3.38}$$

The weak setting of the elastoplastic IBVP (3.1), (3.29), (3.30) may be formulated in the following manner.

$$\boxed{\begin{array}{c} \text{Find the pair } (\boldsymbol{u}, \dot{\lambda}) \in H^1([0,T], V) \times H^1_0([0,T], K) \text{ such that} \\ \begin{array}{rcll} a(\boldsymbol{u}, \boldsymbol{v}) - p\left(\boldsymbol{E}^p(\boldsymbol{u}, \dot{\lambda}), \boldsymbol{v}\right) & = & f(\boldsymbol{v}) & \forall\, \boldsymbol{v} \in V \\ \left\langle -G\left(\boldsymbol{E}(\boldsymbol{u}), \boldsymbol{E}^p(\boldsymbol{u}, \dot{\lambda})\right), \gamma - \dot{\lambda} \right\rangle & \geq & 0 & \forall\, \gamma \in K \end{array} \end{array}} \tag{3.39}$$

with, for $\boldsymbol{x} \in \Omega$ and fixed $t \in (0, T]$,

$$\boldsymbol{E}^p(\boldsymbol{u}, \dot{\lambda}) = \int_{t^0}^{t} \dot{\lambda}(\boldsymbol{x}, \tau)\, \mathbb{A}^{-1}[\boldsymbol{M}(\boldsymbol{u}(\boldsymbol{x}, \tau))]\; \mathrm{d}\tau. \tag{3.40}$$

Thus, our elastoplastic deformation process is governed by the system that consists of a variational equality $(3.39)_1$ and a variational inequality $(3.39)_2$. In the language of mechanics the variational equality assures the equilibrium of the body during the process, whereas the variational inequality controls the development of admissible plastic strains within the body and may be regarded as a weak formulation of the consistency condition. Notice that although the variational inequality (3.39) contains rates, it differs from classical parabolic inequalities [27]. From the computational viewpoint, in order to solve the system (3.39) effectively in practical problems we have to employ numerical techniques based on approximations in space and time.

Let us consider the incremental problem in time, applying an implicit integration scheme known as the *catching-up algorithm*. Within a typical time-step $t_{n-1} \to t_n$ the state of a body at time $t = t_{n-1} \in (0, T)$ is given and the task is to determine its state at time $t = t_n \in (t_{n-1}, T]$. We shall denote the quantities at a fixed $t = t_n$ with the subscript $n$, thus e.g. $\boldsymbol{u}_n \equiv \boldsymbol{u}(t_n, \cdot)$ is a function only of the space variable $\boldsymbol{x}$. By $\Delta$ we shall denote a finite increment operator, e.g.

$$\boldsymbol{u}_n = \boldsymbol{u}_{n-1} + \Delta \boldsymbol{u}_n, \tag{3.41}$$

$$\lambda_n = \lambda_{n-1} + \Delta \lambda_n. \tag{3.42}$$

The finite increment of the function $G(\boldsymbol{E}(\boldsymbol{u}_n), \boldsymbol{E}_n^p)$ can be expressed as

$$\begin{aligned}\Delta G_n &\equiv \left.\frac{\partial g}{\partial \boldsymbol{E}^e}\right|_{t=t_n} \cdot (\Delta \boldsymbol{E}_n - \Delta \boldsymbol{E}_n^p) + \left.\frac{\partial \kappa}{\partial \lambda}\right|_{t=t_n} \Delta\lambda_n \\ &= \boldsymbol{M}(\boldsymbol{u}_n) \cdot \boldsymbol{E}(\Delta \boldsymbol{u}_n) - \big(\boldsymbol{M}(\boldsymbol{u}_n) \cdot \mathbb{A}^{-1}[\boldsymbol{M}(\boldsymbol{u}_n)] + \kappa_n'\big)\, \Delta\lambda_n. \qquad (3.43)\end{aligned}$$

The incremental problem for the system (3.39) at time $t = t_n$ takes up the form

Find the pair $(\Delta \boldsymbol{u}_n, \Delta\lambda_n) \in V \times K$ such that

$$a(\Delta \boldsymbol{u}_n, \boldsymbol{v}) - p(\Delta\lambda_n \mathbb{A}^{-1}[\boldsymbol{M}_n], \boldsymbol{v}) = f_{n,n-1}(\boldsymbol{v})$$

$$\big\langle -G_{n-1} - \boldsymbol{M}_n \cdot \boldsymbol{E}(\Delta \boldsymbol{u}_n) + \big(\boldsymbol{M}_n \cdot \mathbb{A}^{-1}[\boldsymbol{M}_n] + \kappa_n'\big)\, \Delta\lambda_n,\ \gamma - \Delta\lambda_n \big\rangle \geq 0$$

for all $(\boldsymbol{v}, \gamma) \in V \times K$.

(3.44)

In (3.44) $G_{n-1}$ is the known space distribution of the yield function at previous time level $t = t_{n-1}$ and

$$f_{n,n-1}(\boldsymbol{v}) = f_n(\boldsymbol{v}) - a(\boldsymbol{u}_{n-1}, \boldsymbol{v}) + p(\boldsymbol{E}_{n-1}^p, \boldsymbol{v}). \qquad (3.45)$$

Note that the normal $\boldsymbol{M}_n \equiv \boldsymbol{M}(\boldsymbol{u}_n)$ is evaluated at the current state from the displacement vector $\boldsymbol{u}_n$ which makes the VI (3.44) nonlinear. An iterative algorithm for solving the system (3.44) and results of numerical experiments for a test problem are contained in [90]. Here we wish only to mention that the algorithm consists of the equilibrium and the projection step. In the next section we investigate the question of existence and uniqueness of solutions to the problem (3.44).

### 3.1.3 Existence and uniqueness

In this section we show that the operator $A$ corresponding to the VI formulation (3.44) is Lipschitz continuous and strongly monotone. These properties of $A$ guarantees the existence of a unique solution to system (3.44). In studying this question we simplify the notations by introducing the following sets and elements

$$\mathcal{V} \equiv V \times \Lambda, \qquad \Lambda = L^2(\Omega), \qquad (3.46)$$

$$\mathcal{K} \equiv V \times K, \qquad K \subset \Lambda, \qquad (3.47)$$

$$u \equiv (\boldsymbol{u}, \lambda), \qquad v \equiv (\boldsymbol{v}, \gamma), \qquad (3.48)$$

with the corresponding norm of $v \in \mathcal{V}$ defined by

$$\|v\|_{\mathcal{V}}^2 = \|\boldsymbol{v}\|_V^2 + \|\gamma\|_\Lambda^2. \tag{3.49}$$

For brevity in notation we drop the index of time $n$ and we denote:

$$\boldsymbol{M}_{\boldsymbol{u}_n} \equiv \boldsymbol{M}(\boldsymbol{u}_{n-1} + \Delta\boldsymbol{u}_n), \qquad \Delta u_n \equiv (\Delta\boldsymbol{u}_n, \Delta\lambda_n), \tag{3.50}$$

$$\langle\, l_{n,n-1},\, v\,\rangle \equiv f_{n,n-1}(\boldsymbol{v}) + \langle\, G_{n-1},\, \gamma\,\rangle\,. \tag{3.51}$$

We introduce the operator $A : \mathcal{V} \longrightarrow \mathcal{V}^*$ by

$$\langle\, Au,\, v\,\rangle \equiv a(\boldsymbol{u},\, \boldsymbol{v}) - \tilde{p}(\lambda,\, \boldsymbol{v}) - e(\boldsymbol{u},\, \gamma) + h(\lambda,\, \gamma) \tag{3.52}$$

wherein $a$ is same as in (3.33), $\tilde{p}$ corresponds to (3.36) and the others are

$$a(\boldsymbol{u},\boldsymbol{v}) = \int_\Omega \boldsymbol{E}(\boldsymbol{v}) \cdot \mathbb{A}[\boldsymbol{E}(\boldsymbol{u})]\ \mathrm{d}x\ =\ \int_\Omega \nabla\boldsymbol{v} \cdot \mathbb{A}[\nabla\boldsymbol{u}]\ \mathrm{d}x, \tag{3.53}$$

$$\tilde{p}(\lambda,\, \boldsymbol{v}) = \int_\Omega \boldsymbol{E}(\boldsymbol{v}) \cdot \boldsymbol{M}_{\boldsymbol{u}}\,\lambda\ \mathrm{d}x\ =\ \int_\Omega \nabla\boldsymbol{v} \cdot \boldsymbol{M}_{\boldsymbol{u}}\,\lambda\ \mathrm{d}x, \tag{3.54}$$

$$e(\boldsymbol{u},\gamma) = \int_\Omega \boldsymbol{M}_{\boldsymbol{u}} \cdot \boldsymbol{E}(\boldsymbol{u})\ \gamma\ \mathrm{d}x\ =\ \int_\Omega \boldsymbol{M}_{\boldsymbol{u}} \cdot \nabla\boldsymbol{u}\,\gamma\ \mathrm{d}x, \tag{3.55}$$

$$h(\lambda,\gamma) = \int_\Omega (\boldsymbol{M}_{\boldsymbol{u}} \cdot \mathbb{A}^{-1}[\boldsymbol{M}_{\boldsymbol{u}}] + \kappa')\lambda\,\gamma\ \mathrm{d}x. \tag{3.56}$$

It is interesting to notice that the linearization and implicit time integration procedure we use lead to a symmetric elastic-plastic boundary value problem.

With the above notations we can rewrite the problem (3.44) as the variational inequality:

Find $\Delta u_n \in \mathcal{K}$ such that

$$\langle\, A(\Delta u_n),\, v - \Delta u_n\,\rangle \geq \langle\, l_{n,n-1},\, v - \Delta u_n\,\rangle \quad \forall\, v \in \mathcal{K}. \tag{3.57}$$

We show that the operator $A$ possesses some useful properties.

**Lemma 3.2.** *The operator $A$ is Lipschitz continuous, that is, there exists a positive constant $k < \infty$ such that*

$$\|Av - Au\|_{\mathcal{V}^*} \leq k\,\|v - u\|_{\mathcal{V}}. \tag{3.58}$$

**Proof.** By virtue of $(3.6)_2$ and (3.27) it follows by standard arguments (Cauchy-Schwartz inequality and equivalence of norms) that the bilinear forms

$a$, $\tilde{p}$, $h$ and the form $e$ are continuous in the sense that there exist positive constants $k_1$, $k_2$, $k_3$, $k_4$ such that

$$|a(\boldsymbol{u},\, \boldsymbol{v})| \leq k_1\, \|\boldsymbol{u}\|_V\, \|\boldsymbol{v}\|_V, \tag{3.59}$$

$$|\tilde{p}(\lambda,\, \boldsymbol{v})| \leq k_2\, \|\lambda\|_\Lambda\, \|\boldsymbol{v}\|_V, \tag{3.60}$$

$$|e(\boldsymbol{u}, \gamma)| \leq k_3\, \|\boldsymbol{u}\|_V\, \|\gamma\|_\Lambda, \tag{3.61}$$

$$|h(\lambda, \gamma)| \leq k_4\, \|\lambda\|_\Lambda\, \|\gamma\|_\Lambda. \tag{3.62}$$

To show the requirement (3.58) we consider

$$\begin{aligned}\langle\, Av - Au,\, w\,\rangle \;&=\; a(\boldsymbol{v}-\boldsymbol{u},\, \boldsymbol{w}) - \tilde{p}(\gamma-\lambda,\, \boldsymbol{w}) - e(\boldsymbol{v}-\boldsymbol{u},\, \zeta) + \\ &\quad\; h(\gamma-\lambda,\, \zeta)\end{aligned} \tag{3.63}$$

with $w = (\boldsymbol{w}, \zeta)$, and make use of estimations (3.59) to (3.62)

$$\begin{aligned}|\,\langle\, Av - Au,\, w\,\rangle\,| \;&\leq\; k_1\|\boldsymbol{v}-\boldsymbol{u}\|_V\, \|\boldsymbol{w}\|_V + k_2\|\gamma-\lambda\|_\Lambda\, \|\boldsymbol{w}\|_V + \\ &\quad\; k_3\|\boldsymbol{v}-\boldsymbol{u}\|_V\, \|\zeta\|_\Lambda + k_4\|\gamma-\lambda\|_\Lambda\, \|\zeta\|_\Lambda \\ &\leq\; \frac{1}{2}k\, \left(\|\boldsymbol{v}-\boldsymbol{u}\|_V + \|\gamma-\lambda\|_\Lambda\right)\left(\|\boldsymbol{w}\|_V + \|\zeta\|_\Lambda\right) \\ &=\; k\, \|v-u\|_{\mathcal{V}}\, \|w\|_{\mathcal{V}}\end{aligned} \tag{3.64}$$

where $k = 2\,\max\{k_1,\, k_2,\, k_3,\, k_4\}$ and we have used the inequality $\alpha + \beta \leq \sqrt{2}\left(\alpha^2+\beta^2\right)^{1/2}$. Now, in the light of the definition

$$\|Av - Au\|_{\mathcal{V}^*} = \sup_{w\in\mathcal{V}-0} \frac{|\,\langle\, Av - Au,\, w\,\rangle\,|}{\|w\|_{\mathcal{V}}} \tag{3.65}$$

and condition (3.64), the requirement (3.58) is satisfied. ❑

We shall need a modification of Korn's inequality.

**Lemma 3.3.** *Let* $\Omega \in \mathcal{C}^{0,1}$. *Then there exists a positive constant* $k_K > 0$ *such that*

$$\int_\Omega |\boldsymbol{E}(\boldsymbol{v})|^2\; \mathrm{d}x \geq k_K\; \|\boldsymbol{v}\|_V^2 \qquad \textit{for every} \quad \boldsymbol{v} \in V. \tag{3.66}$$

**Proof.** See Lemma 6.2 of Kikuchi & Oden [70]. ❑

Further we are concerned with the case of an elastic-plastic material that work-hardens, i.e. the function $\kappa$ is strictly monotone, $\kappa' \geq H_p > 0$. Moreover, let $k_A$ denote the lower bound of $\mathbb{A}$, cf. (3.6), and let $\bar{\beta} = 1 - \beta$ with $\beta \in (0,1)$. Our proof follows that of Jiang [65] who studied an elastic-plastic problem with a similar mathematical structure, see also Reddy & Griffin [154].

**Lemma 3.4.** *Let the elastic-plastic material exhibit strictly positive strain hardening. Then the operator $A$ is strongly monotone, that is, there exists a constant $k_0 > 0$ such that*

$$\langle\, Av - Au,\; v - u \,\rangle \geq k_0 \, \|v - u\|_{\mathcal{V}}^2 \tag{3.67}$$

**Proof.** Let us denote

$$L \equiv \langle\, Av - Au,\; v - u \,\rangle \,.$$

We have

$$\begin{aligned}
L &= a(\boldsymbol{v}-\boldsymbol{u},\, \boldsymbol{v}-\boldsymbol{u}) - \tilde{p}(\gamma-\lambda,\, \boldsymbol{v}-\boldsymbol{u}) - e(\boldsymbol{v}-\boldsymbol{u},\, \gamma-\lambda) + h(\gamma-\lambda,\, \gamma-\lambda) \\
&= \int_\Omega (\boldsymbol{E}(\boldsymbol{v}-\boldsymbol{u}) - \mathbb{A}^{-1}[\boldsymbol{M}_{\boldsymbol{u}}](\gamma-\lambda)) \cdot \mathbb{A}[\boldsymbol{E}(\boldsymbol{v}-\boldsymbol{u}) - \mathbb{A}^{-1}[\boldsymbol{M}_{\boldsymbol{u}}](\gamma-\lambda)] \,\mathrm{d}x + \\
&\quad \int_\Omega \kappa'(\gamma-\lambda)(\gamma-\lambda)\,\mathrm{d}x \\
&\geq \int_\Omega k_A(\boldsymbol{E}(\boldsymbol{v}-\boldsymbol{u}) - \mathbb{A}^{-1}[\boldsymbol{M}_{\boldsymbol{u}}](\gamma-\lambda)) \cdot (\boldsymbol{E}(\boldsymbol{v}-\boldsymbol{u}) - \mathbb{A}^{-1}[\boldsymbol{M}_{\boldsymbol{u}}](\gamma-\lambda))\,\mathrm{d}x + \\
&\quad \int_\Omega \kappa'(\gamma-\lambda)(\gamma-\lambda)\,\mathrm{d}x \\
&\geq \int_\Omega \Bigg\{ k_A\beta \boldsymbol{E}(\boldsymbol{v}-\boldsymbol{u}) \cdot \boldsymbol{E}(\boldsymbol{v}-\boldsymbol{u}) + k_A \left( \sqrt{\bar{\beta}}\boldsymbol{E}(\boldsymbol{v}-\boldsymbol{u}) - \frac{1}{\sqrt{\bar{\beta}}} \mathbb{A}^{-1}[\boldsymbol{M}_{\boldsymbol{u}}](\gamma-\lambda) \right) \\
&\quad \cdot \left( \sqrt{\bar{\beta}}\boldsymbol{E}(\boldsymbol{v}-\boldsymbol{u}) - \frac{1}{\sqrt{\bar{\beta}}} \mathbb{A}^{-1}[\boldsymbol{M}_{\boldsymbol{u}}](\gamma-\lambda) \right) - \frac{k_A\beta}{\bar{\beta}} \boldsymbol{M}_{\boldsymbol{u}} \cdot \mathbb{A}^{-1}[\boldsymbol{M}_{\boldsymbol{u}}](\gamma-\lambda)^2 \\
&\qquad + H_p(\gamma-\lambda)(\gamma-\lambda) \Bigg\} \,\mathrm{d}x \\
&\geq \int_\Omega \left\{ k_A\beta\, |\boldsymbol{E}(\boldsymbol{v}-\boldsymbol{u})|^2 - \frac{k_A\beta}{1-\beta} \boldsymbol{M}_{\boldsymbol{u}} \cdot \mathbb{A}^{-1}[\boldsymbol{M}_{\boldsymbol{u}}](\gamma-\lambda)^2 + H_p(\gamma-\lambda)^2 \right\} \,\mathrm{d}x \\
&\geq \int_\Omega \left\{ k_A\beta\, |\boldsymbol{E}(\boldsymbol{v}-\boldsymbol{u})|^2 + (H_p - \frac{k_A\beta k_M}{1-\beta})(\gamma-\lambda)^2 \right\} \,\mathrm{d}x,
\end{aligned} \tag{3.68}$$

where $k_A$ and $k_M$ are positive constants defined in (3.6) and (3.28). Now taking $\beta = \frac{H_p}{(H_p + 2k_A k_M)}$ and using (3.66) we have

$$\langle\, Av - Au,\; v - u \,\rangle \geq \frac{k_A H_p k_K}{H_p + 2k_A k_M} \, \|\boldsymbol{v}-\boldsymbol{u}\|_V^2 + \frac{1}{2} H_p \, \|\gamma - \lambda\|_\Lambda^2 \,. \tag{3.69}$$

Hence for this choice of $\beta$, (3.67) is satisfied with

$$k_0 = \min\left\{ \frac{k_A H_p k_K}{H_p + 2k_A k_M}, \frac{1}{2} H_p \right\}. \qquad ❑$$

Finally, we summarize the results in the following theorem on the existence and uniqueness of solutions to (3.57). Recall that (3.57) is merely a re-written expression for the elastic-plastic boundary value problem (3.44).

**Theorem 3.5.** *Under the assumptions made on the data, there exists a unique solution of the problem (3.57). The solution depends continuously on data* $l \in \mathcal{V}^*$.

**Proof.** In the light of Lemmas (3.2) and (3.4), the proof is a standard result in the theory of variational inequalities, cf. Theorem 2.9 and Theorem 2.2. Since the operator $A$ is Lipschitz continuous and strongly monotone, it is pseudomonotone and coercive. The uniqueness and continuity of the solution is assured due to the strong monotonicity of $A$. Indeed, let $u_i$ be two solutions of (3.57),

$$\langle Au_i,\, v - u_i \rangle \geq \langle l_i,\, v - u_i \rangle \quad \forall\, v \in \mathcal{K}, \tag{3.70}$$

with $l_i \in \mathcal{V}^*$, $i = 1, 2$.

Setting $v = u_{3-i}$ in inequality (3.70) for $i = 1, 2$, we have

$$\begin{aligned} \langle Au_1,\, u_2 - u_1 \rangle &\geq \langle l_1,\, u_2 - u_1 \rangle\,, \\ \langle Au_2,\, u_1 - u_2 \rangle &\geq \langle l_2,\, u_1 - u_2 \rangle\,. \end{aligned}$$

Adding the above two inequalities, we finally obtain

$$\langle Au_2 - Au_1,\, u_2 - u_1 \rangle \leq \langle l_2 - l_1,\, u_2 - u_1 \rangle\,,$$

so

$$k_0 \, \|u_2 - u_1\|_{\mathcal{V}}^2 \leq \|l_2 - l_1\|_{\mathcal{V}^*} \, \|u_2 - u_1\|_{\mathcal{V}}\,.$$

Hence, inequality

$$\|u_2 - u_1\|_{\mathcal{V}} \leq \frac{1}{k_0} \, \|l_2 - l_1\|_{\mathcal{V}^*} \tag{3.71}$$

completes the continuity and uniqueness assertion. ❑

## 3.2 Skeletal structural systems with clearances

In this section we are concerned with the skeletal structural systems which may exhibit both the instantaneous elastic-plastic response as well as the time-dependent viscoelastic-plastic one. An additional feature of these systems is the presence of clearances. On the level of the discrete matrix description we use, the latter may be the nodal values of functions describing the inherent property of the material obtained by a finite element approximation, or represent the existing gaps between different constituents of the structural system, e.g. an engineering structure and its foundation, unilateral constraints at supports. The source of inequality relations governing the problem considered here is the yield function and the clearance function, defined in a piecewise linear fashion. As concerns these general concepts we follow PRAGER [146], MAIER & CORRADI [104, 22] and GAWĘCKI [43]. We have enhanced the elastic-plastic material model in two aspects: (i) material behaviour inside the yield surface may be viscoelastic and, (ii) the associated IBVP is formulated and solved as a sequence of nested (mixed) linear complementarity problems.

In the proposed material model the viscoelastic and plastic strains are governed by different constitutive laws. The basic assumption is that the plastic strains do not influence the viscoelastic properties of the material, the customary assumption in elastoplasticity. This macroscopic model is based on more than one micromechanism responsible for the development of stress in a solid body. First, if some measure of deformation is smaller than a threshold value (clearance function), then there is no stress in the material point. The reversible changes in the microstructure of the material are described by viscoelastic laws, whereas the third mechanism is activated when the stresses reach some threshold (yield function). Upon releasing the stresses when the third mechanism is induced there is permanent (plastic) deformation. In brief, whilst the second mechanism accounts for viscous and rate effects in material behaviour, the role of the third mechanism is in limiting the stresses which the material can sustain and in accounting for instantaneous permanent deformation. Notice that, depending on the kind of the viscoelastic model used, the second mechanism may also contribute to the final permanent deformation. Owing to this particular succession of the mechanisms the suggested model does not directly fall into the well-known viscoplasticity theories, e.g. [142, 27, 93, 110]. In developing the model, our motivation was to extend the viscoelastic model of [79] in order to cover the possibility of instantaneous permanent deformation. Thus, a combination of [79] and [45] has led us to [81]. Yet, we have realized recently that the idea of a conceptual combination in series of viscoelastic and plastic basic elements (spring, dashpot and slide) is not new, and dates back at least to the early sixties, see e.g.

[124, 145, 155, 119, 55]. Our considerations here are restricted to initially isotropic, non-aging linearly viscoelastic-plastic media undergoing small deformations under isothermal quasistatic conditions.

In the next section we first recall the constitutive relation and formulate the discrete-in-space but continuous-in-time problem. The characteristic matrix notations used for structural systems are explained. Next the time integration scheme is outlined and the resulting time-step LCP are derived. The question of existence and uniqueness of solutions to the incremental problems is discussed. Finally, results of numerical experiments for illustrative examples of a beam/foundation system subjected to nonproportional loading histories are included. The results clearly demonstrate the impact of the history of loading and the unilateral constraints upon the current state of the structural system.

### 3.2.1 Constitutive relations

In this section we present the fundamental relations that define our model of slackened-viscoelastic-plastic behaviour. The description is purely phenomenological and derived in the context of one-dimensional structural elements. (The viscoelastic relations for 3D and 2D cases are given in [82].) The total strain is additively decomposed into a clearance part $\epsilon^l$, a viscoelastic part $\epsilon^{ve}$ and a plastic part $\epsilon^p$, see Fig. 1,

$$\epsilon = \epsilon^l + \epsilon^{ve} + \epsilon^p, \tag{3.72}$$

or in incremental form

$$\dot{\epsilon} = \dot{\epsilon}^l + \dot{\epsilon}^{ve} + \dot{\epsilon}^p. \tag{3.73}$$

The rate form can also be written, for some combinations of the mechanical basic elements, as the following decomposition

$$\dot{\epsilon} = \dot{\epsilon}^l + \dot{\epsilon}^{ep} + \dot{\epsilon}^v \tag{3.74}$$

in which an instantaneous strain rate $\dot{\epsilon}^{ep}$ and a delayed strain rate $\dot{\epsilon}^v$ are separated. In fact, the split (3.74) together with $\dot{\epsilon}^v = 0$ will be employed later at the times at which stress $\sigma$ suffers a discontinuity of first order.

For the plastic strain rate an associative flow rule is used, whilst the evolution of the viscoelastic strain is assumed to be governed by the following linear differential equation

$$a_0\sigma + a_1\dot{\sigma} + a_2\ddot{\sigma} = b_0\epsilon^{ve} + b_1\dot{\epsilon}^{ve} + b_2\ddot{\epsilon}^{ve} \tag{3.75}$$

wherein $a_i, b_i$ $(i = 1, 2, 3)$ are viscoelastic material constants. In the particular case of the standard three-parameter solid shown in Fig. 1, equation (3.75) simplifies to the equation of first order

$$\frac{E_1 + E_2}{\eta_2}\sigma + 1.0\,\dot{\sigma} = \frac{E_1 E_2}{\eta_2}\epsilon^{ve} + E_1\dot{\epsilon}^{ve}. \tag{3.76}$$

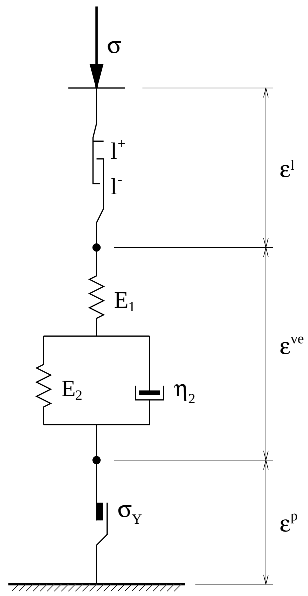


Figure 1: Conceptual model for viscoelastic-plastic behaviour, with clearance strain

Let us assume that the stress history is known, then we can solve equation (3.75) for strains and express the result at a time $t$ in the form of linear hereditary constitutive relation

$$\epsilon^{ve}(t) = \int_{t_0}^{t} J(t-\tau)\frac{\partial\sigma(\tau)}{\partial\tau}\,d\tau \equiv \mathcal{F}^{t}_{\tau=t_0}[\sigma(\tau)] \tag{3.77}$$

which emphasizes the fact that the strain at a current moment $t$ depends upon the entire history of stress from a time $t = t_0$ to the time $t$. Usually one takes $t_0 = 0$ and zero initial condition which should be defined at the left-hand side of time $t$, i.e. $t = t_0^- \equiv t_0 - 0$. In (3.77) $J(s)$ denotes a creep function, which e.g. for the viscoelastic three-parameter solid shown in Fig. 1 is

$$J(s) = \frac{1}{E_1}\left[1 + \frac{E_1}{E_2}\left(1 - \exp(-\frac{E_2}{\eta_2}s)\right)\right]. \tag{3.78}$$

Suppose the deformation process of a slackened system made of the viscoelastic-plastic material has taken place on times $\tau$ along the interval $(0, t]$, i.e. $\tau \in (0,t]$. Then the state of the system at the present instant $t \in \mathcal{R}_+$, with $\tau \in (0,t]$, is governed by the following relations.

$$
\begin{array}{rrcll}
 & \multicolumn{4}{l}{\text{GENERAL RELATIONS}} \\
1) & \boldsymbol{\epsilon}(t) & = & \boldsymbol{C}\,\boldsymbol{u}(t), & \text{kinematic compatibility,} \\
2) & \boldsymbol{p}(t) & = & \boldsymbol{C}^{\mathrm{T}}\boldsymbol{\sigma}(t), & \text{equilibrium,} \\
 & \multicolumn{4}{l}{\text{STRAIN DECOMPOSITION}} \\
3) & \boldsymbol{\epsilon}(t) & = & \boldsymbol{\epsilon}^{l}(t) + \boldsymbol{\epsilon}^{ve}(t) + \boldsymbol{\epsilon}^{p}(t), & \\
 & \multicolumn{4}{l}{\text{LINEAR VISCOELASTICITY}} \\
4) & \boldsymbol{\epsilon}^{ve}(t) & = & \mathcal{F}_{\tau=0}^{t}[\boldsymbol{\sigma}(\tau)], & \\
 & \multicolumn{4}{l}{\text{PLASTICITY}} \\
5) & \boldsymbol{\epsilon}^{p}(t) & = & \boldsymbol{N}\boldsymbol{\lambda}(t), \quad \boldsymbol{\lambda}(t) = \int_0^t \dot{\boldsymbol{\lambda}}(\tau)\,d\tau, & \text{associative flow rule,} \\
6) & \dot{\boldsymbol{\lambda}}(\tau) & \geq & \boldsymbol{0}, & \\
7) & \boldsymbol{f}(\tau) & = & \boldsymbol{N}^{\mathrm{T}}\boldsymbol{\sigma}(\tau) - \boldsymbol{H}\boldsymbol{\lambda}(\tau) - \boldsymbol{k} \leq \boldsymbol{0}, & \text{yield function,} \\
8) & \dot{\boldsymbol{\lambda}}(\tau)\cdot\boldsymbol{f}(\tau) & = & 0, & \\
 & \multicolumn{4}{l}{\text{SLACKENING (UNILATERAL CONTACT)}} \\
9) & \boldsymbol{\sigma}(\tau) & = & \boldsymbol{M}\boldsymbol{\psi}(\tau), & \text{normality law,} \\
10) & \boldsymbol{\psi}(\tau) & \geq & \boldsymbol{0}, & \\
11) & \boldsymbol{g}(\tau) & = & \boldsymbol{M}^{\mathrm{T}}\boldsymbol{\epsilon}^{l}(\tau) - \boldsymbol{l} \leq \boldsymbol{0}, & \text{clearance function,} \\
12) & \boldsymbol{\psi}(\tau)\cdot\boldsymbol{g}(\tau) & = & 0. &
\end{array}
\tag{3.79}
$$

The manner in which the time dependence of the problem quantities is displayed in the relations (3.79) is just to indicate which of the quantities are time-dependent and where the history of the deformation process is involved; of course, the conditions of equilibrium $(3.79)_2$ and of geometric compatibility $(3.79)_1$ must be satisfied at each instant $\tau \in (0,t]$. Furthermore it should be mentioned that relations (3.79) represent the finite-dimensional model of the whole structure/foundation system obtained by means of the finite element method, which consists of the structure's elements and those modelling its foundation. In fact, the similar relations as (3.79) are valid at the elemental level, the system (3.79) being obtained by the usual assembly process. Although the aspects of finite dimensional approximation are very important, in this paper we treat (3.79) as granted and wish to focus our attention rather on the time approximation of the problem at hand. Yet, let us recall merely the notations used in (3.79). The geometric compatibility condition $(3.79)_1$ states a relation between the vector of nodal displacements $\boldsymbol{u}(t)$ and the vector of generalized strains, with $\boldsymbol{C}$ being called the kinematic compatibility matrix whose transpose $\boldsymbol{C}^{\mathrm{T}}$ defines the equilibrium condition $(3.79)_2$. By $\boldsymbol{p}(t)$, $\boldsymbol{\sigma}(t)$ we denote the vector of external nodal forces and the vector of generalized stresses, respectively. Notice that the vectors $\boldsymbol{u}$, $\boldsymbol{p}$, and $\boldsymbol{\epsilon}$, $\boldsymbol{\sigma}$ should satisfy the compatibility condition of virtual work, $\boldsymbol{p} \cdot \boldsymbol{u} = \boldsymbol{\sigma} \cdot \boldsymbol{\epsilon}$. The development of plasticity effects is governed by the associative flow rule $(3.79)_5$ and complementarity conditions $(3.79)_6$ - $(3.79)_8$, in which the piecewise linear yield function $(3.79)_7$ is defined by (constant) matrix $\boldsymbol{N}$ collecting outward normal vectors to all segments of yield function $\boldsymbol{f}$ and linear hardening matrix $\boldsymbol{H}$, $\dot{\boldsymbol{\lambda}}$ is the rate of plastic multiplier $\boldsymbol{\lambda}$. The slackening (or unilateral contact) relations $(3.79)_9$ - $(3.79)_{12}$ have a similar structure. Vectors $\boldsymbol{k}$ and $\boldsymbol{l}$ contain values of the plastic and clearance moduli defined at the elemental level. It should be stressed that entries and dimensions of the above matrices depend on the space approximations applied.

### 3.2.2 Time discretization and the nLCP formulation

#### Time discretization method

The viscoelastic-plastic model proposed in the preceding section governs an evolutionary deformation process in which the dependence on time is two-fold. First, the viscoelastic part $\epsilon^{ve}$ is time-dependent, whereas for the plastic part, which is path-dependent, the time variable $t$ merely labels the succession of events. For the time integration of the viscoelastic part of strains we will use the method due to Świtka & Husiar [176], already applied for unilateral contact problems [79, 87, 88]. In the framework of nonlinear viscoelasticity [4], such a method is called the *creep approach*, other integration schemes are discussed in [196, 189, 161]. Now, by selecting instants $t_n$ on the time axis, i.e. $t_n \in \mathcal{R}_+$, we can divide it into a number of finite intervals $\vartheta_n \equiv t_n - t_{n-1} \subset \mathcal{R}_+$. In the sequel we indicate a function of $t$ at instant $t = t_n$ by a subscript $n$, e.g. $\epsilon_n \equiv \epsilon(t_n)$. In the method [176], the strain $\epsilon$ is solved from the differential equation (3.75) for a piecewise polynomial approximation of stress successively within each time interval, which leads to the following recurrent expressions

$$\epsilon_n^{ve} = \gamma_n \sigma_n + \tilde{\epsilon}_{n,n-1}, \qquad \dot{\epsilon}_n^{ve} = \dot{\gamma}_n \sigma_n + \dot{\tilde{\epsilon}}_{n,n-1}, \qquad n = 1, 2, \dots, \tag{3.80}$$

with

$$\begin{aligned} \tilde{\epsilon}_{n,n-1} &\equiv \boldsymbol{h}_n \cdot \boldsymbol{s}_{n-1}^{ve}, \qquad & \boldsymbol{h}_n &= \{h_{1n}, h_{2n}, h_{3n}, h_{4n}, h_{5n}, h_{6n}\}^{\mathrm{T}}, \\ \dot{\tilde{\epsilon}}_{n,n-1} &\equiv \dot{\boldsymbol{h}}_n \cdot \boldsymbol{s}_{n-1}^{ve}, \qquad & \dot{\boldsymbol{h}}_n &= \{\dot{h}_{1n}, \dot{h}_{2n}, \dot{h}_{3n}, \dot{h}_{4n}, \dot{h}_{5n}, \dot{h}_{6n}\}^{\mathrm{T}}. \end{aligned}$$

In the above relations, scalars $\gamma_n$, $\dot{\gamma}_n$ and vectors $\boldsymbol{h}_n, \dot{\boldsymbol{h}}_n$ depend upon the viscoelastic properties of a material and the degree of approximation (linear, or quadratic), whereas $\boldsymbol{s}_{n-1}$ is a vector which describes the state of the material at a previous instant, accounting only for the viscoelastic strain part,

$$\boldsymbol{s}_{n-1}^{ve} = \{\epsilon_{n-1}^{ve},\, \dot{\epsilon}_{n-1}^{ve},\, \sigma'_{n-1},\, \dot{\sigma}'_{n-1},\, \sigma_{n-1},\, \dot{\sigma}_{n-1}\}. \tag{3.81}$$

By ($'$) we denote in (3.81) and in the sequel the right-hand value of the relevant quantity, e.g. for stress $\sigma$ we have, $\sigma'_n = \sigma_n + \Delta\sigma_n$, where $\Delta$ is the symbol of a finite increment. The discontinuities which may appear in some state variables are induced by discontinuous changes in the external loading $\boldsymbol{p}(t)$ on the structure. At such time-discontinuity points $t_n$ we suppose an instantaneous elastoplastic material response, and consequently a finite increment of strain is defined as

$$\Delta\epsilon_n = \Delta\epsilon_n^l + \Delta\epsilon_n^{ve} + \Delta\epsilon_n^p, \qquad n = 0, 1, 2, \ldots\,, \tag{3.82}$$

$$\text{with} \qquad \Delta\epsilon_n^{ve} \equiv \Delta\epsilon_n^e = \gamma_0 \Delta\sigma_n, \qquad \Delta\dot{\epsilon}_n^{ve} = \gamma_0 \Delta\dot{\sigma}_n + \dot{\gamma}_0 \Delta\sigma_n. \tag{3.83}$$

The rate of stress depends on the degree of the polynomial approximation:

— the linear approximation: $\dot{\sigma}_n = \frac{1}{\vartheta_n}(\sigma_n - \sigma'_{n-1})$,

— the quadratic approximation: $\dot{\sigma}_n = \frac{2}{\vartheta_n}(\sigma_n - \sigma'_{n-1}) - \dot{\sigma}'_{n-1}$.

It should be remarked here that in the case when the linear approximation is used the increment of the velocity $\Delta\dot{\epsilon}_n^{ve}$ in $(3.83)_2$ need not to be determined, only $\Delta\epsilon_n^{ve}$ in $(3.83)_1$ is needed. Summing up, we want to point out that the increments of (3.82) can be determined by solving system (3.79), which now must be satisfied at the right-hand side of instant $t = t_n$.

Depending on the order of the time approximation applied and the character of time changes of loadings on the structure, we have to solve from one to three problems at the selected times $t = t_n$. These will be discussed in the sequel.

### Time-step $t_{n-1} \to t_n^-$

Because the system (3.79) is nonlinear it is necessary to approach it in an incremental way. A typical time-step $t_{n-1} \to t_n$ consists in updating the known state of the system at previous time level $t_{n-1}$ to the state at current time level $t_n$. Making use of the successive relation (3.80) we obtain the following updating formula for the viscoelastic strain vector

$$\boldsymbol{\epsilon}_n^{ve} = \boldsymbol{F}_n \boldsymbol{\sigma}_n + \tilde{\boldsymbol{\epsilon}}_{n,n-1} \tag{3.84}$$

in which $\boldsymbol{F}_n$ is a matrix that corresponds to the scalar $\gamma_n$ in (3.80) and plays a role similar to that of the flexibility matrix in elasticity, but here being updated from step to step. Associated with the scalar $\tilde{\epsilon}_{n,n-1}$ is the vector $\tilde{\boldsymbol{\epsilon}}_{n,n-1}$ by which the viscoelastic state of the system at the preceded instant is accounted for. At a time discontinuity point $t = t_n$, according to $(3.83)_2$ the following relation between the finite increments holds

$$\Delta \dot{\boldsymbol{\epsilon}}_n^{ve} = \boldsymbol{F}_0 \Delta \dot{\boldsymbol{\sigma}}_n + \dot{\boldsymbol{F}}_0 \Delta \boldsymbol{\sigma}_n. \tag{3.85}$$

The updating of the plastic strain and plastic multiplier vectors is defined in a usual way

$$\begin{aligned} \boldsymbol{\lambda}_n &= \boldsymbol{\lambda}_{n-1} + \Delta \boldsymbol{\lambda}_n, \\ \boldsymbol{\epsilon}_n^p &= \boldsymbol{\epsilon}_{n-1}^p + \Delta \boldsymbol{\epsilon}_n^p. \end{aligned} \tag{3.86}$$

At any two successive time levels we may express the relations (3.79) in the following incremental form.

$$\begin{array}{rrcl|rcl}
 & \multicolumn{3}{c}{\text{TIME LEVEL } t = t_{n-1}} & \multicolumn{3}{c}{\text{TIME LEVEL } t = t_n} \\
1) & \boldsymbol{\epsilon}_{n-1} & = & \boldsymbol{C}\,\boldsymbol{u}_{n-1}, & \boldsymbol{\epsilon}_n & = & \boldsymbol{C}\,\boldsymbol{u}_n, \\
2) & \boldsymbol{p}_{n-1} & = & \boldsymbol{C}^{\mathrm{T}} \boldsymbol{\sigma}_{n-1}, & \boldsymbol{p}_n & = & \boldsymbol{C}^{\mathrm{T}} \boldsymbol{\sigma}_n, \\
3) & \boldsymbol{\epsilon}_{n-1} & = & \boldsymbol{\epsilon}_{n-1}^l + \boldsymbol{\epsilon}_{n-1}^{ve} + \boldsymbol{\epsilon}_{n-1}^p, & \boldsymbol{\epsilon}_n & = & \boldsymbol{\epsilon}_n^l + \boldsymbol{\epsilon}_n^{ve} + \boldsymbol{\epsilon}_n^p, \\
4) & \boldsymbol{\epsilon}_{n-1}^{ve} & = & \boldsymbol{F}_{n-1} \boldsymbol{\sigma}_{n-1} + \tilde{\boldsymbol{\epsilon}}_{n-1,n-2}, & \boldsymbol{\epsilon}_n^{ve} & = & \boldsymbol{F}_n \boldsymbol{\sigma}_n + \tilde{\boldsymbol{\epsilon}}_{n,n-1}, \\
5) & \Delta \boldsymbol{\epsilon}_{n-1}^p & = & \boldsymbol{N}\,\Delta \boldsymbol{\lambda}_{n-1}, & \Delta \boldsymbol{\epsilon}_n^p & = & \boldsymbol{N}\,\Delta \boldsymbol{\lambda}_n, \\
6) & \Delta \boldsymbol{\lambda}_{n-1} & \geq & \mathbf{0}, & \Delta \boldsymbol{\lambda}_n & \geq & \mathbf{0}, \\
7) & \boldsymbol{f}_{n-1} & = & \boldsymbol{N}^{\mathrm{T}} \boldsymbol{\sigma}_{n-1} - \boldsymbol{H} \boldsymbol{\lambda}_{n-1} - \boldsymbol{k} & \boldsymbol{f}_n & = & \boldsymbol{N}^{\mathrm{T}} \boldsymbol{\sigma}_n - \boldsymbol{H}(\boldsymbol{\lambda}_{n-1} + \Delta \boldsymbol{\lambda}_n) - \boldsymbol{k} \\
 & & \leq & \mathbf{0}, & & \leq & \mathbf{0}, \\
8) & 0 & = & \Delta \boldsymbol{\lambda}_{n-1} \cdot \boldsymbol{f}_{n-1}, & 0 & = & \Delta \boldsymbol{\lambda}_n \cdot \boldsymbol{f}_n, \\
9) & \boldsymbol{\sigma}_{n-1} & = & \boldsymbol{M} \boldsymbol{\psi}_{n-1}, & \boldsymbol{\sigma}_n & = & \boldsymbol{M} \boldsymbol{\psi}_n, \\
10) & \boldsymbol{\psi}_{n-1} & \geq & \mathbf{0} & \boldsymbol{\psi}_n & \geq & \mathbf{0}, \\
11) & \boldsymbol{g}_{n-1} & = & \boldsymbol{M}^{\mathrm{T}} \boldsymbol{\epsilon}_{n-1}^l - \boldsymbol{l} \leq \mathbf{0}, & \boldsymbol{g}_n & = & \boldsymbol{M}^{\mathrm{T}} \boldsymbol{\epsilon}_n^l - \boldsymbol{l} \leq \mathbf{0}, \\
12) & 0 & = & \boldsymbol{\psi}_{n-1} \cdot \boldsymbol{g}_{n-1}, & 0 & = & \boldsymbol{\psi}_n \cdot \boldsymbol{g}_n.
\end{array} \tag{3.87}$$

By substituting the stress from $(3.87)_9$ into $(3.87)_2$ and $(3.87)_7$, and making use of the split $(3.87)_3$, for $t = t_n$, we can reduce (3.87) to the conditions

$$\begin{aligned} \boldsymbol{C}^{\mathrm{T}} \boldsymbol{M} \boldsymbol{\psi}_n - \boldsymbol{p}_n &= \mathbf{0}, \\ \boldsymbol{H} \Delta \boldsymbol{\lambda}_n - \boldsymbol{N}^{\mathrm{T}} \boldsymbol{M} \boldsymbol{\psi}_n + \boldsymbol{k} + \boldsymbol{H} \boldsymbol{\lambda}_{n-1} &\geq \mathbf{0}, \\ \boldsymbol{M}^{\mathrm{T}} \boldsymbol{N} \Delta \boldsymbol{\lambda}_n - \boldsymbol{M}^{\mathrm{T}} \boldsymbol{C} \boldsymbol{u}_n + \boldsymbol{M}^{\mathrm{T}} \boldsymbol{F}_n \boldsymbol{M} \boldsymbol{\psi}_n + \boldsymbol{M}^{\mathrm{T}} \tilde{\boldsymbol{\epsilon}}_{n,n-1} + \boldsymbol{l} + \boldsymbol{M}^{\mathrm{T}} \boldsymbol{\epsilon}_{n-1}^p &\geq \mathbf{0}, \end{aligned} \tag{3.88}$$

with the side conditions

$$\Delta\boldsymbol{\lambda}_n \geq \mathbf{0}, \quad \boldsymbol{\psi}_n \geq \mathbf{0} \quad \text{and} \quad \Delta\boldsymbol{\lambda}_n \cdot \boldsymbol{f}_n = 0, \quad \boldsymbol{\psi}_n \cdot \boldsymbol{g}_n = 0. \tag{3.89}$$

The two unknown vectors of (3.88), $\Delta\boldsymbol{\lambda}_n$ and $\boldsymbol{\psi}_n$, should satisfy the non-negativity condition, cf. (3.89), and the orthogonality condition with respect to the conjugate variable, $(3.88)_2$ and $(3.88)_3$, respectively.

We can formulate the incremental problem under consideration (3.88) as the following nested linear complementarity problem (nLCP)— *Problem I*:

$$\boxed{\begin{array}{c} \bar{\boldsymbol{A}}_n \boldsymbol{x}_n + \boldsymbol{y}_n = \boldsymbol{b}_{n,n-1}, \\ \boldsymbol{x}_{2,n} \geq \mathbf{0}, \quad \boldsymbol{x}_{3,n} \geq \mathbf{0}, \quad \boldsymbol{y}_{1,n} = \mathbf{0}, \quad \boldsymbol{y}_{2,n} \geq \mathbf{0}, \quad \boldsymbol{y}_{3,n} \geq \mathbf{0}, \quad \boldsymbol{x}_n \cdot \boldsymbol{y}_n = 0, \end{array}} \tag{3.90}$$

where the following notations are used:

$$\bar{\boldsymbol{A}}_n = \begin{bmatrix} \mathbf{0} & \mathbf{0} & -\boldsymbol{C}^{\mathrm{T}}\boldsymbol{M} \\ \mathbf{0} & -\boldsymbol{H} & \boldsymbol{N}^{\mathrm{T}}\boldsymbol{M} \\ \boldsymbol{M}^{\mathrm{T}}\boldsymbol{C} & -\boldsymbol{M}^{\mathrm{T}}\boldsymbol{N} & -\boldsymbol{M}^{\mathrm{T}}\boldsymbol{F}_n\boldsymbol{M} \end{bmatrix},$$

$$\boldsymbol{x}_n = \left\{ \begin{array}{c} \boldsymbol{u}_n \\ \Delta\boldsymbol{\lambda}_n \\ \boldsymbol{\psi}_n \end{array} \right\}, \qquad \boldsymbol{b}_{n,n-1} = \left\{ \begin{array}{c} -\boldsymbol{p}_n \\ \boldsymbol{k}_{n-1} \\ \tilde{\boldsymbol{l}}_{n,n-1} \end{array} \right\},$$

given $\boldsymbol{p}_n$, $\boldsymbol{k}_{n-1} = \boldsymbol{k} + \boldsymbol{H}\boldsymbol{\lambda}_{n-1}$, $\tilde{\boldsymbol{l}}_{n,n-1} = \boldsymbol{l} + \boldsymbol{M}^{\mathrm{T}}(\tilde{\boldsymbol{\epsilon}}_{n,n-1} + \boldsymbol{\epsilon}^p_{n-1})$.

### Step $t_n^- \to t_n^+$ at a time discontinuity point $t = t_n$

At these times $t_n$ at which the load vector suffers a jump discontinuity in time, i.e. $\Delta\boldsymbol{p}_n \neq \mathbf{0}$, we have to determine the state of the system at the right-hand side of $t_n$, i.e. at $t = t_n^+ \equiv t_n + 0$. This leads to a problem II defined below which must be solved in addition to Problem I in the case of both the linear and quadratic time approximations.

The state of the structural system at the time-discontinuity point $t = t_n$ is defined by the following relations.

$$
\begin{array}{rrclrcl}
 & \multicolumn{3}{c}{\textsc{Time level } t = t_n - 0} & \multicolumn{3}{c}{\textsc{Time level } t = t_n + 0} \\
1) & \boldsymbol{\epsilon}_n & = & \boldsymbol{C}\,\boldsymbol{u}_n, & \boldsymbol{\epsilon}'_n & = & \boldsymbol{C}\,\boldsymbol{u}'_n, \\
2) & \boldsymbol{p}_n & = & \boldsymbol{C}^{\mathrm{T}}\boldsymbol{\sigma}_n, & \boldsymbol{p}'_n & = & \boldsymbol{C}^{\mathrm{T}}\boldsymbol{\sigma}'_n, \\
3) & \boldsymbol{\epsilon}_n & = & \boldsymbol{\epsilon}^l_n + \boldsymbol{\epsilon}^{ve}_n + \boldsymbol{\epsilon}^p_n, & \boldsymbol{\epsilon}'_n & = & \boldsymbol{\epsilon}^{l\prime}_n + (\boldsymbol{\epsilon}^{ve}_n + \Delta\boldsymbol{\epsilon}^{ve}_n) \\
 & & & & & & +(\boldsymbol{\epsilon}^p_n + \Delta\boldsymbol{\epsilon}^{p\prime}_n), \\
4) & \boldsymbol{\epsilon}^{ve}_n & = & \boldsymbol{F}_n\boldsymbol{\sigma}_n + \tilde{\boldsymbol{\epsilon}}_{n,n-1}, & \Delta\boldsymbol{\epsilon}^{ve}_n & = & \boldsymbol{F}_0\,\Delta\boldsymbol{\sigma}_n, \\
5) & \Delta\boldsymbol{\epsilon}^p_n & = & \boldsymbol{N}\,\Delta\boldsymbol{\lambda}_n, & \Delta\boldsymbol{\epsilon}^{p\prime}_n & = & \boldsymbol{N}\,\Delta\boldsymbol{\lambda}'_n, \\
6) & \Delta\boldsymbol{\lambda}_n & \geq & \boldsymbol{0}, & \Delta\boldsymbol{\lambda}'_n & \geq & \boldsymbol{0}, \\
7) & \boldsymbol{f}_n & = & \boldsymbol{N}^{\mathrm{T}}\boldsymbol{\sigma}_n - \boldsymbol{H}\boldsymbol{\lambda}_n - \boldsymbol{k} & \boldsymbol{f}'_n & = & \boldsymbol{N}^{\mathrm{T}}\boldsymbol{\sigma}'_n - \boldsymbol{H}(\boldsymbol{\lambda}_n + \Delta\boldsymbol{\lambda}'_n) - \boldsymbol{k} \\
 & & \leq & \boldsymbol{0}, & & \leq & \boldsymbol{0}, \\
8) & 0 & = & (\Delta\boldsymbol{\lambda}_n)\cdot\boldsymbol{f}_n, & 0 & = & \left(\Delta\boldsymbol{\lambda}'_n\right)\cdot\boldsymbol{f}'_n, \\
9) & \boldsymbol{\sigma}_n & = & \boldsymbol{M}\boldsymbol{\psi}_n, & \boldsymbol{\sigma}'_n & = & \boldsymbol{M}\boldsymbol{\psi}'_n, \\
10) & \boldsymbol{\psi}_n & \geq & \boldsymbol{0} & \boldsymbol{\psi}'_n & \geq & \boldsymbol{0}, \\
11) & \boldsymbol{g}_n & = & \boldsymbol{M}^{\mathrm{T}}\boldsymbol{\epsilon}^l_n - \boldsymbol{l} \leq \boldsymbol{0}, & \boldsymbol{g}'_n & = & \boldsymbol{M}^{\mathrm{T}}\boldsymbol{\epsilon}^{l\prime}_n - \boldsymbol{l} \leq \boldsymbol{0}, \\
12) & 0 & = & (\boldsymbol{\psi}_n)\cdot\boldsymbol{g}_n, & 0 & = & \left(\boldsymbol{\psi}'_n\right)\cdot\boldsymbol{g}'_n.
\end{array}
\tag{3.91}
$$

The linear complementarity problem associated with (3.91) has a form analogous to the prior nLCP and is stated as the following *Problem II*:

$$
\boxed{
\begin{array}{c}
\bar{\boldsymbol{A}}_0\boldsymbol{x}'_n + \boldsymbol{y}'_n \;=\; \boldsymbol{b}'_{n,n-1}, \\
\boldsymbol{x}'_{2,n} \geq \boldsymbol{0}, \quad \boldsymbol{x}'_{3,n} \geq \boldsymbol{0}, \quad \boldsymbol{y}'_{1,n} = \boldsymbol{0}, \quad \boldsymbol{y}'_{2,n} \geq \boldsymbol{0}, \quad \boldsymbol{y}'_{3,n} \geq \boldsymbol{0}, \quad (\boldsymbol{x}'_n)\cdot\boldsymbol{y}'_n = 0,
\end{array}
}
\tag{3.92}
$$

where

$$\bar{\boldsymbol{A}}_0 = \begin{bmatrix} \mathbf{0} & \mathbf{0} & -\boldsymbol{C}^{\mathrm{T}}\boldsymbol{M} \\ \mathbf{0} & -\boldsymbol{H} & \boldsymbol{N}^{\mathrm{T}}\boldsymbol{M} \\ \boldsymbol{M}^{\mathrm{T}}\boldsymbol{C} & -\boldsymbol{M}^{\mathrm{T}}\boldsymbol{N} & -\boldsymbol{M}^{\mathrm{T}}\boldsymbol{F}_0\boldsymbol{M} \end{bmatrix},$$

$$\boldsymbol{x}'_n = \begin{Bmatrix} \boldsymbol{u}'_n \\ \Delta\boldsymbol{\lambda}'_n \\ \boldsymbol{\psi}'_n \end{Bmatrix}, \quad \boldsymbol{b}'_{n,n-1} = \begin{Bmatrix} -\boldsymbol{p}'_n \\ \boldsymbol{k}_n \\ \tilde{\boldsymbol{l}}'_{n,n-1} \end{Bmatrix},$$

given $\boldsymbol{p}'_n$, $\boldsymbol{k}_n = \boldsymbol{k} + \boldsymbol{H}\boldsymbol{\lambda}_n$, $\tilde{\boldsymbol{l}}'_{n,n-1} = \boldsymbol{l} + \boldsymbol{M}^{\mathrm{T}}(\tilde{\boldsymbol{\epsilon}}_{n,n-1} + \boldsymbol{\epsilon}^p_n) + \boldsymbol{M}^{\mathrm{T}}(\boldsymbol{F}_n - \boldsymbol{F}_0)\boldsymbol{M}\boldsymbol{\psi}_n$.

In this way, the original continuous-in-time problem (3.79) has been transformed into a series of linear complementarity problems (3.90) and (3.92), which describe completely the considered unilateral viscoelastic-plastic contact problem at time $t_n$. In fact, the incremental procedure we have advanced allows us to analyze quite a complex, also non-proportional loading programme of the slackened system in which, within a typical time step, plastic strains are assumed holonomic whilst stresses are approximated with a linear or quadratic polynomial. At all times $t_n$ at which the external load on the system is time-continuous it is sufficient to solve the nLCP (3.90), but otherwise the nLCP (3.92) must be solved additionally afterwards using the known vector $\boldsymbol{x}_n$, the solution of Problem I.

For the solution of the nested linear complementarity problems we have devised a principle pivoting scheme, see Section 2.3. In reference to Lemma 2.10 we want to stress that in the derived LCP (3.90) and (3.92) the properties of the matrix $\bar{\boldsymbol{A}}_n,\ n = 0, 1, 2, \ldots$ depend on both the kinematical and physical properties of the structural system. Firstly, the matrix $-\bar{\boldsymbol{A}}_n \equiv \boldsymbol{A}_n$ is positive semi-definite if the matrices $\boldsymbol{H}$ and $\boldsymbol{M}^{\mathrm{T}}\boldsymbol{F}_n\boldsymbol{M}$ are positive semi-definite. This requirement is satisfied in the case of the used Prager's plastic hardening rule and the convexity of the yield and clearance regions, together with the non-negative hardening modulus $H'(\boldsymbol{x}) \geq 0$ and viscoelastic parameter $\gamma_n(\boldsymbol{x}) \geq 0$ for all points of the system. Secondly, the existence and uniqueness of a solution to our problem depends also on the data $\boldsymbol{b}_{n,n-1}$ which contain information on the applied loading and changes in the physical (plastic strain hardening) and kinematical properties of the structural system in the course of the deformation process. It is clear that the development of plastic strains (hinges) may convert the initially stable structure made of a viscoelastic- perfectly plastic material into a structural mechanism unable to sustain any additional loading.

When using the quadratic polynomial time approximation we need the rate of stress $\dot{\boldsymbol{\sigma}}_n'$ at the right-hand side of the time $t_n$ at which there is a jump in the external load, $\Delta \boldsymbol{p}_n \neq \mathbf{0}$ or/and in its speed $\Delta \dot{\boldsymbol{p}}_n \neq \mathbf{0}$. To this end, an additional *Problem III* must be considered. First, an increment $\Delta \dot{\boldsymbol{u}}_n$ is determined from the equation — *Problem IIIa*:

$$\tilde{\boldsymbol{K}}_0 \, \Delta \dot{\boldsymbol{u}}_n = \Delta \dot{\boldsymbol{p}}_n + \tilde{\boldsymbol{C}}^{\mathrm{T}} \tilde{\boldsymbol{F}}_0^{-1} \dot{\tilde{\boldsymbol{F}}}_0 \, \Delta \tilde{\boldsymbol{\sigma}}_n \tag{3.93}$$

where

$$\tilde{\boldsymbol{K}}_0 = \tilde{\boldsymbol{C}}^{\mathrm{T}} \tilde{\boldsymbol{F}}_0^{-1} \tilde{\boldsymbol{C}}$$

is the stiffness matrix of the structural subsystem, containing only the contributions of these elements of the foundation which are in contact with the structure. With the superscript $\tilde{}$ we denote here the restriction to this subsystem. The boundary conditions on $\Delta \dot{\boldsymbol{u}}_n$ can easily be derived from those imposed on the displacement vector $\boldsymbol{u}_n$. In deriving (3.93) we made use of (3.85) and the equation — *Problem IIIb*:

$$\tilde{\boldsymbol{C}}^{\mathrm{T}} \, \Delta \dot{\tilde{\boldsymbol{\sigma}}}_n = \Delta \dot{\boldsymbol{p}}_n. \tag{3.94}$$

Having determined $\Delta \dot{\boldsymbol{u}}_n$ we can calculate

$$\begin{aligned} \Delta \dot{\tilde{\boldsymbol{\epsilon}}}_n^{ve} &= \tilde{\boldsymbol{C}} \, \Delta \dot{\boldsymbol{u}}_n, \\ \Delta \dot{\tilde{\boldsymbol{\sigma}}}_n &= \tilde{\boldsymbol{F}}_0^{-1} \, \Delta \dot{\tilde{\boldsymbol{\epsilon}}}_n^{ve} - \tilde{\boldsymbol{F}}_0^{-1} \dot{\tilde{\boldsymbol{F}}}_0 \Delta \, \tilde{\boldsymbol{\sigma}}_n, \end{aligned}$$

and finally

$$\dot{\boldsymbol{\sigma}}_n' = \dot{\boldsymbol{\sigma}}_n + \Delta \dot{\boldsymbol{\sigma}}_n. \tag{3.95}$$

The equation (3.93) is valid provided that the matrix $\tilde{\boldsymbol{K}}_0$ is non-singular, which depends both on the matrix $\tilde{\boldsymbol{C}}$ and the matrix $\tilde{\boldsymbol{F}}_0$. Of course, when the matrix $\tilde{\boldsymbol{F}}_0$ is equal to zero, then $\tilde{\boldsymbol{K}}_0$ is singular. This is the case with any viscoelastic model for which the coefficient $\gamma_0 = 0$, in particular with the Kelvin-Voigt model. (In reference to the constitutive equation (3.75) we recall that $\gamma_0$ is defined as follows: $\gamma_0 = a_1/b_1$, if $b_1 \neq 0, b_2 = 0$, and $\gamma_0 = a_2/b_2$ if $b_2 \neq 0$.) In the situation $\tilde{\boldsymbol{F}}_0 = \mathbf{0}$ it is sufficient to satisfy equation (3.94). However, it should be noted that the system of equations (3.94), in which $\tilde{\boldsymbol{C}}^{\mathrm{T}}$ is a $M \times N$ rectangular matrix with $M > N$, may not possess a solution and if any, the solution may be non-unique. Following the idea presented in [46] we can show that there exists a unique solution to (3.94) if rank $\tilde{\boldsymbol{C}}^{\mathrm{T}} = N$ and the structural subsystem whose elements contribute to the matrix $\tilde{\boldsymbol{C}}$ is statically determinate. The requirement on the rank of $\tilde{\boldsymbol{C}}^{\mathrm{T}}$, i.e. rank $\tilde{\boldsymbol{C}}^{\mathrm{T}} = N$ is equivalent to the following condition that det $\tilde{\boldsymbol{C}}\tilde{\boldsymbol{C}}^{\mathrm{T}} \neq 0$.

In the next section we shall discuss the numerical results on examples of practical importance in engineering.

### 3.2.3 Numerical examples

This section contain the numerical results which we have obtained with our material model for some typical engineering test problems. From the four examples considered [81], we present here Examples 1 and 4. We start with the bending problem of a simply supported beam made of different viscoelastic materials. The main purpose of Example 1 is to test the convergence rate of the piecewise linear approximation for the prescribed piecewise quadratic history of loading. Notice that in Example 1 it suffices to divide the beam into only two finite elements in order to get numerical results which are exact as concerns both the statics and kinematics of the problem. More specifically, the description of the kinematics with only a few elements, the number of which is determined by the number of forces applied and supports of the beam, is exact under the assumption that the lumped plastic hinges may appear in the cross-sections where the forces are applied. The latter is true for a beam with ideal I–cross-section and if the material of the beam is perfectly plastic. In other cases, where the plastic hardening modulus $H'$ is positive and/or the beam may come in contact with a foundation, the finite element discretization of the beam must be finer. As checked numerically, the used time integration scheme and numerical algorithm exhibit a good convergence rate even in the case of complex boundary conditions and loading histories, Example 2 in [81], and is capable to solve the difficult interaction problem, cf. [25], for a freely resting structure on a unilateral foundation Example 3 in [81]. A different numerical procedure for similar problems is proposed in [44].

**Example 1**
As the first example we consider a simply supported beam, shown in Fig. 2, made of different viscoelastic materials and loaded with the point force $P = P(t)$ whose time evolution is depicted in Fig. 2a. We assumed the following material parameters $E_1 = E_2 = E = 2.0 \cdot 10^5$ MPa, $\eta_1 = \eta_2 = \eta = 4.0 \cdot 10^5$ MPa$\cdot$ hr, which are used in the governing differential equations of the following viscoelastic models [164], for the standard model see (3.76):
— the Maxwell model

$$\frac{1}{\eta}\sigma + \frac{1}{E}\,\dot{\sigma} = \dot{\epsilon}^{ve},$$

— the Kelvin-Voigt model

$$\sigma = E\,\epsilon^{ve} + \eta\,\dot{\epsilon}^{ve},$$

— the Burgers model

$$\sigma + \left(\frac{\eta_1}{E_1} + \frac{\eta_1}{E_2} + \frac{\eta_2}{E_2}\right)\dot{\sigma} + \frac{\eta_1\eta_2}{E_1E_2}\,\ddot{\sigma} = \eta_1\dot{\epsilon}^{ve} + \frac{\eta_1\eta_2}{E_2}\,\ddot{\epsilon}^{ve}.$$

Figure 2b shows the time evolution of the deflection of the midspan point for the different viscoelastic material models when the load $P$ varies piecewise linearly with a jump at $t = 4.00$ hr. Note that in this case the piecewise linear time approximation furnishes the exact solution for any time step $\vartheta_\tau \leq 4.00$ hr, in particular in order to determine the states at $t = 4.00$ and $t = 8.00$ it suffices to take $\vartheta_1 = \vartheta_2 = 4.00$, and then we just solve Problem I at times $4.00, 8.00$ and Problem II at $t = 4.00$. The same results we can obtain by employing the piecewise quadratic time approximation, but now at times $t = 0.00$ and $t = 4.00$ we have to additionally solve Problem III. However, if the evolution of $P$ is piecewise quadratic, then the other time approximation furnishes the exact solution to the whole deformation process which is illustrated in Fig. 2c for the characteristic midspan deflection. In other words, with the piecewise quadratic approximation we can determine exactly the state of the beam at $t = 4.00$ and $t = 8.00$ by taking $\vartheta_1 = \vartheta_2 = 4.00$ and solving Problem I at these times and Problems II and III at $t = 4.00$. Moreover, it is interesting to remark that the deflection $u(t)$ is a non-monotone function for times $t > 4.00$ while the evolution of the load is monotone. This effect is even more pronounced in case of the quadratic load history.

Fig. 3 shows the convergence results of the midspan deflection of the beam for the piecewise linear approximation of the quadratic evolution of loading $P(t)$. The time step $\vartheta_i$ is varying (but being constant along the time interval [0.00,8.00]) from $\vartheta_0 = \bar{\vartheta} = 4.00$ hr to $\vartheta_5 = 0.125$ hr by the formula $\vartheta_i = \bar{\vartheta}/2^i$ with $i = 0, 1, \ldots, 5$. (On the abscissa of Fig. 3 the locations of $\log \vartheta_i$ are marked merely with the coefficients $1/2^i$.) As can be seen the piecewise linear variant of the time integration method exhibits a very good convergence rate, since the error is from about 0.6 % for the standard model to 2 % for the Kelvin-Voigt model at $t = 4.00^-$, when the basic time step is divided into only four steps, i.e. $\vartheta_i = \bar{\vartheta}/4 = 1.00$ hr. Due to the particular changes of load $P(t)$ the errors at $t = 8.00$ are even smaller.

**Example 2**

In the present example 2 (example 4 of [81]) the material response of the beam is assumed to be elastic-perfectly plastic with plastic hinges lumped at nodes. The foundation is treated as the viscoelastic-plastic medium of Winkler-type. The beam is discretized with the two-node four-parameter cubic elements and the foundation is modeled with the truss elements located at the beam nodes. The material of the beam is characterized by the Young modulus $E = 2.0 \cdot 10^5$ MPa, $H' = 0.0$, inertia moment of the cross-section $I = 10^{-4}$ m$^4$, yield moment $M_Y = 0.16$ MNm. The viscoelastic response of the foundation is described by the standard three-parameter solid, Fig. 1. We have assumed the following material parameters: $E_1 = 60.0$ MPa/m, $E_2 = 30.0$ MPa/m,

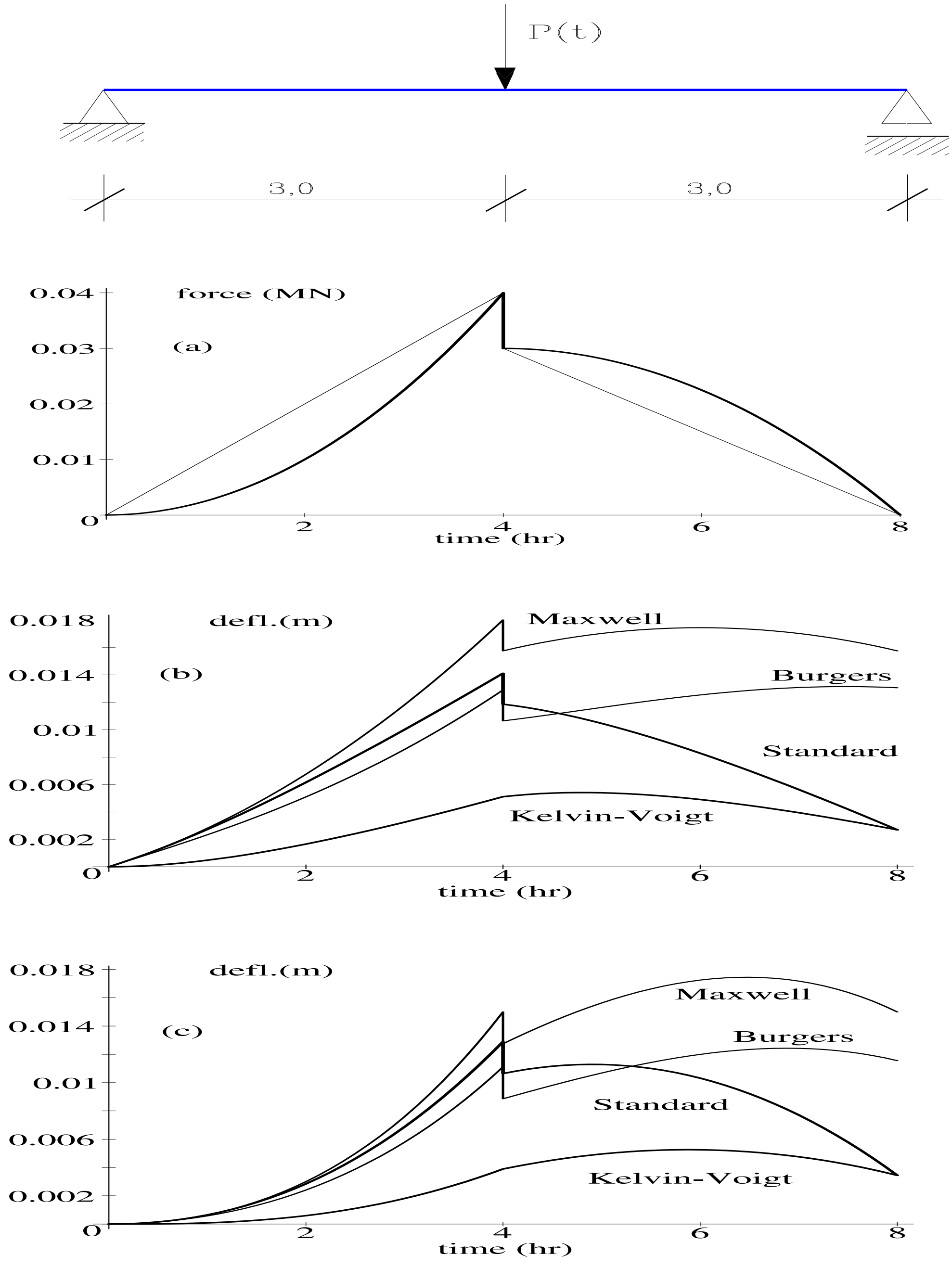


Figure 2: Example 1. Simply supported beam subjected to force $P(t)$. (a) Piecewise linear (thin line) and piecewise quadratic (thick line) history of $P$; Deflections of the midspan of the beam for various viscoelastic models under the piecewise linear (b), and piecewise quadratic (c) evolution of $P$

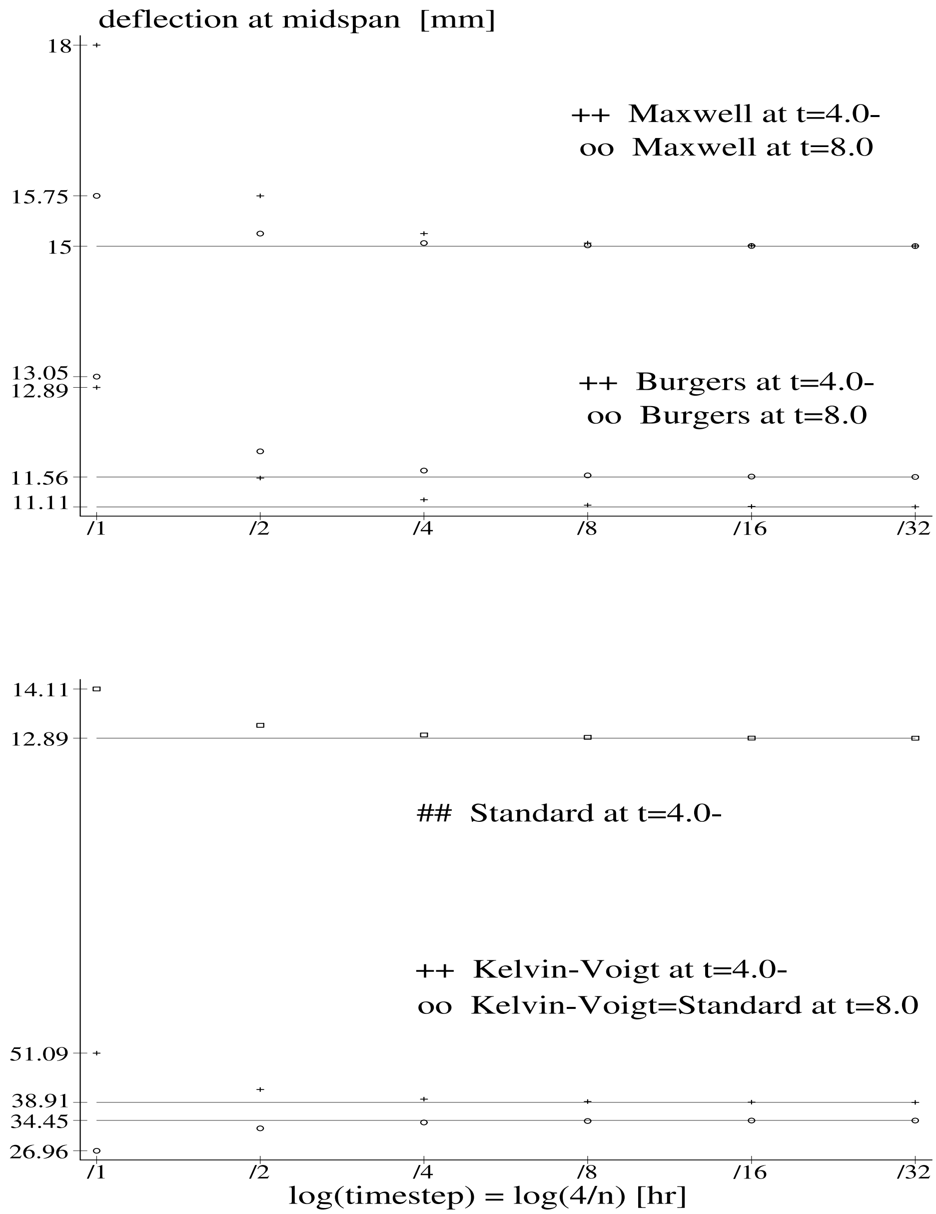


Figure 3: Example 1. Results of the convergence test of the piecewise linear approximation of the piecewise quadratic history of loading, for various viscoelastic models

$\eta_2 = 10^3$ MPa·hr (hour), $H' = 10.0$ MPa/m, $\sigma_Y = 0.15$ MPa/m. For the purposes of the numerical examples presented here the values of the material parameters of the viscoelastic-plastic models are chosen to represent properties of a generic material (different for the beam and for the foundation) rather than a specific material. The gap between the beam and the foundation is modelled as clearance strains with the modulus $l^+$ equally distributed under the beam ($l^-$ is assumed to be a sufficiently great number). We have analyzed a two-span fixed-ended beam shown in Fig. 4. The moduli of the clearance strains at the supports are equal, $l^+ = l^- = 0.01$ rad. The beam of 12 meters in length was divided into 120 finite elements. In the calculations the piecewise linear time approximation method was applied with constant time step $\vartheta_n = 1.0$ hr. The gap between the beam and its foundation is $l^+ = 0.005$ m. The beam is subjected to two point loads $P_1$ and $P_2$ whose variation in time is shown in Fig. 4a. The load $P_1$ has a jump of 0.10 MN at time $t = 8.00$ hr, and at time $t = 32.00$ hr both forces $P_1$ and $P_2$ are quickly removed (another jump) from the beam. Note that at times $t = 8.00^-$ (i.e. on the left-hand side of that instant), $t = 16.00$, and $t = 32.00^-$ the load levels are equal, i.e. $P_1 = 0.25$ MN, $P_2 = 0.15$ MN. The results for the beam without clearances at the supports are shown in Figs. 4b, c, d, e at time $t = 8.00$ hr where the force $P_1$ is suddenly increased from 0.25 MN to 0.35 MN. We can see that at $t = 8.00^-$ the displacement $u$ is a smooth function, the bending moment does not reach its limit value of $M_Y = 0.16$ MNm, and the contact appears for $x \in (1.6, 4.5) \cup (8.1, 10.0)$, with the plastic stress of $\sigma_Y = 0.15$ MPa being reached in the foundation in the region $x \in (2.3, 3.8)$. The situation is drastically changed after the load increase from 0.25 MN which induces plastic hinges in the beam, at the left support, $x = 0.00$ m, and at $x = 3.00$ m where $P_1$ is applied. The contact pressure spreads over a larger area under the first span of the beam, whilst it shrinks under the second one.

Fig. 5 shows the states of the beam/foundation system at time $t = 32.00$ hr at which the external load is instantaneously removed from the beam. Owing to the previous plastic deformation of the beam at its supports and beneath forces $P_1$ and $P_2$, there are some residual deformations in the beam, see Fig. 5a, which are accompanied by the residual bending moments, Fig. 5d.

At $t = 32.00^+$ the foundation exhibits both permanent deformations, thick line in Fig. 5b and some viscoelastic ones which will eventually disappear in the case of the tree-parameter solid model we used. That the history of the deformation process plays a great role is again demonstrated in Fig. 5c, where the distributions of the foundation pressure at the same load level, $P_1 = 0.25$ MN, $P_2 = 0.15$ MN, but at different times can be compared. Note that under the first span of the beam the pressure is nearly equally distributed at time

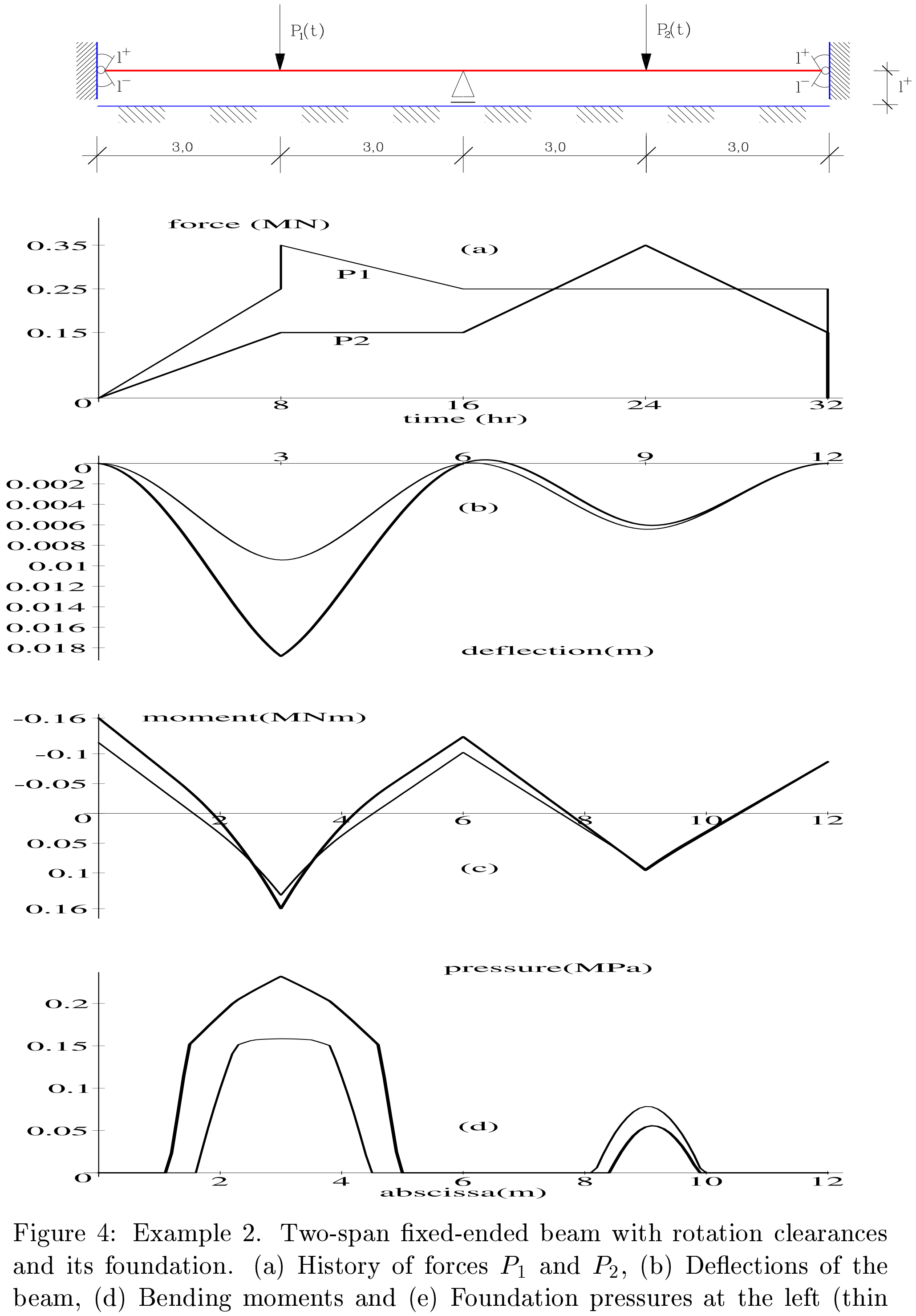


Figure 4: Example 2. Two-span fixed-ended beam with rotation clearances and its foundation. (a) History of forces $P_1$ and $P_2$, (b) Deflections of the beam, (d) Bending moments and (e) Foundation pressures at the left (thin line) and the right (thick line) hand-side of instant $t = 8.00$ hr, for the beam without clearances at the supports, $l^- = l^+ = 0$

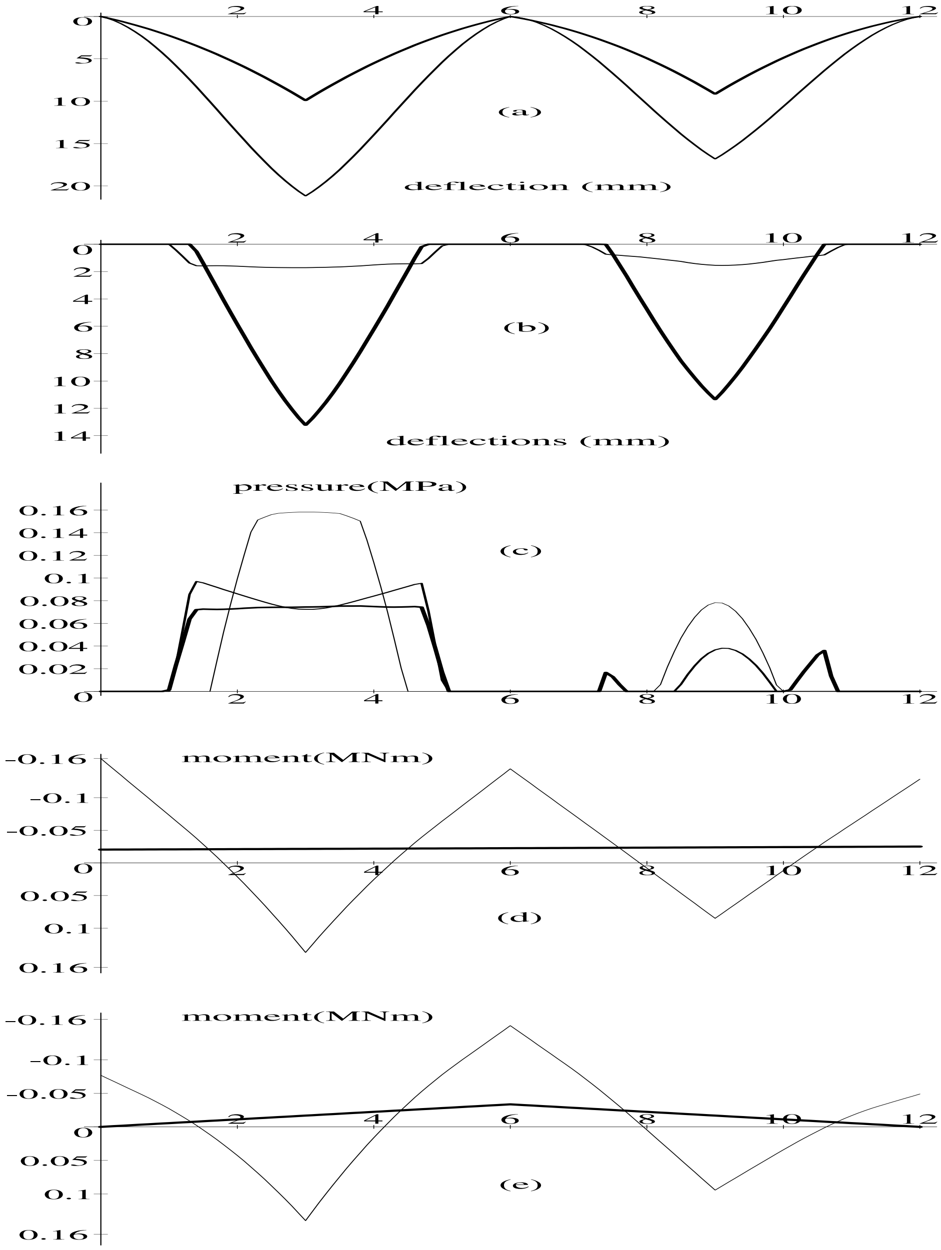


Figure 5: Example 2 cntd. (a) Deflections of the beam at $t = 32.00^-$ (thin line), $t = 32.00^+$ (thick line). (b) Viscoelastic displacements (thin line) and plastic displacements of the foundation (thick line) at $t = 32.00^+$ hr. (c) Distribution of foundation pressure for the same level of loads at different times: $t = 8.00^-$ hr (thin line), $t = 16.00$ hr (medium line), $t = 32.00^-$ (thick line). Distribution of bending moments at $t = 32.00^-$ (thin line), $t = 32.00^+$ (thick line), for the beam without (d) and with (e) clearances at the supports

$t = 32.00^-$. The residual moment in the beam with clearances is different from that without clearances, compare case (d) and (c) in Fig. 5.

## 3.3 Concluding remarks

The main idea behind the variational inequality approach developed in Section 3.1 is a weak form expression of the loading/unloading criteria which, as has been shown, are equivalent to a variational inequality. The existence of unique, stable solutions to the associated incremental boundary value problem is established, under the commonly taken hypotheses. From the computational viewpoint the advantage of the VI formulation is in satisfying the consistency condition as well as loading/unloading conditions automatically, and what is equally important not only pointwise at the Gauss points (see e.g. [163]) but in a weak sense for the body $\Omega$ as a whole. In the presented formulation the Huber – von Mises yield function has been employed, but this approach can be applied also to other yield criteria, e.g. non-associative plasticity or to multi-surface non-smooth plasticity as presented in [89]. It is quite easy to directly extend this formulation to gradient dependent plasticity [120] where higher-order spatial gradients of the plastic multiplier $\lambda$ are included. The proof of Lemma 3.4 shows that the associated operator $A$ will remain strongly monotone even if the requirements on the function $\kappa(\lambda)$ are weakened, provided one replaces the latter by $\kappa[\lambda] = \kappa(\lambda)+$ gradient terms (cf. Eqns. (4) and (9) in [120]).

A new material model accounting for slackening, viscous and plastic effects is suggested. The model formulated in the computer-oriented format of structural mechanics. The results of many numerical experiments indicate that in the viscoelastic-plastic structural system subjected to variable loads some complex evolution processes are taking place, including unloading, reloading and redistribution of stresses due to plastic effects, creep and stress relaxation, and clearances. The simple case of residual stresses in Fig. 5 is just a signal of the complex situation in rails, e.g. cf. Orkisz [136]. But, as defined here, our model describes only very roughly the surface phenomena. For a better description of the complex processes taking place on the contact surface, Szefer has introduced the concept of a singular surface, see e.g. [179].

# 4 Martensitic phase transformations

In this chapter an attempt is made to develop a workable model for a 3D body made of a material undergoing martensitic phase transformations under complex nonproportional loading conditions. The model is intended to describe the hysteretic behaviour of shape memory alloys (SMA) in the temperature range of pseudoelasticity, i.e. for temperatures $\theta > A_f^0$ where $A_f^0$ is the conventional austenite-finish temperature at the stress-free state. The most decisive characteristics of this kind of phase transformations (PT) are outlined in Section 1.2, where many relevant references are cited. Recall that martensitic PT is a deformation process that consists of sudden changes in the crystal lattice of the high temperature phase with greater symmetry (*austenite*) and that of the low temperature phase with lower symmetry (*martensite*). The new crystal structure replaces the parent material in the areas where PT have taken place. All possible crystal lattice rearrangements which appear in new phase orientations are called *variants* of martensite and can be determined from the symmetry of the parent phase (from crystallographic relations). Martensitic PT lead mainly to distortions in shape and only to small volumetric changes.

It is generally agreed that martensitic PT are the result of competition between changes in chemical free energy, surface energy and the potential energy of the heterogeneous system during the transformation. Although the resulting microstructures are crystallographically reversible, martensitic PT are thermodynamically irreversible for they induce hysteretic effects, accompanied by dissipation of energy. Hence the use of irreversible thermodynamics in a description of PT is expedient. In a general framework of thermodynamics, two additional ideas are apparently advantageous. These are the concept of *constrained equilibrium* introduced by KESTIN and RICE [68, 156] and that of threshold values of the driving force for PT which has been used by RANIECKI *et al.* [151] and others, and was formalized by LEVITAS [97] as the *postulate of realizability*. We recall that at constrained equilibrium the rate of some internal variables may vanish even though the corresponding thermodynamically conjugate force is non-zero.

The approach proposed here is based on minimization of an effective free energy for the mixture of phases, in which volume fractions play the role of internal variables. The effective free energy of the phase system, $\widetilde{W}$, is a result of the homogenization procedure (relaxation at fixed volume fractions $\boldsymbol{c}$) of the piecewise quadratic potential adopted. At a constant temperature $\theta$, it may be written in the form

$$\widetilde{W}(\boldsymbol{E}, \boldsymbol{c}) = \frac{1}{2}\,(\boldsymbol{E} - \boldsymbol{D}(\boldsymbol{c}))\cdot\mathbb{A}\,[\boldsymbol{E} - \boldsymbol{D}(\boldsymbol{c})] + \varpi(\boldsymbol{c}) + W_{\mathrm{mix}}(\boldsymbol{c}). \tag{4.1}$$

In (4.1) we designate by $\boldsymbol{E}$ the tensor of total strains, $\boldsymbol{c}$ the $N$-tuple of volume fractions of martensite, $\boldsymbol{D}(\boldsymbol{c})$ the effective transformation strain, $\mathbb{A}$ the (common) tensor of elastic moduli, $\varpi(\boldsymbol{c})$ the energy of the mixture at the stress free state and temperature $\theta$. The last term $W_{\text{mix}}(\boldsymbol{c})$ that accounts for misfits of the parent and product phases (variants) we call the *energy of mixing*, but it is also called *interfacial energy* [122], and is related to *energy of unaccommodation* [150]. We consider the PT process as a problem of evolution, with the natural constraints imposed on the volume fractions $c_m$, $1 \le m \le N$, where $N$ is the number of martensitic variants, e.g. $N = 1$ for the two-phase system under study in Sections 4.1 and 4.2, where $\boldsymbol{c}$ reduces to just one entry denoted by $c$, which must satisfy the constraint $0 \le c \le 1$. In a general case, the constraints imposed on the volume fractions $\boldsymbol{c}$ are defined in (4.73). Our point of departure is directly motivated by the developments due to Kohn [75], Levitas *et al.* [99], I. Müller *et al.* [59], and Raniecki *et al.* [151]. In the proposed model the evolution of the volume fractions of phases is governed by phase transformation criteria (PTC) derived from a form of the second principle of thermodynamics (Clausius-Duhem inequality). The PTC are finally expressed in a weak form as a variational inequality that together with the conditions of quasistatic equilibrium are solved incrementally in time as a sequence of linear complementarity problems.

The plan of this chapter is the following. First, by way of motivation we consider the one-dimensional model, where the peculiarities of the martensitic phase transformation IBVP may be demonstrated to some extent also by analytical calculations. Our main finding here are the great differences in the local behaviour at a material point and the system behavior at a global level. In particular the internal loops at the global level are observed only if the hardening is significantly larger than the material inhomogeneities. The effects of thermomechanical couplings due to the exothermic character of the forward (i.e., austenite $\to$ martensite) PT and the endothermic character of reverse PT is investigated. We conclude the 1D case with a brief discussion on the modelling of internal hysteresis loops. Observe that in the 1D case we use the usual notations $\sigma$ and $\varepsilon$ for the stress and strain, respectively. After that, the two-phase system is considered again but in the variational setting for a three-dimensional body. The existence of unique solutions to the incremental IBVP is proved and the results of numerical simulations of the tensile test on two-phase strips are provided. The obtained numerical results revealed the influence of the boundary conditions on the deformation modes of the specimen, and they are in good qualitative agreement with the available laboratory experiments. Finally the qualitative analysis is extended to a 3D body made of a multi-phase material. We close this chapter with a few conclusions.

## 4.1 The one-dimensional model problem

We wish to analyze here the macroscopic stress-strain (force-elongation) relations describing the PT process as a simplified one-dimensional problem. The material point $x$ of a body $\Omega$ is an element of an interval on reals $\mathcal{R}$, i.e. $x \in \Omega = (0, l_B)$, where $l_B$ is the length of the bar. The reason is that the majority of laboratory experiments have been carried out on wires and, on the mathematical side, for the 1D problem even tedious analytical derivations are still tractable, also numerical algorithms can be devised more directly. Our aim here is to impart the characteristic features of the constitutive relations governing the hysteretic behaviour and to lay grounds for further developments related to the 3D case to be considered in the next sections.

More specifically, we are concerned with the mathematical modelling and computational simulation of hysteretic behaviour typically exhibited by shape memory alloys in the pseudoelastic temperature range, as observed by I. Müller and his co-workers in experimental tests on a bar made of a CuZnAl monocrystal. The internal hysteresis loops are described by means of a discrete memory variable which can be handled by a monotone path rule. Existence and uniqueness of solutions is shown in the presence of hardening. We investigate the limit of vanishing hardening and vanishing material inhomogeneity and show that the limit depends on their relative size within the limit procedure. The analytical and numerical results show that under small hardening the phase transformation process is very sensitive to any inhomogeneities which may be present (e.g. geometric ones) or are developed in the two-phase system in the course of the loading/unloading sequences. Surprisingly enough, we obtained great differences in the local response at a material point and the system behaviour, in particular the system displays internal loops only if the hardening is significantly larger than the material inhomogeneities.

The one-dimensional static theory of elastic bars whose material behaviour is described by a non-monotone physical law has been studied in [31, 63], with the energy criterion of material stability for a non-convex smooth strain energy function. In [1] the authors derived the kinetics of phase transformations by making use of thermal activation theory. Finally we note that hysteresis operators of similar problems have been analyzed in [78, 186] and others. Our approach is different.

### 4.1.1 The mechanical model

Let us first record the relations that define the model of ideal pseudoelasticity following [59, 99, 151]. The model describes the phase transformation phenomenon in the shape memory alloy at temperatures above $A_f^0$, and the adjective "ideal" refers to the idealized situation with horizontal yield and recovery lines in the stress-strain diagram. In what follows we shall assume a more general case with hardening. With the traditional notations, $\sigma$ for

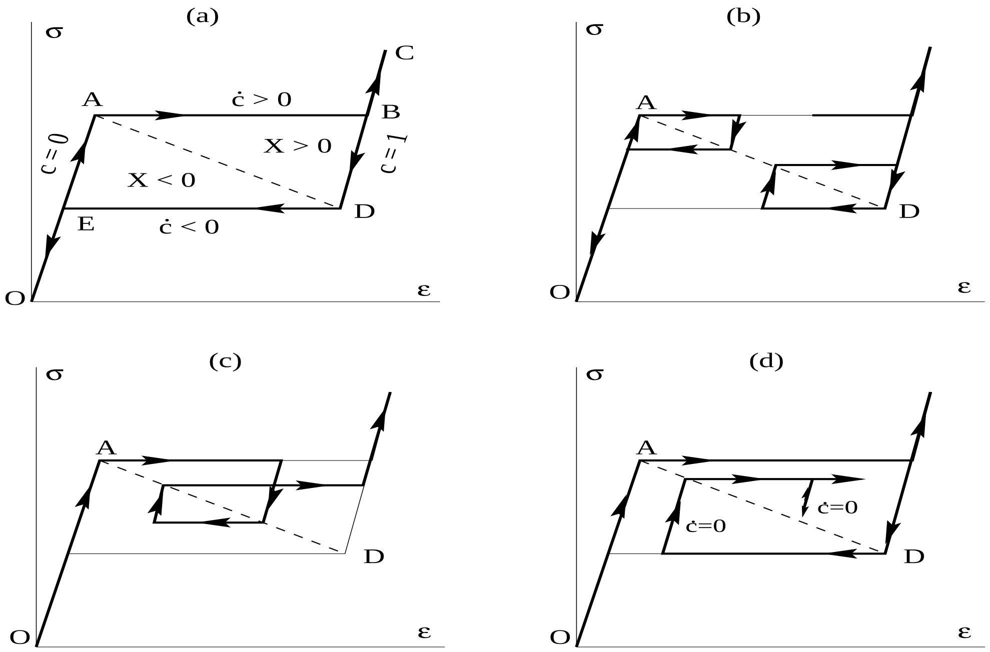


Figure 6: Stress vs strain diagram of ideal pseudoelastic behaviour. Phase transformation starts at the diagonal AD: (a) Yield and recovery; outer loop. (b) Internal yield and internal recovery. (c) Internal loop. (d) Internal elasticity and history dependence

stresses and $\varepsilon$ for strains, some typical pseudoelastic paths in the stress-strain diagram are shown in Fig. 6. In the macroscopic description of a PT process, a useful internal variable very often applied is a scalar $c$ which is defined as a volume fraction of martensite in the (infinitesimal) volume of the austenite-martensite mixture, i.e. $0 \leq c \leq 1$. In terms of the phase fraction rate $\dot{c}$ we can in general distinguish the following three characteristic stages of the PT deformation process, cf. Fig. 6:

1. reversible, purely elastic deformation of the parent (austenite, or 1) phase and product (martensite, or 2) phase, or austenite/martensite mixture, with $\dot{c} = 0$;

2. forward PT: austenite $\rightarrow$ martensite (or, $1 \rightarrow 2$), with $\dot{c} > 0$;

3. reverse PT: martensite $\rightarrow$ austenite (or, $2 \rightarrow 1$), with $\dot{c} < 0$.

Notice that at points in the triangle ABD and line BC the rate $\dot{c}$ is positive or equal to zero, whereas at points in the triangle ADE and interval OE, $\dot{c} \leq 0$. The diagonal AD (including points A and D) plays a critical role in the process. As can be seen in Fig. 6, on the diagonal the phase transformation initiates and its direction can be reversed, depending on the sense of strain increments. In fact, the diagonal is a phase equilibrium line but the states therein are not in a stable thermodynamic equilibrium.

We consider the simplified case that Young's moduli in both phases are equal, i.e. $E = E_1 = E_2$. The elastic parts of the strain in each phase are

$$\varepsilon_1^e = \varepsilon, \qquad \varepsilon_2^e = \varepsilon - \eta$$

where $\varepsilon = \partial u/\partial x$ is the derivative of displacement $u$, and $\eta$ is the transformation strain, a positive material constant. The free energy of the mixture is the sum of contributions

$$\widetilde{W} = (1-c)W_1(\varepsilon_1^e) + cW_2(\varepsilon_2^e) + W_{\text{mix}}(c) \tag{4.2}$$

in which $W_i = 0.5\, E(\varepsilon_i^e)^2 + \varpi_i(\theta)$ is the assumed form of the free energy for each phase that is quadratic in elastic strain. The material constant $B$ in the expression for energy of mixing, $W_{\text{mix}} = 0.5\, B(1-c)c$, is a measure of the area of the outer hysteresis loop. The function $\varpi_i(\theta)$ depends on temperature $\theta$, treated here as a parameter, and we adopted the formula

$$\varpi_i(\theta) = C_v(\theta - \theta^0) - C_v\theta \ln(\theta/\theta^0) + e_i^0 - \theta s_i^0 \tag{4.3}$$

where $e_i^0$, $s_i^0$ are the energy and entropy constants of $i$-th phase, $C_v$ the common specific heat, and $\theta^0$ a reference temperature. Using the fact that we have $\varepsilon_1^e = \varepsilon_2^e$ (due to the same stresses and Young moduli in both phases) we obtain for (4.2) the final expression

$$\widetilde{W}(\varepsilon, c) = \frac{1}{2}\, E\, (\varepsilon - c\eta)^2 + (1-c)\varpi_1 + c\varpi_2 + \frac{1}{2}\, B(1-c)c. \tag{4.4}$$

With $s$ indicating entropy, the rate of mechanical dissipation per unit volume, $\mathcal{D} = \sigma\dot{\varepsilon} - \dot{\widetilde{W}} - s\dot{\theta}$, takes the form

$$\mathcal{D} = \left(\sigma - \frac{\partial \widetilde{W}}{\partial \varepsilon^e}\right)\dot{\varepsilon}^e + \sigma\eta\dot{c} - \left(s + \frac{\partial \widetilde{W}}{\partial \theta}\right)\dot{\theta} - \frac{\partial \widetilde{W}}{\partial c}\dot{c} \geq 0. \tag{4.5}$$

Further, assuming the constrained equilibrium and making use of the standard argument,

$$\sigma \equiv \frac{\partial \widetilde{W}}{\partial \varepsilon^e} = E(\varepsilon - c\eta), \qquad s \equiv -\frac{\partial \widetilde{W}}{\partial \theta} = -(1-c)\frac{\partial \varpi_1}{\partial \theta} - c\frac{\partial \varpi_2}{\partial \theta} \tag{4.6}$$

we can reduce (4.5) to the following inequality

$$D = X\,\dot{c} \geq 0 \tag{4.7}$$

where

$$X = \sigma\eta - \Delta\varpi - \frac{1}{2}\,B(1-2c) \tag{4.8}$$

is, as a variable conjugate to $\dot{c}$, the thermodynamic driving force for phase transformation. In the case of zero stress, $X$ reduces to the phase chemical potential $X^0$,

$$X = X^0 \equiv -\Delta\varpi - \frac{1}{2}\,B(1-2c), \tag{4.9}$$

which is the driving force for temperature-induced martensitic transformations at the stress-free state. The difference in the free energies of the phases, $\Delta\varpi \equiv \varpi_2 - \varpi_1$ is a linear function of temperature, cf. (4.3).

The equilibrium line $X = 0$, diagonal A-D in Fig. 6, has a negative slope, so all equilibrium states are unstable. The instability of equilibrium states is an origin of the dissipative character of phase transformation process manifested by hysteresis loops. Note that the driving force is positive in the triangle ABD and negative in the triangle ADE. In order to consistently account for the experimental findings of Müller *et al.*, it is advantageous to use a concept of threshold values for $X$. Accordingly, the phase transformation may take place only if its driving force $X$ equals the threshold value of $\kappa^+$ or $\kappa^-$, where $\kappa^+ \geq 0$ and $\kappa^- \leq 0$ are given functions of the current state of the phase mixture. This idea, together with the requirement of dissipation inequality (4.7) lead to the following phase transformation criteria (PTC)

$$\boxed{\begin{array}{lccc} \text{if} & X(c) = \kappa^+(c) & \text{then} & \dot{c} \geq 0, \\ \text{if} & X(c) = \kappa^-(c) & \text{then} & \dot{c} \leq 0, \\ \text{if} & \kappa^-(c) < X(c) < \kappa^+(c) & \text{then} & \dot{c} = 0. \end{array}} \tag{4.10}$$

The following situations concerning the conditions $(4.10)_1$ and $(4.10)_2$ deserve further comment. First, the case $X = 0$ corresponds to the states on the phase equilibrium line, the diagonal AD in Fig. 6. These states are unstable and any process along the phase equilibrium line is accompanied by no dissipation. Further, the situations $X = \kappa^+(c) > 0$ and $\dot{c} = 0$, and $X = \kappa^-(c) < 0$ and $\dot{c} = 0$ correspond to a degenerate problem in which both the complementary variables, $y^+ \equiv \kappa^+(c) - X$ and $\dot{c}$ are equal to zero, similarly for

$y^- \equiv X - \kappa^-(c)$ and $\dot{c}$. That the phase transformation process, and not another one, starts on the phase equilibrium line and carry on when the condition $X = \kappa^+(c)$, or $X = \kappa^-(c)$ is satisfied, may be motivated by the principle of least work, [190]. The threshold quantities, $\kappa^+$ for forward PT and $\kappa^-$ for reverse PT are assumed here to be dependent only on the volume fraction $c$ and a new internal variable $p$. We adopt the functions $\kappa^+$ and $\kappa^-$ in the form

$$\kappa^+ = \max\{L(c-p), 0\} \geq 0, \qquad \kappa^- = \min\{L(c-p), 0\} \leq 0. \tag{4.11}$$

The new material parameter $L$ should be greater than or equal to $B$. Notice that the functions $\kappa^+$ and $\kappa^-$ are a measure of the dissipated energy in the course of the forward and the reverse phase transformation, respectively. In fact, relations (4.11) can be derived from the dissipation potential $\Phi$ of the form

$$\Phi(c,p) = \frac{1}{2}L(c-p)^2, \tag{4.12}$$

which is a homogeneous quadratic function of the difference $c-p$. Expression (4.12) shows that the physical meaning of material parameter $L > 0$ is that of the energy which is dissipated while transforming a unit volume of one phase into the other. We assume that $L \geq B$, whereas the case $L = B > 0$ corresponds to the ideal pseudoelastic flow shown in Fig. 6.

Condition $(4.10)_1$ is relevant for all horizontal intervals in the "upper" triangle ABD, whilst $(4.10)_2$ controls the phase transformation process along horizontal segments in the "lower" triangle ADE. All the states on intervals parallel to lines OA and DC are governed by condition $(4.10)_3$. These three conditions (4.10) when supplemented with the auxiliary one, $0 \leq c \leq 1$, allow us to describe completely the stress-strain relationship illustrated in Fig. 6, including the proper succession of states. The latter is guaranteed by a suitable updating of the variable $p$. On the outer intervals, i.e. AB and DE, we take $p = 0$ and $p = 1$, respectively. As applied in this model, the variable $p \in [0, 1]$ plays the role of a discrete memory that "remembers" only the latest characteristic state of the two-phase system, and it is stipulated here that $p$ is changed at the intersection point of the actual stress-strain path and the diagonal AD. A further discussion of the evolution law for quantity $p$ will be given in Section 4.1.5.

We remark that the considered model of hysteretic behaviour is defined by five parameters: $E, \eta, B, L, \Delta\varpi$ which can easily be determined from the stress-strain (force-elongation) diagram in Fig. 6 as shown in [85].

The mechanical problem is now completed by associating the cross-sectional area $\alpha(x)$ to each value of the axial variable $x \in [0, l_B]$, where $l_B$ is the length of the bar. Thus, the effective elastic modulus at $x$ is $\alpha(x)E$.

The mechanical problem is now given as follows: For each $t \in [0, T]$ and each $x \in (0, l_B)$ we have

$$\boxed{\begin{gathered}\frac{\mathrm{d}}{\mathrm{d}x}\Big(\alpha(x)E[\varepsilon(t,x) - c(t,x)\eta]\Big) = 0,\\ \int_0^{l_B} \varepsilon(t,x)\,\mathrm{d}x = \ell(t),\\ (c(t,x), p(t,x)) \text{ satisfy the PTC (4.10).}\end{gathered}} \tag{4.13}$$

The first equation is the elastic equilibrium equation and the second one is equivalent to the displacement conditions $u(t,0) = 0$ and $u(t, l_B) = \ell(t)$.

Note that although the phase transformation problem is treated as a quasistatic one, it possesses time derivatives of the internal variable $c$. These derivatives have to satisfy inequality constraints which generate history dependence and the constraint $c \in [0,1]$ must be assured. Hence, it is convenient to approach this phenomenon in an incremental manner. In the next section we shall present the formulation of (4.13) that leads to the numerical algorithm based on the axial force $F(t)$, being constant along the bar due to the elastic equilibrium, is the characteristic quantity in the 1D case,

$$F(t) = \alpha(x)\sigma(t,x) = \alpha(x)E(\varepsilon(t,x) - c(t,x)\eta).$$

In experiments one usually plots only the curve $(F(t), \ell(t))$ which gives the stress-strain relation. We will associate to this curve the name "*system behaviour*" as it averages over all the material points $x \in [0, l_B]$ where different local material behaviour may occur. Another, more general approach based on complementarity conditions and variational inequality formulation was shown in the note [84] and will be presented in the context of 3D problems later on.

### 4.1.2 Analytical results

We analyze the phase transformation in a bar as a strain-driven process by prescribed hard loadings $\ell(t)$ that is a continuous function of time $t$. First, we are concerned with the case with hardening that allows us to construct the unique solution of problem (4.13). Here we use the special feature in the one-dimensional theory that the sign of $\dot{\ell}(t)$ determines for each point $x$ whether there is loading or unloading. Second, we analyze the case of a homogeneous bar made of a material without hardening and show that the set of solutions is very rich. Third, we consider the case $L = B + \omega$ and $\alpha(x) = \alpha_0 + \omega\rho\alpha_1(x)$

in the limit $\omega \to 0$, which provides special solutions for the homogeneous case without hardening. In particular, we show the differences in the unloading depending on the parameter $\rho$ which measures the size of the inhomogeneity relative to the hardening parameter $\omega = L - B$. We have found that small $\rho$ gives rise to the internal loops presented in Fig. 8 while large $\rho$ leads to so-called external loops.

The main observation here is that in every material point the values $\sigma(t)$, $c(t)$ and $p(t)$ can be given as functions of $\varepsilon(t)$ and the values of $c(t_{n-1})$ and $p(t_{n-1})$ as long as $\varepsilon(\cdot)$ is monotone on $[t_{n-1}, t]$. We denote these functions as

$$\begin{aligned} \sigma(t) &= \Sigma(\varepsilon(t), c(t_{n-1}), p(t_{n-1})), \\ c(t) &= \mathcal{C}(\varepsilon(t), c(t_{n-1}), p(t_{n-1})), \\ p(t) &= \mathcal{P}(\varepsilon(t), c(t_{n-1}), p(t_{n-1})). \end{aligned} \tag{4.14}$$

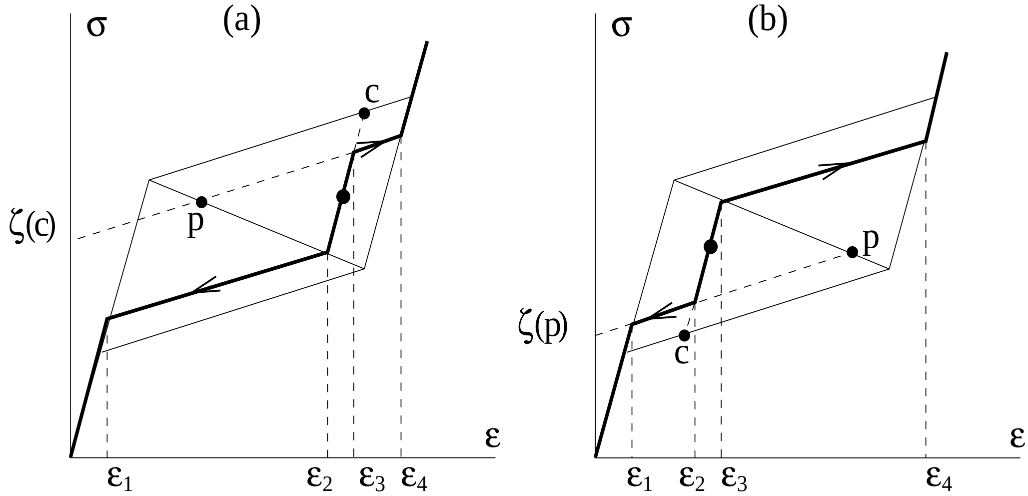


Figure 7: Illustration for determining the function $\Sigma$: (a) Case $c > p$, (b) Case $c < p$

Some elementary calculations using the phase transformation conditions (4.10) give the following explicit expressions.

$$\Sigma(\varepsilon, c, p) = \begin{cases} E\varepsilon & \text{for} \quad \varepsilon \le \varepsilon_1(c,p), \\ \tilde{E}\varepsilon + E\eta\xi(\max\{c,p\}) & \text{for } \varepsilon_1(c,p) \le \varepsilon \le \varepsilon_2(c,p), \\ E\varepsilon - \mu c & \text{for } \varepsilon_2(c,p) \le \varepsilon \le \varepsilon_3(c,p), \\ \tilde{E}\varepsilon + E\eta\xi(\min\{c,p\}) & \text{for } \varepsilon_3(c,p) \le \varepsilon \le \varepsilon_4(c,p), \\ E\varepsilon - \mu & \text{for } \varepsilon_4(c,p) \le \varepsilon, \end{cases} \tag{4.15}$$

wherein the characteristic strains, $\varepsilon_i$, and $\xi$ are given by

$$\begin{array}{rcl} \varepsilon_1(c,p) & = & (\gamma - L\max\{c,p\})/\mu, \\ \varepsilon_2(c,p) & = & (\gamma + \nu c - L\max\{c,p\})/\mu, \\ \varepsilon_3(c,p) & = & (\gamma + \nu c - L\min\{c,p\})/\mu, \\ \varepsilon_4(c,p) & = & (\gamma + \nu - L\min\{c,p\})/\mu, \\ \xi(z) & = & (\gamma - Lz)/\nu, \end{array} \tag{4.16}$$

with the material parameters $\mu = E\eta$, $\tilde{E} = (L-B)E/\nu$, $\nu = L - B + E\eta^2$ and $\gamma = B/2 + \Delta\varpi$. Moreover, we obtain

$$\mathcal{C}(\varepsilon,c,p) = \begin{cases} 0 & \text{for } \varepsilon \le \varepsilon_1(c,p), \\ \mu\varepsilon/\nu - \xi(\max\{c,p\}) & \text{for } \varepsilon_1(c,p) \le \varepsilon \le \varepsilon_2(c,p), \\ c & \text{for } \varepsilon_2(c,p) \le \varepsilon \le \varepsilon_3(c,p), \\ \mu\varepsilon/\nu - \xi(\min\{c,p\}) & \text{for } \varepsilon_3(c,p) \le \varepsilon \le \varepsilon_4(c,p), \\ 1 & \text{for } \varepsilon_4(c,p) \le \varepsilon, \end{cases} \tag{4.17}$$

$$\mathcal{P}(\varepsilon,c,p) = \begin{cases} p & \text{if } (\varepsilon > \varepsilon_2(c,p) \text{ and } c > p) \text{ or if } (\varepsilon < \varepsilon_3(c,p) \text{ and } c < p), \\ c & \text{if } (\varepsilon \le \varepsilon_2(c,p) \text{ and } c > p) \text{ or if } (\varepsilon \ge \varepsilon_3(c,p) \text{ and } c < p). \end{cases} \tag{4.18}$$

With these three functions we are able to construct a solution of (4.13) which, under the assumptions adopted, is unique as stated in the following theorem proved in [85].

**Theorem 4.1.** *Assume $L > B$ and let $\ell : [0,T] \to \mathcal{R}$ be a continuous, piecewise monotone function. Then, problem (4.13) has a unique solution which is also piecewise monotone in $\varepsilon$ on the same time intervals.* ❏

In the sequel we wish to address the question why the case $L = B$ ($\tilde{E} = 0$, no hardening) is highly degenerate and how the limit $L \to B$ can be understood in cases where the material inhomogeneity is also small, further details are contained in [85].

**The homogeneous case without hardening**

It can be shown analytically that the case $L = B$ leads to a big variety of solutions if additionally $\alpha(x) \equiv \alpha_0$, that is the bar is homogeneous. To illustrate this fact let us consider a simple loading and unloading cycle $\ell(t) = \ell_{\max}(1-|1-t|)$ which however only reaches the maximal value $\ell_{\max} = l_B(\gamma/\mu + \eta/2)$ that is half way in the hysteresis loop. Starting with $c(0,x) = p(0,x) = 0$ we obtain for $\ell(t) \le l_B\gamma/\mu$ that $c(t,x)$ and $p(t,x)$ remain 0 since we are below the critical strain. However, for $\ell(t) > l_B\gamma/\mu$ and $t < 1$ the only constraints on $c(t,x)$ are

$$\frac{\partial}{\partial t}c(t,x) \ge 0, \quad \int_0^{l_B} \left(\frac{\gamma}{\mu} + c(t,x)\eta\right) \mathrm{d}x = \ell(t).$$

Of course, there are a lot of ways to satisfy these conditions. For instance we may take $c(t,x) = (\mu\ell(t) - l_B\gamma)/(\mu\eta l_B)$ or we choose $c(t,x) = 1$ for $x \in [x_1(t), x_2(t)]$ and 0 otherwise, where $\dot{x}_1(t) \le 0$ and $\dot{x}_2(t) \ge 0$ with $x_2(t) - x_1(t) = (\mu\ell(t) - l_B\gamma)/(\mu\eta)$. The function $p(t,x)$ remains 0 for all $t \in [0,1]$. In this loading process we still have the same axial force $F(t)$ for all the different solutions, namely $F(t) = \alpha_0 E \min\{\gamma/\mu, \ell(t)/l_B\}$, so the system behaviour does not reflect the nonuniqueness. However, upon unloading the system behaviour will be completely different.

We illustrate more precisely the effects of nonuniqueness by considering the system behaviour under the sequence of loading, unloading and reloading for two extreme situations: Case 1, the homogeneous state, $c(t,x) \equiv c(t)$, and Case 2, the $c$-inhomogeneous case of $c(t,x) \in \{0,1\}$. To this end we extend the loading program $\ell(t)$ by adding a reloading step, i.e. $\ell(t) = \ell_{\max}\max\{1 - |1-t|, t - 2/3\}$. The derived expressions for the axial force $F_i(t)$ in each case are given below and the corresponding hysteresis loops are depicted in Fig. 8.

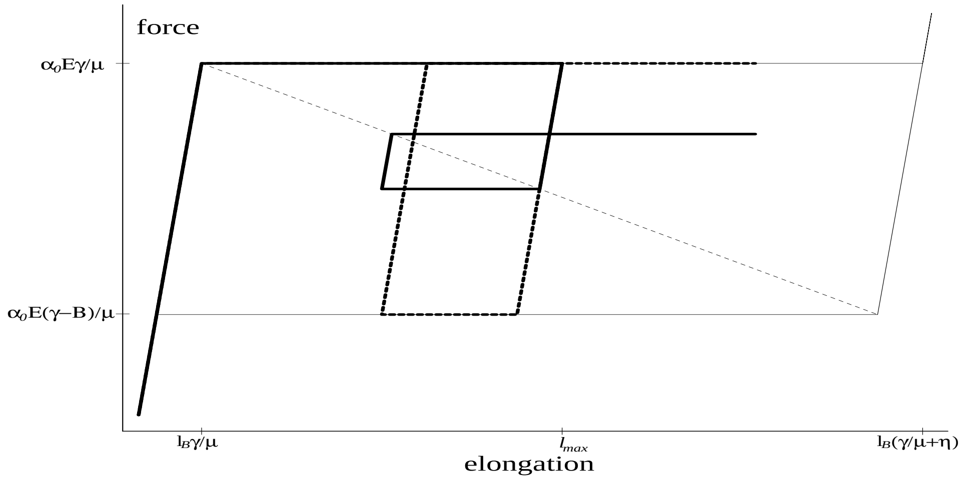


Figure 8: Nonunique system behaviour of a homogeneous bar: (i) for homogeneous distribution of $c(t) \in [0,1]$ (solid bold line), (ii) for inhomogeneous distribution of $c$, $c(t,x) \in \{0,1\}$ (dotted bold line)

**Case 1:** For the homogeneous distribution of $c$ we have the following evolution of force $F_1$,

$$F_1(t) = \begin{cases} \alpha_0 E \min\{\ell(t)/l_B, \gamma/\mu\} & t \in [0,1], \quad \text{(loading)} \\ \alpha_0 E \max\{\ell(t)/l_B - \eta/2, \gamma/\mu - B/(2\mu)\} & t \in [1,4/3], \quad \text{(unloading)} \\ \alpha_0 E \min\{\ell(t)/l_B - A_0, A_1\} & t \in [4/3,2], \quad \text{(reloading)} \end{cases}$$

where $A_0 = \eta/3 - \gamma/(3\mu) + B/(2\mu)$, $A_1 = (4\gamma + 2\nu + B + B(2\gamma - 3B)/\nu)/(6\mu)$.

**Case 2:** We consider the case that $c(t,x) = 1$ for $x \le x_f(t)$ and $c(t,x) = 0$ else. Hence, only the position of $x_f(t)$ has to be determined. Using the phase transformation conditions we easily obtain

$$F_2(t) = \begin{cases} \alpha_0 E \min\{\ell(t)/l_B, \gamma/\mu\} & t \in [0,1], \quad \text{(loading)} \\ \alpha_0 E \max\{\ell(t)/l_B - \eta/2, (\gamma - B)/\mu\} & t \in [1, 4/3], \quad \text{(unloading)} \\ \alpha_0 E \min\{\ell(t)/l_B - A_2, \gamma/\mu\} & t \in [4/3, 2], \quad \text{(reloading)} \end{cases}$$

where $A_2 = (3B + \eta\mu - \gamma)/(3\mu)$.

**Small hardening versus small inhomogeneity**

We now briefly mention the physically interesting case that the hardening parameter $\omega = L - B > 0$ as well as the inhomogeneity of the bar, $\alpha'(x)$ are small. To this end consider the following ansatz

$$L = B + \omega\,, \qquad \alpha(x) = \alpha_0 + \omega\rho\alpha_1(x).$$

According to theorem 4.1 there is for each piecewise monotone loading curve $\ell(t)$ a unique solution $(\varepsilon_{\omega,\rho}(t,x), c_{\omega,\rho}(t,x), c_{0,\omega,\rho}(t,x))$ which for $\omega \to 0$ converges, as shown in [85], to a well-defined limit $(\varepsilon_{*,\rho}(t,x), c_{*,\rho}(t,x), c_{0,*,\rho}(t,x))$. This limit is in fact one of the solutions for the homogeneous problem without hardening considered above. The interesting thing is, that it is the specific solution which still has information on the relative size of the inhomogeneity and the hardening which is expressed in the parameter $\rho$. We will omit here the rather lengthy analytical derivations discussed in [85], and illustrate only the final force-elongation diagram for the unloading step.

Relations in Fig. 9 were obtained by unloading with $\ell(t) = 8 - t$ for $t \in [4,8]$ from the state reached by loading with $\ell(t) = 4 - |4 - t|$, $t \in [0,4]$. We remark that the loading process is not dependent on the parameter $\rho$. For simplicity, the following data were used

$$E = 1,\ l_B = 1,\ \eta = 4,\ B = 1,\ \gamma = 8,\ L = 1 + \omega,\ \alpha(x) = 1 + \omega\rho x.$$

By $\rho_0$ we denote a parameter that depends on both geometry and material of the bar, $\rho_0 = \alpha_0/(\gamma l_B) = 1/8$. Let $F(t) = F_*(t) + \mathcal{O}(\omega)$ be an expansion of the axial force.

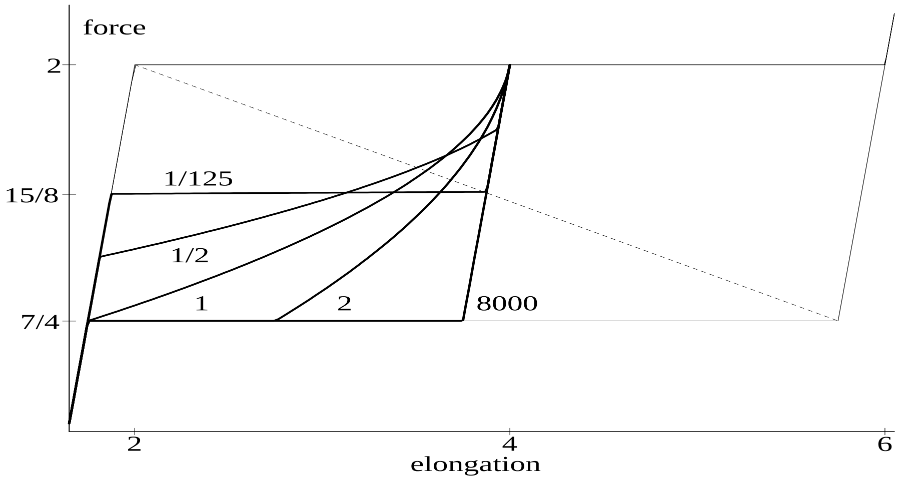


Figure 9: Force $F$ during unloading as the function of elongation $\ell(t) = 8 - t,\ t \in [4, 8]$, for various (scaled) inhomogeneity parameters $\rho/\rho_0$

The system behaviour, shown in Fig. 9, strongly depends on $\rho$:

For $t \in [4, 8]$ and $\rho \geq 1/8$ we have $\ell(t) = 8 - t$

$$F_*(t) = \begin{cases} 2 + \frac{\rho}{8} - \frac{1}{4}\sqrt{(\rho/2)^2 + 4\rho(t-4)} & \text{for } t \in [4, 17/4 + 1/(4\rho)], \\ 7/4 & \text{for } t \in [17/4 + 1/(4\rho), 25/4], \\ 8 - t & \text{for } t \geq 25/4. \end{cases}$$

For $t \in [4, 8]$ and $\rho \leq 1/8$ we have $\ell(t) = 8 - t$

$$F_*(t) = \begin{cases} 6 - t, & t \in [4, \frac{33}{8} - \rho], \\ 2 + \frac{\rho}{8} - \frac{1}{4}\sqrt{(\rho/2)^2 + 4\rho(t-6) + (1/2 + 4\rho)^2}, & t \in [\frac{33}{8} - \rho, \frac{49}{8} + \rho], \\ 8 - t, & t \geq \frac{49}{8} + \rho. \end{cases}$$

We especially recall the two extreme cases of (i) hardening without inhomogeneity ($\rho \to 0$) and (ii) of large inhomogeneity and small hardening ($\rho \to \infty$). In both cases we have two purely elastic regions close to $\ell = 0$ and $\ell = 4$. In between there is a flat part of the curve which has the level 15/8 in case (i) and the level 7/4 in case (ii), see Fig. 9. Thus, the case (ii) yields weaker system behaviour. Let us observe that the curve $(F_*(t), \ell(t))$ does not behave monotonously in $\rho$. For analysis of more complex loading cycles we will apply a numerical algorithm to be described next.

### 4.1.3 Numerical results

First we formulate an incremental problem for system (4.13) and describe an iterative algorithm for its solution. Then we present a numerical study of the dependence of internal hysteresis loops on the relative size of hardening and inhomogeneity.

**Monotone path rule**

We discretize the problem in time by selecting on the time interval $[0, T]$ nodal points $t_n$, $n = 1, ..., N$, so a typical time-step $t_{n-1} \Longrightarrow t_n$ is defined on the subinterval $[t_{n-1}, t_n]$. We apply the implicit time integration scheme in which the evolution of the hysteretic system (4.13) is treated as piecewise monotone. This means that in **one** time step the path of a material point evolves according to the following monotone path rule.

**Monotone path rule for time steps** (MPR)

In each time-step $t_{n-1} \Longrightarrow t_n$ the deformation process in a material point $x$ is either pure loading $[\ \dot{\varepsilon} > 0\, (\dot{\sigma} \geq 0)\ ]$ or pure unloading $[\ \dot{\varepsilon} < 0\, (\dot{\sigma} \leq 0)\ ]$.

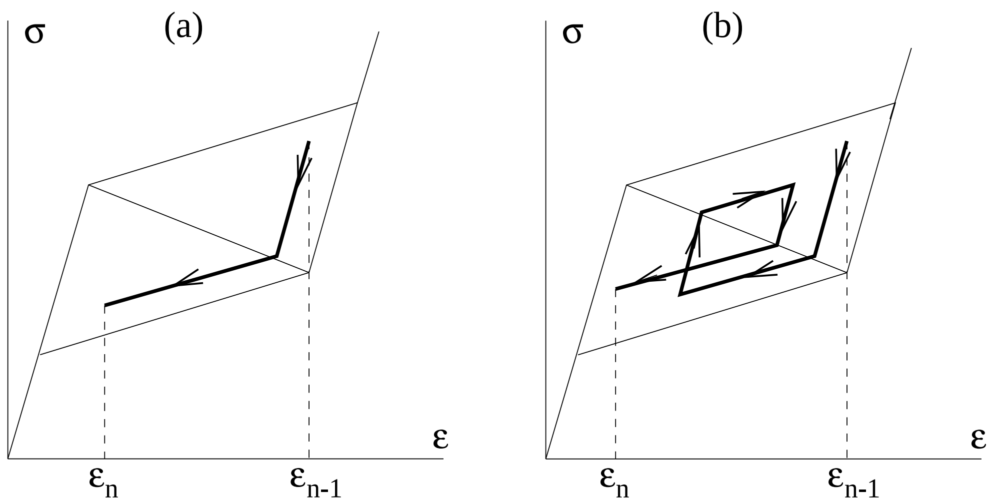


Figure 10: (a) An allowed path and, (b) an excluded path in one time-step

Thus, using the MPR we admit to the paths as shown, for example, in Fig. 10a, but exclude loops around the diagonal $X = 0$ as illustrated in Fig. 10b, within one time-step, at the material point at a fixed temperature. Of course, in different material points $x \in \Omega$ we may have loading or unloading. In our 1D case one may expect that in each $x \in \Omega$ the monotonicity intervals of $[0, T]$ coincide with those of the loading function $\ell(t)$ (the latter are determined by the points $t_n$ at which the rate of $\ell(t)$ changes sign).

**Numerical algorithm**

The numerical algorithm is developed for a slightly more general problem including a volume forcing $f(t, x)$ along the bar, so now the elastic equilibrium equation reads

$$\frac{\mathrm{d}}{\mathrm{d}x}\left(\alpha(x)E(\varepsilon(t,x) - c(t,x)\eta)\right) = f(t,x) \quad \text{for } x \in (0, l_B).$$

Due to this generalization the monotonicity argument employed in the case $f(t, x) \equiv 0$ is no longer valued. We may have loading and unloading at the same time instant but at different material points. The ability to handle such circumstances is necessary when considering higher-dimensional problems, since then one cannot guarantee simultaneous loading or unloading even when no volume forces are present.

In the implicit time integration scheme we determine the state of the process $S_n \equiv (u_n, c_n, p_n)$ at time level $t_n$ for the given values of driving quantities $l_n = \ell(t_n)$ and $f_n = f(t_n, \cdot)$ at this moment, and previous state $S_{n-1}$. By virtue of the MPR, the quantities of interest $\sigma, c$ and $p$ can be written as functions of $\varepsilon$ and the old values of $c_{n-1}, p_{n-1}$ using the function $\Sigma$, $\mathcal{C}$ and $\mathcal{P}$ defined in (4.15) - (4.18),

$$\sigma_n = \Sigma(\varepsilon_n, c_{n-1}, c_{n-1}), \; c_n = \mathcal{C}(\varepsilon_n, c_{n-1}, p_{n-1}), \; p_n = \mathcal{P}(\varepsilon_n, c_{n-1}, p_{n-1}). \tag{4.19}$$

The hysteretic evolution of the binary alloy can now be approximated by the following time-incremental problem

Given $S_{n-1} = (u_{n-1}, c_{n-1}, p_{n-1})$, find $S_n = (u_n, c_n, p_n)$ from $u_n(x) = \int_0^x \varepsilon_n(y)\,\mathrm{d}y$ and the following relations:

$$\alpha(x)\,\Sigma\left(\varepsilon_n(x), c_{n-1}(x), p_{n-1}(x)\right) = F_n - \int_x^{l_B} f_n(y)\,\mathrm{d}y, \;\; x \in [0, l_B],$$
$$\int_0^{l_B} \varepsilon_n(x)\,\mathrm{d}x = \ell_n,$$

with

$$c_n(x) = \mathcal{C}(\varepsilon_n(x), c_{n-1}(x), p_{n-1}(x)),$$
$$p_n(x) = \mathcal{P}(\varepsilon_n(x), c_{n-1}(x), p_{n-1}(x)).$$

(4.20)

For $L > B$ we obtain a unique solution of the incremental problem by determining the unknown axial force $F_n$ such that the length condition holds. The existence and uniqueness follows from the fact that $\Sigma$ is strictly monotone in $\varepsilon$, namely piecewise linear with slopes either $E > 0$ or $\tilde{E} > 0$.

The first two equations in (4.20) have to be solved numerically. This can be done as follows. The function $\mathcal{E}(\sigma, c, p)$ as the inverse of $\sigma = \Sigma(\varepsilon, c, p)$ is known explicitly (provided $L - B > 0$). Hence it remains to solve

$$\begin{aligned} \ell_n \;\; &= \;\; \mathcal{L}_n(F_n) \stackrel{\text{def}}{=} \int_0^{l_B} \mathcal{E}(\sigma_n(x), c_{n-1}(x), p_{n-1}(x))\,\mathrm{d}x \\ \text{with} \qquad & \sigma_n(x) = (F_n - \int_x^{l_B} f_n(y)\,\mathrm{d}y)/\alpha(x). \end{aligned} \tag{4.21}$$

To solve this nonlinear scalar problem we introduce a node spacing $x_i = ih$, $i = 0, 1, 2, \ldots, M$, with $h = l_B/M$. The integrals are calculated by a trapezoidal rule and the nonlinear scalar function is solved using bisection with a relative error in $\ell_n$ smaller than $10^{-12}$. The quantities $\varepsilon_n$, $c_n$ and $p_n$ are obtained on the nodes $x_i$ via $\mathcal{E} \equiv \Sigma^{-1}$, $\mathcal{C}$ and $\mathcal{P}$ of (4.19).

The convergence of this algorithm was checked numerically for many test examples. The results for an inhomogeneous bar subjected to a body force $f(x, t)$ and a displacement loading $\ell(t)$ are included in [85]. Here we would like to restrict ourselves to the numerical analysis of hysteretic behaviour in a number of loading/unloading cycles.

**Numerical study of internal loops**

The analysis here complements the analytical results obtained in the previous section. Our goal here is to test the influence of the measure of inhomogeneity $\rho$ on the system behaviour. We have analyzed the test examples as the displacement-driven loading process of the bar of unit length, say $l_B = 1.00\,\mathrm{m}$. The considered bar possesses a linearly varying cross-sectional area $\alpha(x) = 0.9999 + 0.0002|x|$, $x \in (-0.5, 0.5)$. The hardening modulus $L$ is expressed in terms of the parameter $\rho$, i.e. $L = B + 0.0002/\rho$. We have used the data provided in [59]. After some calculations we obtain the following values: temperature $\theta = 292.6$ K, yielding stress $\sigma_Y = 64.227$ MPa, recovery stress $\sigma_R = 45.277$ MPa, elasticity modulus $E = 12\,300.0$ MPa, material constant $B = 1.30$ MPa, phase transition strain $\eta = 0.0686$, density of the alloy $\rho_{\mathrm{dens}} = 7750.0$ kg/m$^3$, difference in energies $\Delta\varpi = 3.756$ J/m$^3$, $\gamma = 4.406$ MPa, $\mu = 843.78$ MPa. The following initial distribution of the volume fraction, $c(0, x) = 0$, and the discrete memory, $p(0, x) = 1$, are taken.

**Example 1.** First, we subject the bar to the loading program $\ell(t) = 0.07308t + 0.019538\sin(5.712t)$, which has a local maximum at $t = 0.40$ and a local minimum at $t = 0.70$: $\ell(0.4) = 0.044$ and $\ell(0.7) = 0.03639$. This loading program induces one internal loop, whereas the loading function used in the next example produces 3 internal loops, cf. Fig. 13b. The system behaviour is displayed in Fig. 11 for some representative values of the inhomogeneity parameter $\rho$ scaled against the characteristic value $\rho_0 = \alpha_0/(\gamma l_B)$. By a dotted line the diagonal and the recovery segment for the ideal pseudoelastic case $L = B = 1.30$ are marked. As established in Section 4.1.2, the internal loops are realized if the inhomogeneity of the process is sufficiently small, $\rho < \rho_0/200$, which results in uniform distributions of volume fraction $c$, see Fig. 12 for $\rho = \rho_0/500$. Otherwise we have in terms of strain a localization phenomenon. It should be stressed that the localization effect, even if not present after a first loading/unloading cycle, it may occur later in the course of the loading/unloading sequences.

**Example 2.** To further check the impact of some inhomogeneity induced by previous loading/unloading loops we have subjected the bar to the loading history shown in Fig. 13b. We denote by L1,L2,L3 and U1,U2,U3 the turning points of the sequential loading and unloading steps. The elongation program induces three internal loops with the same unloading amplitude of 0.6%. In Fig. 13 presented are the results which illustrate three types of the system behaviour. First, when the inhomogeneity is high (or hardening is small) there is no internal loop, in this example for $\rho = \rho_0/2 = 0.22694$. Then for $\rho = \rho_0/500$ even although the first loading/unloading cycle is accompanied by a regular hysteresis internal loop, the inhomogeneous state of strains which is

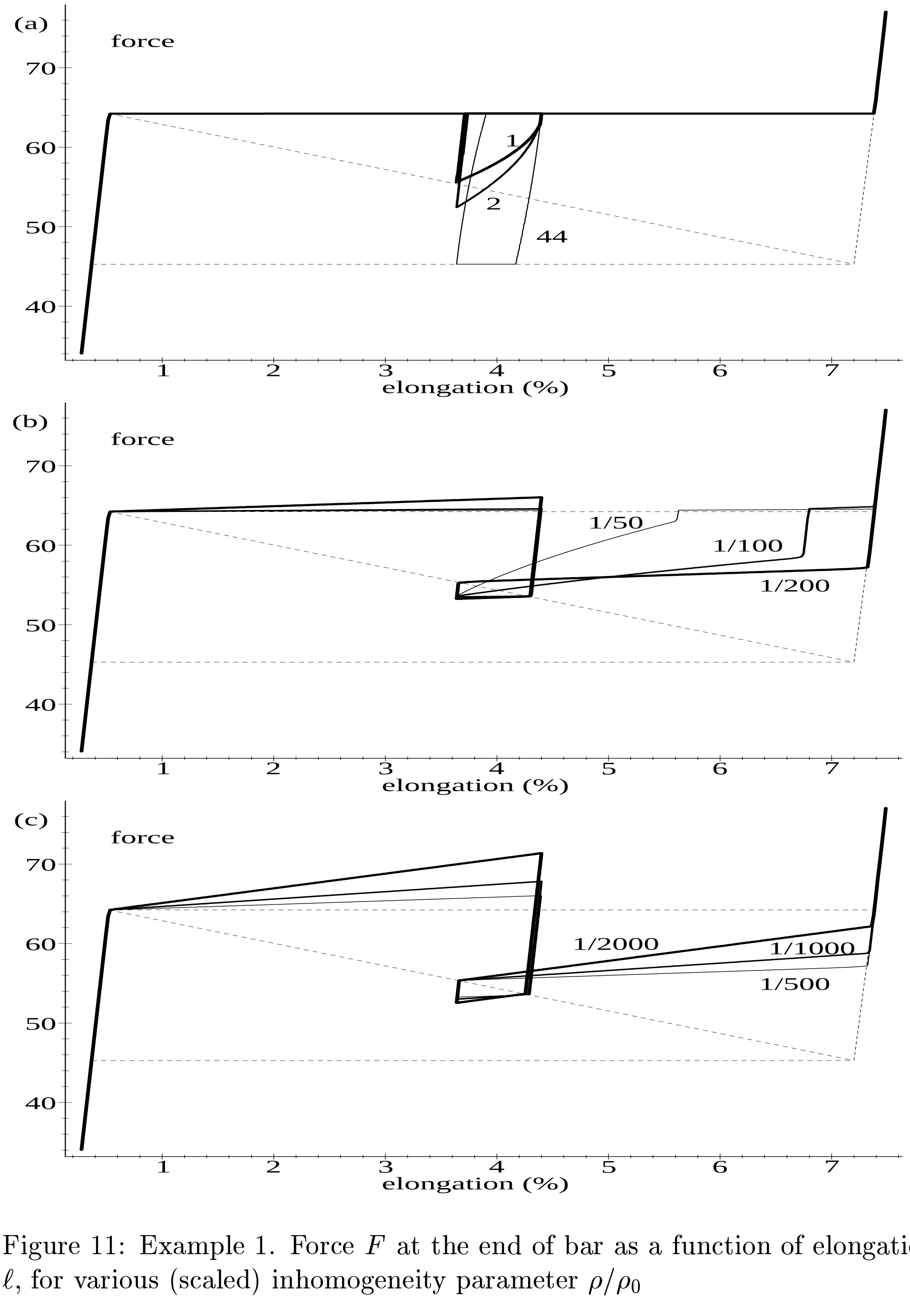


Figure 11: Example 1. Force $F$ at the end of bar as a function of elongation $\ell$, for various (scaled) inhomogeneity parameter $\rho/\rho_0$

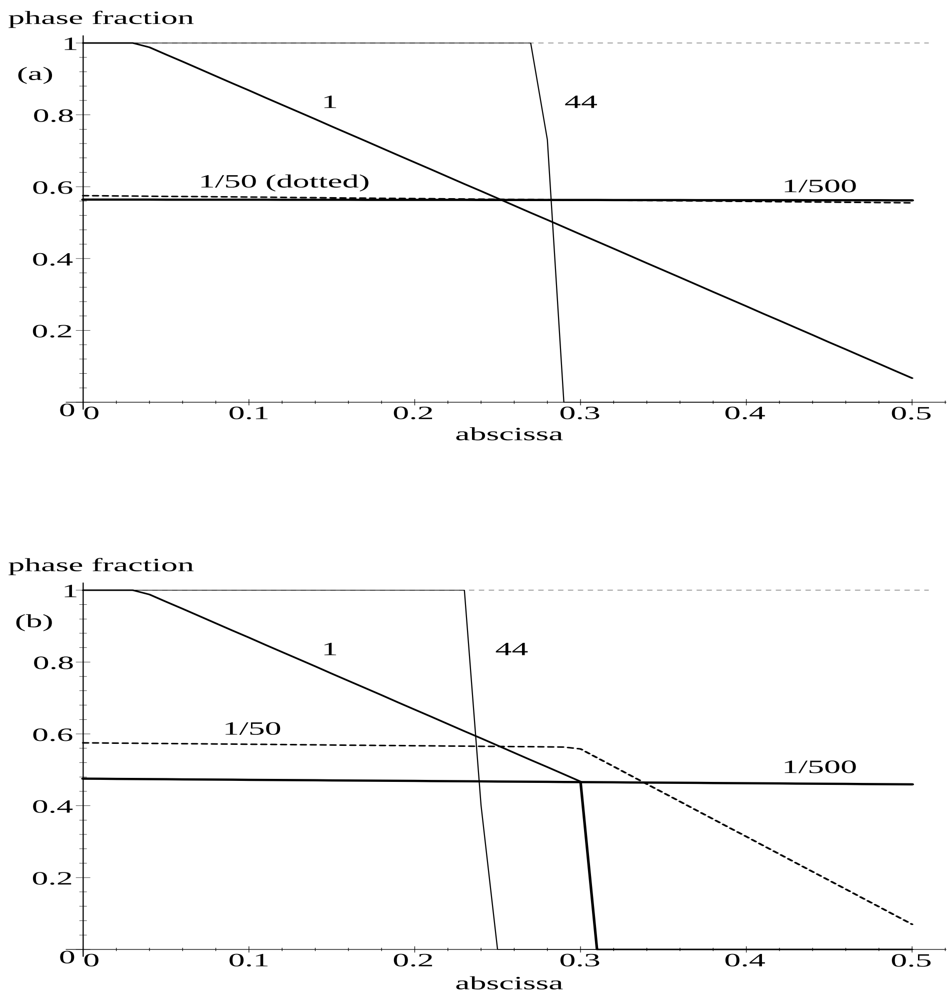


Figure 12: Example 1. Distribution of volume fraction $c(x)$ along the bar at the end of loading (a) and unloading (b), for various (scaled) inhomogeneity parameter $\rho/\rho_0$

induced by that cycle disturbs subsequently the regular response of the system, compare Figs. 13a and 11c. Notice the sharp knicks in Fig. 14a and b. Finally, some accumulation of the deformation history can also be observed in the case of the very small inhomogeneity $\rho = \rho_0/2000$ corresponding to the hardening modulus $L = 1.68B = 2.1813$, see Fig. 14c.

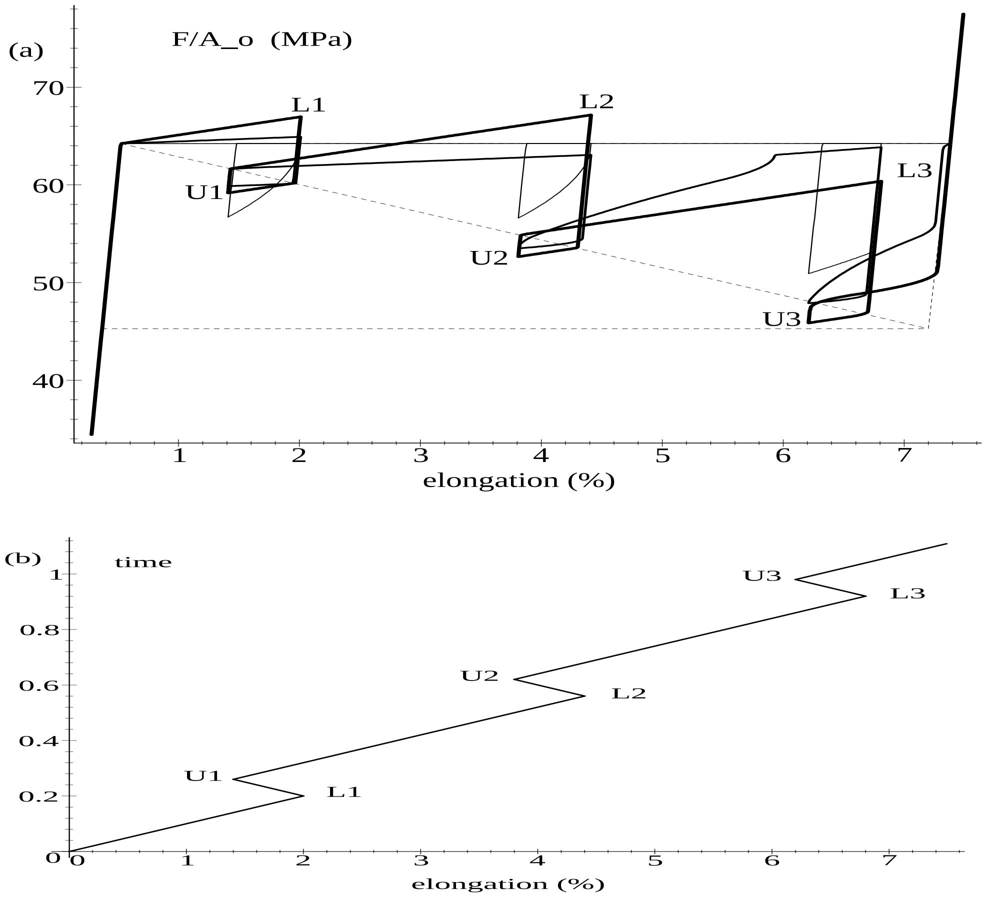


Figure 13: Example 2. (a) Force $F$ at the end of bar as a function of elongation $\ell(t)$ shown in (b), for various (scaled) inhomogeneity parameter: $\rho/\rho_0 = 1$ (thin line), $\rho/\rho_0 = 1/500$ (medium line), $\rho/\rho_0 = 1/2000$ (thick line)

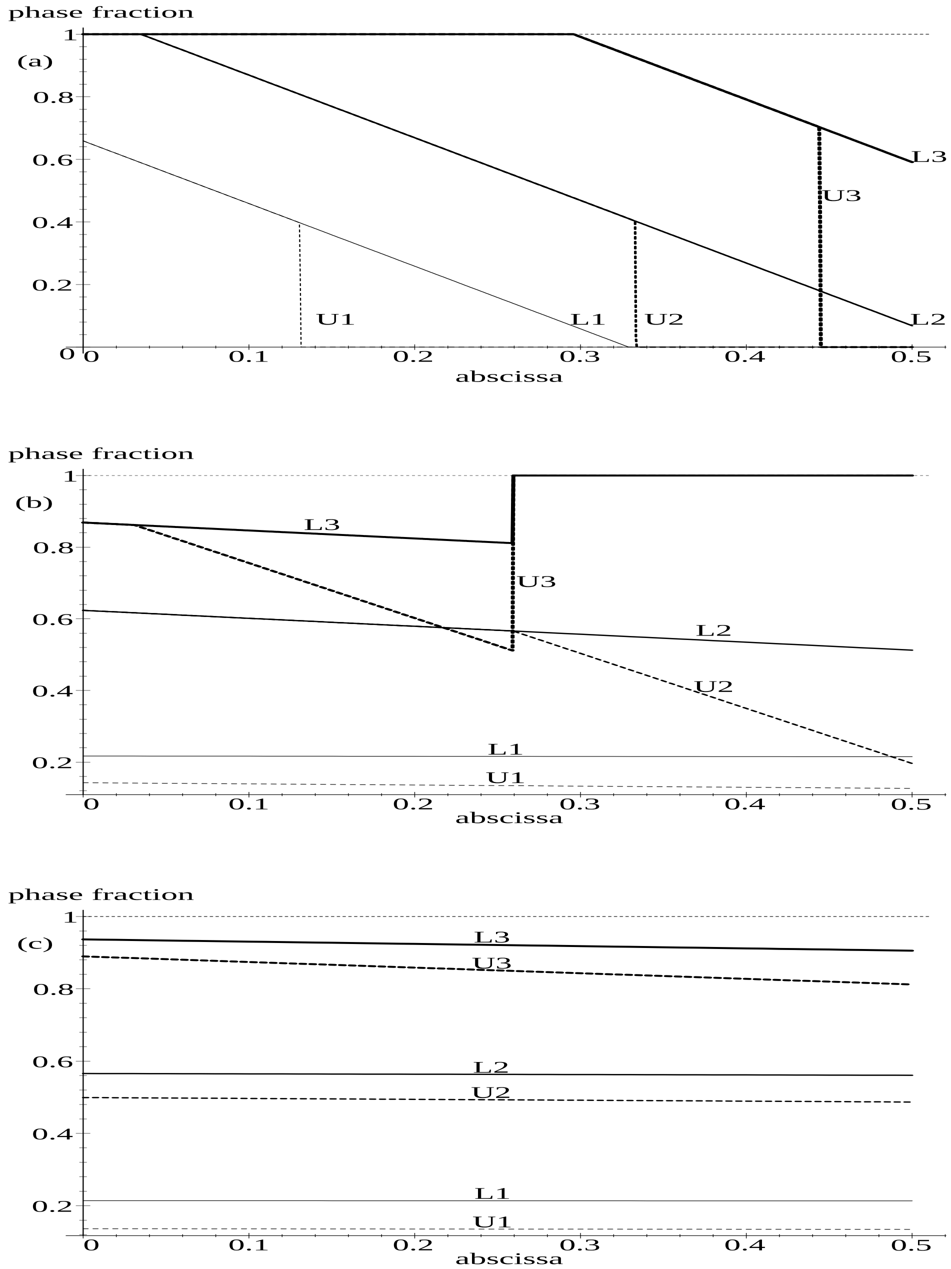


Figure 14: Example 2. Distribution of volume fraction $c(x)$ along the bar at the end of the loading and unloading steps shown in Fig. 13b, for (a) $\rho/\rho_0 = 1$, (b) $\rho/\rho_0 = 1/500$, (c) $\rho/\rho_0 = 1/2000$

### 4.1.4 The non-isothermal problem

As evidenced in experimental tests on shape memory alloys, during the phase transformation process (latent) heat is generated (in case of forward PT) or absorbed (reverse PT), e.g. [166, 160, 187]. Furthermore, the experiments carried out at various temperatures of bath, $\theta_0$, show that the transformation stress depends on the temperature, and that this dependence may be assumed linear as a first approximation. MÜLLER and his co-workers, e.g. [122] revealed that the area of external (limit) hysteresis loops in the force-elongation diagram remains constant. In simple terms, we may say that the stress-strain diagram moves up when the temperature is increasing, or moves down upon a decrease in the temperature. Note that the place where the heat is generated or absorbed is not known in advance, because the location of the phase transformation front is an unknown of the problem. Similar in some aspects to the present problem, the one-dimensional IBVP for phase transformations with temperature coupling has been considered in [130, 34, 17, 94, 197].

The heat equation for the phase transformation problem we have derived from the first law of thermodynamics, cf. e.g. [59, 151], by making use of Fourier's law of heat diffusion

$$\dot{q} = -k\frac{\partial \theta}{\partial x} \tag{4.22}$$

where the proportionality factor $k$ is known as the thermal conductivity, and Newton's law of cooling

$$\dot{r} = \beta_{en}[\theta^{en} - \theta(x,t)]A_s \tag{4.23}$$

which incorporates the heat transfer from the sides of the bar, with $\beta_{en}$ being the coefficient of heat transfer, $\theta^{en}$ the temperature of the bath (environment) and $A_s$ is the area of the bar's surface per unit length. Finally, we arrive at the coupled heat equation of the form

$$d(\varepsilon, c)\dot{c} + \tilde{C}\dot{\theta} - k\theta_{,xx} + E\beta_0\theta\dot{\varepsilon} - \beta_{en}[\theta^{en} - \theta(x,t)]A_s = 0, \tag{4.24}$$

where

$$d(\varepsilon, c) = B/2 + (e_2^0 - e_1^0) - E\eta(\varepsilon + \beta_0\theta^0) + (E\eta^2 - B)c$$

and $\tilde{C} = \rho C_v$ with $\rho$ and $C_v$ being the density and specific heat of the alloy, respectively, $\beta_0$ is the coefficient of thermal expansion at reference temperature $\theta^0$. In what follows we restrict ourselves to a reduced form of (4.24) in which the piezoelectric effect and the heat transfer through the sides of the bar are neglected,

$$d(\varepsilon, c)\dot{c} + \tilde{C}\dot{\theta} - k\theta_{,xx} = 0. \tag{4.25}$$

A typical time step for the non-isothermal evolution of the two-phase bar can be defined as follows.

Given $S_{n-1} = (u_{n-1}, c_{n-1}, p_{n-1}, \theta_{n-1})$, find $S_n = (u_n, c_n, p_n, \theta_n)$ from $u_n(x) = \int_0^x \varepsilon_n(y)\,\mathrm{d}y$ and the following conditions:

$$\alpha(x)\,\Sigma\left(\varepsilon_n(x), \theta_n(x), c_{n-1}(x), p_{n-1}(x)\right) = F_n - \int_x^{l_B} f_n(y)\,\mathrm{d}y, \quad x \in (0, l_B),$$

$$d(\varepsilon_{n-\xi}(x), c_{n-\xi}(x))\frac{c_n(x) - c_{n-1}(x)}{\Delta t_n} + \tilde{C}\frac{\theta_n(x) - \theta_{n-1}(x)}{\Delta t_n} - k\frac{\mathrm{d}^2\theta_n(x)}{\mathrm{d}x^2} = 0,$$

$$\int_0^{l_B} \varepsilon_n(x)\,\mathrm{d}x = \ell_n,$$

with

$$c_n(x) = \mathcal{C}(\varepsilon_n(x), \theta_n(x), c_{n-1}(x), p_{n-1}(x)),$$
$$p_n(x) = \mathcal{P}(\varepsilon_n(x), \theta_n(x), c_{n-1}(x), p_{n-1}(x)).$$

(4.26)

where $0 \leq \xi \leq 1$ and $\Delta t_n = t_n - t_{n-1}$. Approximating the operator $\mathrm{d}^2/\,\mathrm{d}x^2$ by a second centered difference, we finally integrate the nonisothermal phase transformation problem by a backward in time and centered in space scheme.

The functions $\Sigma$, $\mathcal{C}$ and $\mathcal{P}$ are defined as in (4.15), (4.17) and (4.18), but now depend also on the changing temperature $\theta$ through the characteristic strains (4.16) and $\gamma$ which is a function of $\theta$, i.e. $\gamma = B/2 - (e_2^0 - e_1^0) - (s_2^0 - s_1^0)\theta$. The length of the bar is $l_B = 0.015$ m, and the following initial and boundary conditions were considered:

$$\theta(x, 0) = \theta_0, \quad c(x, 0) = 0, \quad u(x, 0) = 0,$$

$$\theta(0, t) = \theta(l_B, t) = \theta^0, \quad u(0, t) = 0, \quad u(l_B, t) = \ell(t).$$

The temperature at the ends of the bar was kept equal to $\theta^0 = 273.00$ K, while the bar was stretched by a bilinear loading $\ell(t)$ with various speeds which was constant in each run, $|\dot{\ell}(t)| =$ constant. The elongation is at first increasing for $t \leq 0.925$ seconds and then decreasing. Following [34, 17] we have used $B = 0.60$ MPa, $L = 1.001B$, $\eta = 0.06$, $\tilde{C} = 3.4265$ MPa/K, $k = 376.0$ W/mK, $\rho = 8900.0$ kg/m$^3$, $E = 10000.0$ MPa.

For solving the nonisothermal problem we have used two numerical schemes. In the first case, the time-step $t_{n-1} \Longrightarrow t_n$ is split in a strain-step and a temperature step, so the problem is treated as semi-coupled. At instant $t_n$, for given state $S_{n-1} = (u_{n-1}, c_{n-1}, p_{n-1}, \theta_{n-1})$ and frozen temperature $\theta = \theta_{n-1}$, first the conditions $(4.26)_{1,3}$ are satisfied, and then for the determined $(u_n, c_n, p_n)$ the temperature is updated by solving the heat equation $(4.26)_2$. In the second case, the fully coupled strain-temperature steps are calculated, where we require that the state $S_n$ at a material point must satisfy all the strain-stress-temperature relations (4.26) at the current time $t_n$. As the stop-criterion we have checked the relative error in elongation and relative changes in temperature and other quantities. Obviously, the convergence rate of the fully coupled scheme is lower.

The scaled force-elongation diagram, $(F/A_0) - (\ell(t)/l_B)$, displayed in Fig. 15, was obtained with the two schemes at the elongation rate of 6.67 %/s. Fig. 16 illustrates the dependence of the force-elongation loops on the speed of elongation. The obtained results are in agreement with the experimental observations [100], and show that the influence of temperature on the phase transformation process in the bar is important.

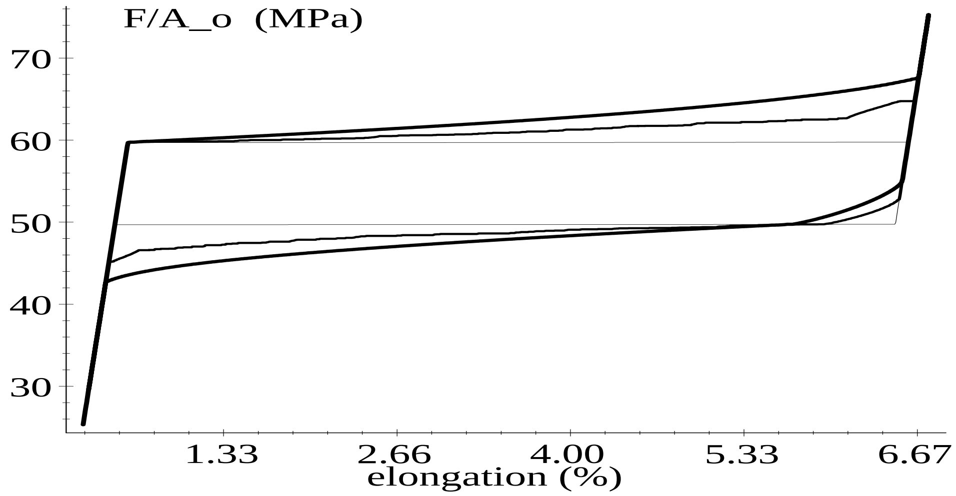


Figure 15: Scaled force $F/A_0$ at the end of the bar as a function of (scaled) elongation $\ell/l_B$. Thin line: isothermal case, medium line: semi-coupled strain-temperature steps, thick line: fully coupled strain-temperature steps

The evolution of volume fraction $c$ and temperature $\theta$ along the bar can be seen by comparing their distribution at the selected states A,...,C'. Observe

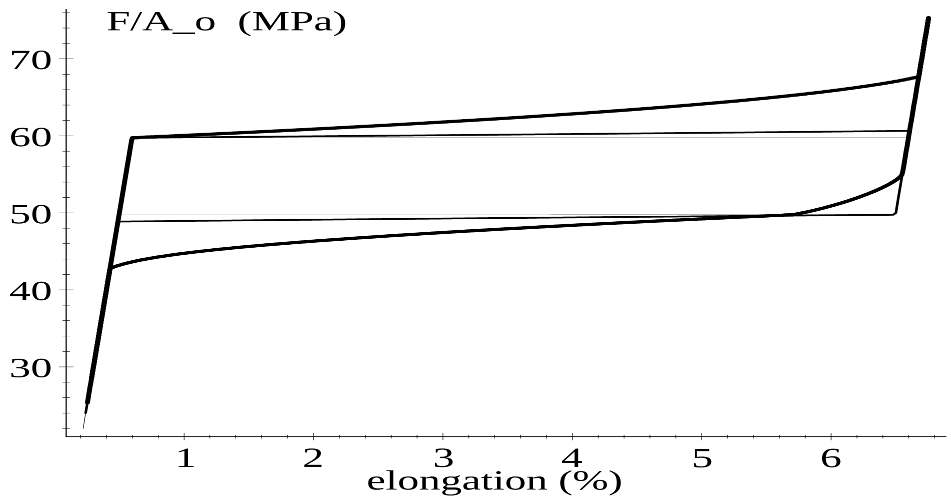


Figure 16: Scaled force $F/A_0$ vs. scaled elongation $\ell/l_B$, obtained with the fully coupled strain-temperature scheme, for various elongation rates. Thin line isothermal case, medium line — 0.667 %/s, thick line — 6.67 %/s

that although each pair of states (A,A'), (B,B'), and (C,C') is associated with the same scaled elongation (overall strain), the corresponding distribution of $c$ and $\theta$ are quite different at A and A', for example. As Fig. 17 shows, the phase transformation starts at the ends of the bar, where the constant temperature condition is imposed. With the semi-coupled scheme we have observed at some places the "algorithmic" unloading for positive elongation increments of the bar's ends, as reported in [17] which have, however, not appeared with the fully coupled scheme. Hence, the characteristic needles were not observed.

Summing up the obtained results, we want to recall two points. The influence of temperature on the stress-assisted phase transformation process (i) is the more pronounced the greater the deformation speed and (ii) it makes the corresponding boundary value problem inhomogeneous. Expressed in other words, point (i) says: the thermomechanical coupling in the thermoelastic phase transformation process results in the *temperature-induced rate dependence* on the level of system behaviour. The observed widening of the stress hysteresis under increasing strain rates is in agreement with the experimental results of Schroeder & Wayman [159] and Lexcellent, Licht & Goo [100].

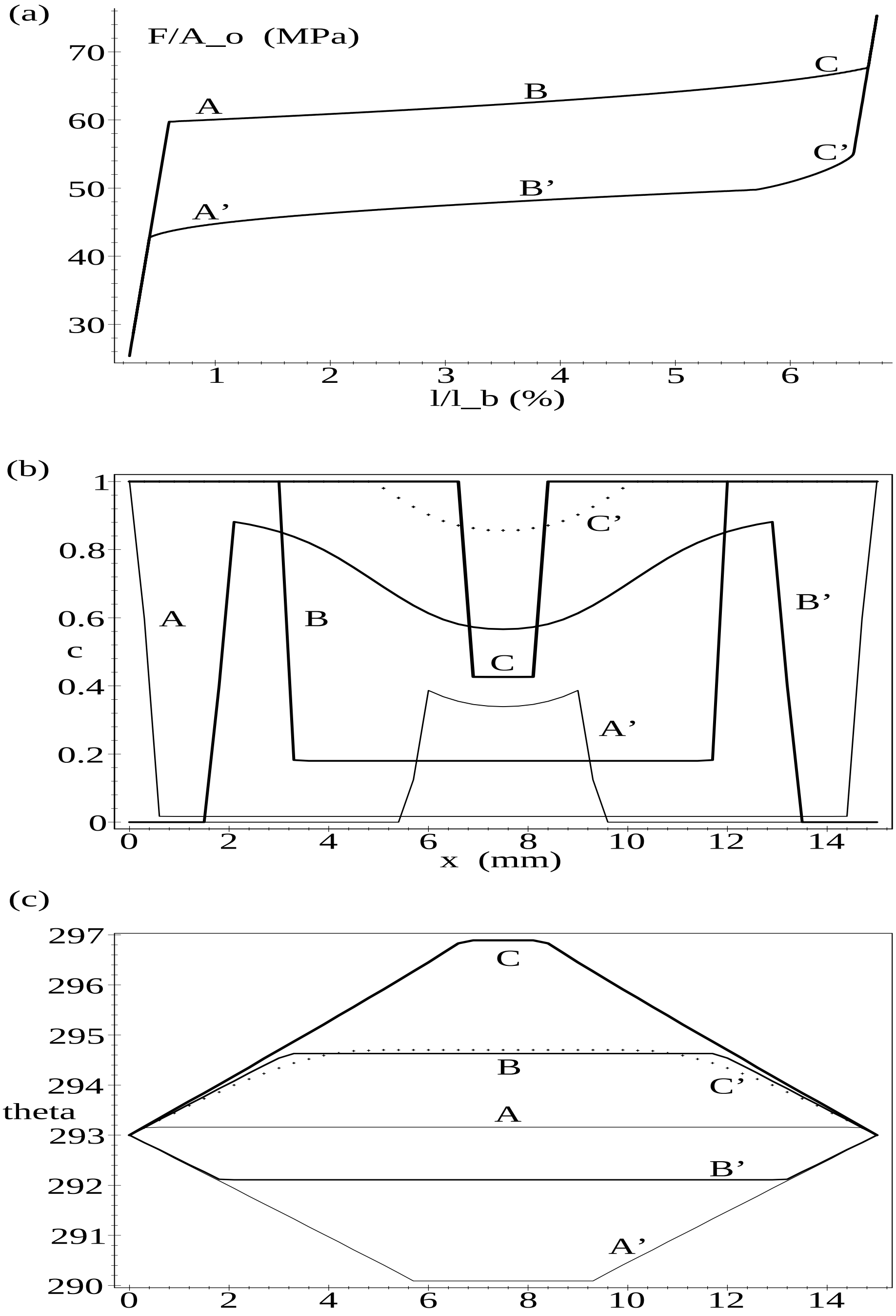


Figure 17: Selected states A,B,...,A' on the force-elongation diagram, (a). Distribution of phase fraction, (b), and temperature, (c), along the bar at the selected states. (The fully coupled strain-temperature scheme)

### 4.1.5 On the description of internal hysteresis loops

The thermomechanical model under consideration accounts for the hysteresis effects of friction type by making use of the threshold functions $\kappa^+$ and $\kappa^-$ in the PTC (4.10). The system (4.10) supplemented with the equations of (static) equilibrium govern completely the evolution of the phase mixture. Nevertheless, the modelling of the internal loops appears to be a delicate matter. In the hysteretic behaviour shown in Fig. 6, it is convenient to introduce a (discrete) memory variable $p$ whose evolution law may be formulated in the form

$$\begin{cases} \dot{p}(t,x,\theta) = 0, & \text{if} \quad X(t,x,\theta) \neq 0, \\ p(t_\star,x,\theta) = c(t_\star,x,\theta), & \text{if} \quad X(t_\star,x,\theta) = 0. \end{cases} \tag{4.27}$$

Thus, as defined above the function $p$ suffers jumps at times $t = t_\star$ at which the driving force $X$ equals zero. However, whenever a loading path slightly crosses the diagonal and then the direction of the response is reversed we have unstable behaviour: compare the paths, at a single material point, in Figs. 18a and 18b, where the deformation process depends discountinuously on the loading history.

The critical point here is the reloading-after-elastic-unloading (and re-unloading-after-elastic-loading) segment in the stress-strain diagram on which, in fact, there is no total consensus among the researches. This situation is illustrated in Fig. 19 where reloading from the state C is the passive, elastic process ($\dot{c} = 0$) in direction CB according to MÜLLER *et al.* [122, 59], whereas by RANIECKI *et al.* [151] it is the active austenite-martensite phase transformation flow ($\dot{c} > 0$) in direction CE.

Accounting for the type of behaviour due to Raniecki we can formally modify the evolution law for the memory variable $p$ to the following form,

$$p(t) = c(t) - \frac{1}{L} X(t) \tag{4.28}$$

where $X$ is the driving force defined in (4.7). Hence for the states on the diagonal – $p$ equals $c$, on the segments of pseudoelastic flow – $p$ remains constant, and during passive processes – $p$ continuously approaches $c$.

Observe that after the change in the evolution law for $p$, the previous formulae (4.15) and (4.17) for $\pm$ and $\mathcal{C}$, together with the formulation of the corresponding incremental boundary value problem (4.20) are still in force. Only for the function $\mathcal{P}$ previously defined in (4.18) we have now the expression

$$\mathcal{P}(\varepsilon, c) = (1 - B/L + E\eta^2/L)\, c - \frac{E\eta}{L}\, \varepsilon + \frac{1}{L}(\Delta\varpi + B/2). \tag{4.29}$$

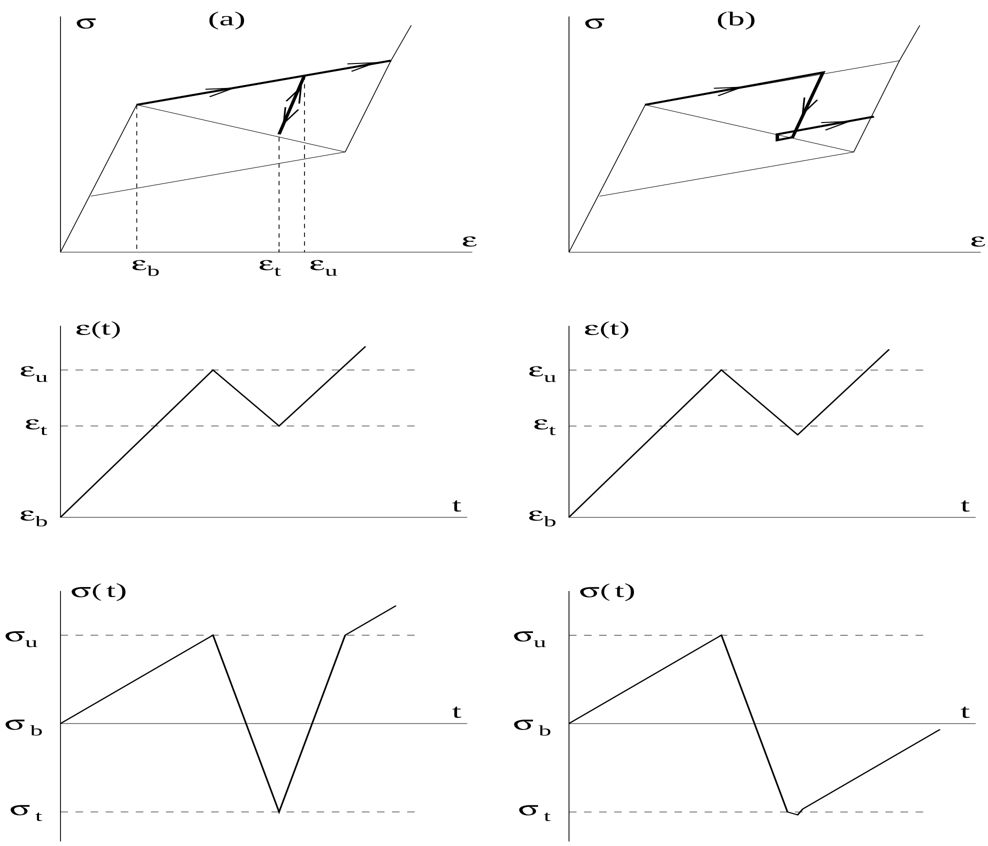


Figure 18: Illustration of a discontinuous response of the thermomechanical model

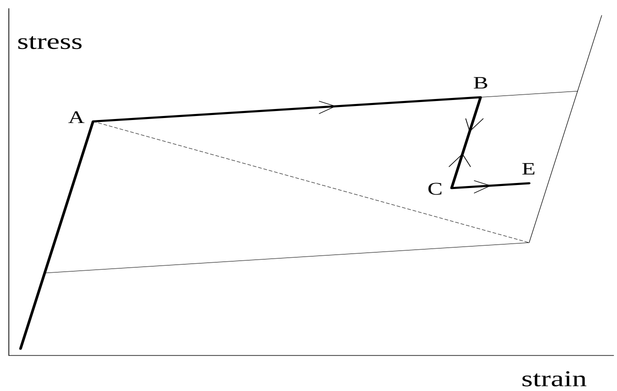


Figure 19: The different reloading responses from the state C: (i) in direction C-B by Müller, (ii) in direction C-E by Raniecki

Applying this new evolution law we have re-calculated Example 2 of Section 4.1.3 with the three loops shown in Fig. 13. The results we obtained this time, cf. Fig. 20, indicate that also in the present case the system behaviour depends upon the inhomogeneity parameter.

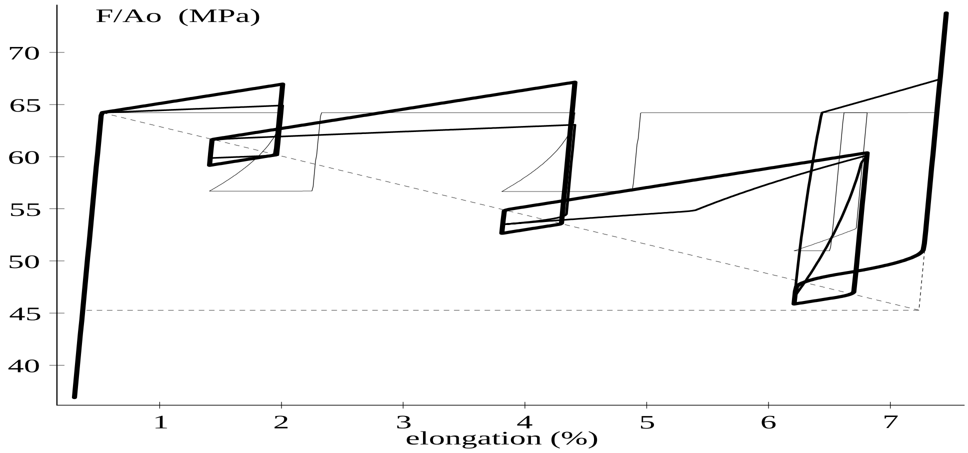


Figure 20: Example 2 of Sec. 4.1.3 recalculated with the evolution law (4.29) for the memory variable $p$, to be compared with the scaled force-elongation $(F/A_0)$ – $(\ell(t)/l_B)$ shown in Fig. 13b, for various (scaled) inhomogeneity parameter: $\rho/\rho_0 = 1$ (thin line), $\rho/\rho_0 = 1/500$ (medium line), $\rho/\rho_0 = 1/2000$ (thick line)

We may conclude that it is not the definition (4.27) of the variable $p$ which is responsible for the discontinuities shown in Figs. 12 and 14, which develop in the inhomogeneous system. The reason seems to be the hysteretic behaviour shown in Fig. 6 itself. It goes without saying that our modelling of the very complex hysteresis loops observed in experiments by means of the variable $p$ should be understood as a first approximation of accounting for this phenomenon, which is based rather on macroscopic observations. How a memory variable evolves in shape memory alloys under cyclic loading is, however, a difficult and subtle question which requires further research, for related discussions see [137, 190, 180, 5, 11]. But, it should be remarked that the use of $p$ is not central to the approach we develop in this work. In particular, we may stipulate that the phase transformation flow will take place only along the interval AB (forward PT with $p = 0$) and the interval DE (reverse PT with $p = 1$). Then, the thresholds assigned in (4.11) become

$$\kappa^+ = \kappa^+(c) = Lc, \qquad \kappa^- = \kappa^-(c) = L(c-1). \tag{4.30}$$

## 4.2 The two-phase system

In this section we develop a variational inequality approach to the hysteretic behaviour of a two-phase thermoelastic material undergoing stress-induced coherent martensitic PT. We shall build on the thermomechanical concepts introduced in the context of the one-dimensional model of Section 4.1. The thermomechanical model applied here was developed by many workers who contributed to its different aspects and generalizations, Müller *et al.* [59], Raniecki *et al.* [151, 152, 148, 150], Levitas *et al.* [97, 99]. The model is based on quadratic free energies for the parent phase, $W_1$ and the product phase, $W_2$. As before, the free energy of the mixture $\widetilde{W}$ (per unit volume) is a weighted sum of the component energies and the 'mixing' energy

$$\widetilde{W} = (1-c)\, W_1 + c\, W_2 + W_{\text{mix}} \tag{4.31}$$

wherein $c \in [0, 1]$ is the volume fraction of the martensite phase. The final form of (4.31) as given in (4.33) resembles the expression rigorously derived in a mathematical way by Kohn [75] who uses a relaxation procedure at fixed volume fractions. The directly related work in metallurgy is by Khachaturyan [69].

Our goal here is to formulate in a unifying manner the corresponding rate boundary value problem for a three dimensional body made from a two-phase material exhibiting the hysteretic behaviour shown in Fig. 6. The proposed formulation takes the form of a variational inequality of the first kind, which is defined on the product set $V \times K$ where $V$ is the space of kinematically admissible (finite increments of) displacements, $\boldsymbol{u} \in V$, and $K$ is the convex set of admissible volume fractions, $c \in K$. Under appropriate hypotheses, the existence and uniqueness of a solution to the incremental-in-time problem is proved. The variational inequality assures the satisfaction in weak form of both the equilibrium conditions and the phase transformation rules. Furthermore, the domain (in a special case: boundary) between the region where the material is the pure austenite phase and that where it is in the pure martensite state, which is the additional unknown of the problem, is determined automatically as a sort of "by-product" by solving the variational inequality. The rate boundary value problem is integrated in time by an implicit scheme and for its space discretization the finite element method is applied. Finally, the governing variational inequality is solved as a sequence of linear complementarity problems. To this end, we have developed two numerical algorithms: one based on the classical idea of pivoting, whereas the other operates in two steps by combining the Symmetric Successive Overrelaxation with Projection method (SSORP) and the Preconditioned Conjugate Gradient method (PCG). We have verified the proposed formulation and algorithms by simulating the uniaxial tension test on shape-memory strips. The strips are initially in an austenitic phase which under prescribed end elongation transforms in a martensitic phase and subsequently, under releasing, returns to the initial state. The numerical results reveal the influence of the phase transformation strain and boundary conditions on the propagation of the transformation front and the deformation mode of the specimen. They are in good qualitative agreement with the available experimental observations.

### 4.2.1 Free energy and thermomechanical relations

The type of hysteretic behaviour we wish to describe is schematically illustrated in Fig. 6. We consider the quasi-static isothermal evolution of a two-phase thermoelastic solid which undergoes a martensitic transformation. The problem is treated in the context of small deformations, under the assumption that the material prefers two strain states: the parent phase (*austenite*), and the product phase (*martensite*). It may be noted that a two-component model for martensitic phase transformations is a conceptual simplification as the martensite phase may, in general, appear in many variants, e.g. six variants of martensite in a cubic to orthorombic transformation, cf. BHATTACHARYA [9]. We consider the multi-phase problem in the next section 4.3. In its natural state at a temperature $\theta^0$ ($\theta^0 > A_f^0$) the body occupies an open region $\Omega \subset \mathcal{R}^d$ with $d = 1, 2, 3$. In a material point (particle) $\boldsymbol{x} \in \Omega$ we postulate the Helmholtz free energy $W_i$, $i = 1, 2$ in the form

$$W_i(\boldsymbol{E}, \theta) = \frac{1}{2}\,(\boldsymbol{E} - \boldsymbol{D}_i) \cdot \mathbb{A}_i\,[\boldsymbol{E} - \boldsymbol{D}_i] + \varpi_i(\theta),$$

where, for simplicity, the 4th order tensors of elasticity $\mathbb{A}_i$ are assumed to be the same for each phase, $\mathbb{A}_1 = \mathbb{A}_2 = \mathbb{A}$. By $\boldsymbol{E} = \boldsymbol{E}(\boldsymbol{u}) = \frac{1}{2}(\nabla\boldsymbol{u} + (\nabla\boldsymbol{u})^{\mathrm{T}})$ we denote the strain tensor, whereas $\boldsymbol{D}_i$ is the *transformation strain* of $i$th phase (structure domain, [69]), and a dot $\cdot$ designates the scalar product of tensors (and vectors). The phase transformation strains $\boldsymbol{D}_i$ are a function of the crystal structures of the parent and product phases and so they may be assumed constant during the deformation process. Taking the austenite lattice as the reference state, we may set $\boldsymbol{D}_1 = \boldsymbol{0}$ and the transformation strain $\boldsymbol{D}_2 \equiv \boldsymbol{D}$. The function $\varpi_i(\theta)$ depends on temperature $\theta$, treated here as a parameter, and $\varpi_i(\theta)$ is defined in (4.3). The free energy function is a two-well functional which is piecewise quadratic

$$W(\boldsymbol{E}) = \min\{W_1(\boldsymbol{E}), W_2(\boldsymbol{E})\}\,. \tag{4.32}$$

But, it is known that if the free energy function of the elastic material is not quasiconvex [6, 7, 18, 113], it is possible to find a boundary value problem for which the energy functional has no minimizer. This mathematical property of the phase transformation problem is connected with the "proclivity" of the material to form a finer and finer microstructure, when minimizing the elastic energy. Quasiconvexification of the phase transformation problem is a remedy used for its regularization which leads to an energetically equivalent solution, that is still of great importance. Denoting by $c$ the volume fraction of martensite we can define the free energy of the mixture by

$$\widetilde{W}(\boldsymbol{E},c) = \frac{1}{2}\,(\boldsymbol{E}-c\boldsymbol{D})\cdot\mathbb{A}[\boldsymbol{E}-c\boldsymbol{D}] + ((1-c)\varpi_1 + c\varpi_2) + \frac{1}{2}Bc(1-c). \quad (4.33)$$

Observe that the function $\widetilde{W}$ defined in (4.33) corresponds to the relaxation at fixed volume fractions $Q_cW(\boldsymbol{E})$ derived by KOHN, see equation (3.11) in [75]. We recall that for the function $W$ specified in (4.32) its relaxation $Q_cW(\boldsymbol{E})$ at fixed $c \in [0,\,1]$ is defined as, cf. [75], (with $|U| \equiv \operatorname{meas} U$)

$$Q_cW(\boldsymbol{E}) = \inf_{\chi}\ \inf_{\boldsymbol{\varphi}|_{\partial U}=\boldsymbol{0}}\ \frac{1}{|U|}\int_U [(1-\chi)W_1(\boldsymbol{E}+\boldsymbol{C}(\boldsymbol{\varphi}))+\chi W_2(\boldsymbol{E}+\boldsymbol{C}(\boldsymbol{\varphi}))] \quad (4.34)$$

where $\boldsymbol{C}(\boldsymbol{\varphi}) = \frac{1}{2}(\nabla\boldsymbol{\varphi} + (\nabla\boldsymbol{\varphi})^{\mathrm{T}})$ and $\chi$, being the characteristic function equal to 0 or 1, describes a partition of $U$ into two phases, with the constraint that the volume fraction of the second phase equals $c$,

$$\frac{1}{|U|}\int_U \chi = c.$$

By $\boldsymbol{\varphi}$ we denote the test displacements with vanishing values at the boundary $\partial U$ of $U$. The minimization in (4.34) is carried out over the physical domain $U \subset \mathcal{R}^d$, with respect to the displacements $\boldsymbol{\varphi}$ and the partitions of $U$ into distinct phases described by distribution of $\chi$. The set $U$ may be related to the "representative volume element" in the theory of composites. However, unlike in an ordinary two-phase composite where inclusions exist at the outset and their placement and concentration are given, cf. [127], here the martensite inclusions nucleate in the course of the deformation loading process, so the volume fractions of constituent phases (variants) are not given *a priori*, but constitute the additional unknowns of the problem. (Homogenization techniques in analysis of periodic media are used in [182].) In our context here, we only remark that the minimization in (4.34) does not depend upon the domain $U$. This is a more general result of the theory on quasiconvexification, see [75] and also [3, 188]. In deriving the expression for $Q_cW(\boldsymbol{E})$, Kohn [75] has used the relaxation via Fourier analysis with $\boldsymbol{\varphi}$ being periodic functions. The relaxation of $W$, denoted by $QW$, can finally be determined by the minimization of $Q_cW(\boldsymbol{E})$ with respect to $c$ over the interval $[0,\,1]$; for a one-dimensional case it is shown schematically in Fig. 21. The most useful property of $QW$ is that it has a minimizer with the corresponding minimal value equal to that of $W$ as defined in (4.32). In this work our point of departure is the function $\widetilde{W}$ by (4.33) which corresponds to Kohn's relaxed energy at fixed volume fractions, $Q_c W(\boldsymbol{E})$. We wish to stress the fundamental rôle which is played here by the term $W_{\mathrm{mix}}$. In the case of the free energy $\widetilde{W}$ of (4.33) $W_{\mathrm{mix}}$ depends on the material parameter $B$, but more general expressions are known in the literature, see [96, 148]. According to [59] the value of $B$ may be related to the area of hysteresis in the elongation-force diagram, another expression for $B$ is given in [75], cf. also [158]. In the case $B = 0$, the phase transformation proceeds at a constant stress (the Maxwell line) determined by the 'double tangent construction', what in mathematical terms amounts to the convexification of the energy $W$ assigned in (4.32) and is illustrated by the dotted bold line in Fig. 21.

In order to take into account the dissipation and hysteresis which are characteristics of the phase transformation behaviour illustrated in Fig. 6, we minimize the free energy $\widetilde{W}$, defined in (4.33), with respect to $c$ under the requirements imposed by the second principle of thermodynamics, supplemented with the postulate of realizability [97].

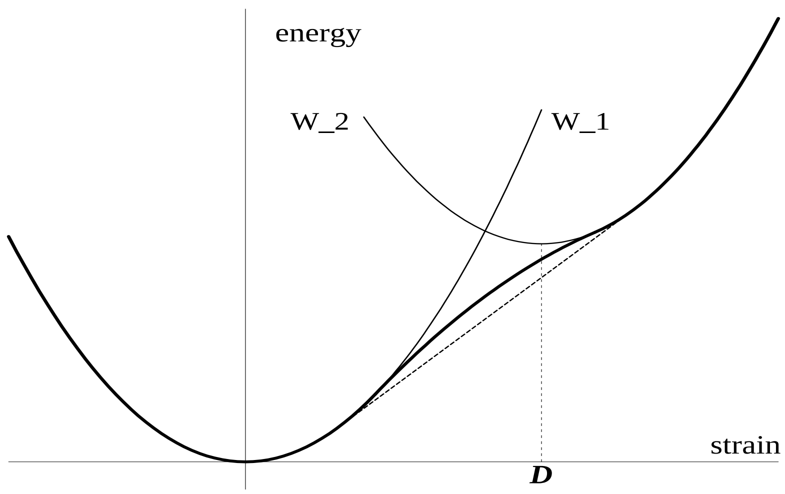


Figure 21: Quasiconvexified energy function $QW$ for a two-phase system with parabolic energies $W_1$ and $W_2$, and transformation strains $\boldsymbol{D}_1 = \boldsymbol{0}, \boldsymbol{D_2} \equiv \boldsymbol{D}$. The dotted bold line corresponds to the convexification of $W$

Requirement of the second law of thermodynamics,

$$\mathcal{D} = \boldsymbol{T} \cdot \dot{\boldsymbol{E}} - (\dot{\widetilde{W}} + s\dot{\theta}) \geq 0, \tag{4.35}$$

leads finally to the inequality, cf. (4.5),

$$\mathcal{D} = X\,\dot{c} \geq 0 \tag{4.36}$$

where the driving force of phase transformation, $X \equiv -\partial\widetilde{W}/\partial c$, is

$$X = \boldsymbol{T} \cdot \boldsymbol{D} - (\varpi_2 - \varpi_1) - \frac{1}{2}B(1 - 2c). \tag{4.37}$$

The condition $X = 0$ defines a plane in the space of stresses $\boldsymbol{T}$, parameterized by the volume fraction $c$. In the one-dimensional case $X = 0$ and $c \in [0,\, 1]$ describe the diagonal AD in Fig. 6. When related to the one-dimensional situation, the driving force $X = X(\boldsymbol{T}, c)$ is positive in the triangle ADB and negative in the triangle ADE of Fig. 6. We recall that the equilibrium states on the diagonal AD are unstable and, according to (4.36), are accompanied by no dissipation. Thus, accounting for the dissipation and consequently for hysteresis effects we assume that phase transformation may take place only if its driving force $X$ reaches some threshold values $\kappa^+$ or $\kappa^-$ defined in (4.11), with possible modifications discussed in section 4.1.5. For completeness we recall here the phase transformation conditions (4.10),

$$\boxed{\begin{array}{llll} \text{if} & X(c) = \kappa^+(c) & \text{then} & \dot{c} \geq 0 \\ \text{if} & X(c) = \kappa^-(c) & \text{then} & \dot{c} \leq 0 \\ \text{if} & \kappa^-(c) < X(c) < \kappa^+(c) & \text{then} & \dot{c} = 0 \end{array}} \tag{4.38}$$

The equilibrium equations for the stress tensor

$$\boldsymbol{T} = \partial\widetilde{W}/\partial\boldsymbol{E} = \mathbb{A}[\boldsymbol{E} - c\boldsymbol{D}] \tag{4.39}$$

take the form

$$\operatorname{div} \mathbb{A}[\boldsymbol{E}(\boldsymbol{u}) - c\boldsymbol{D}] + \boldsymbol{f} = \boldsymbol{0}. \tag{4.40}$$

where $\boldsymbol{f}$ is a body force per unit volume. For the rate boundary value problem considered later on, equations (4.40) should be supplemented by appropriate initial and boundary conditions. We assume that the latter are regular, i.e. they satisfy all the relations defining the problem.

### 4.2.2 Variational inequality formulation

First we reformulate the phase transformation conditions (4.38) in a form suitable later for the numerical solution of associated boundary value problems. To this end, we define the phase transformation functions

$$F^+(\boldsymbol{T}, c, p) \equiv \kappa^+ - X \geq 0, \qquad F^-(\boldsymbol{T}, c, p) \equiv X - \kappa^- \geq 0 \tag{4.41}$$

which correspond to the forward and the reverse phase transformation and $\dot{c}^+$ and $\dot{c}^-$ are the positive and the negative part of the rate of volume fraction, so that $\dot{c} = \dot{c}^+ - \dot{c}^-$, defined by

$$\dot{c}^+ \equiv \max\{\dot{c}, 0\} \geq 0, \qquad \dot{c}^- \equiv \max\{-\dot{c}, 0\} \geq 0. \tag{4.42}$$

Under these definitions we have the following result, compare the equivalence lemma 2.3.

**Lemma 4.2.** *The phase transformation rules (4.38) are equivalent to the rate variational inequality: for* $c \in [0,\, 1]$,

$$F^+(c) \cdot (y_+ - \dot{c}^+) + F^-(c) \cdot (y_- - \dot{c}^-) \geq 0 \quad \textit{for all } y_+,\, y_- \geq 0. \tag{4.43}$$

**Proof.** We prove the assertion in the special case that $c \in (0, 1)$. First, assume the 'if' part of $(4.38)_3$ so that $F^+ > 0$ and $F^- > 0$, then (4.43) implies that $\dot{c}^+ = \dot{c}^- = 0$, otherwise the existence of a $\dot{c}^+ = d > 0$ would lead to the contradiction: $F^+(c) \cdot (y_+ - d) < 0$ for all $y_+ < d$. Further, if one of the phase transformation functions is equal to zero, say, $F^+ = 0$, i.e. the 'if' part of $(4.38)_1$, then $\dot{c}^+ > 0$ satisfies (4.43) (a degenerated case $\dot{c}^+ = 0$ is also covered). Note that by (4.41) $F^+ = F^- = 0$ is possible only for the states on the diagonal AD in Fig. 6 and if the thresholds are defined as in (4.11); such a coincidence is not possible for thresholds assigned by (4.30). Finally, by satisfying inequality (4.43) on the positive cone $\mathcal{R}_+$, with $\dot{c}^+, \dot{c}^- \in \mathcal{R}_+$, we enforce the conditions (4.41). This completes the proof. ❑

*Remark* 1. The case $c = 0$ or $c = 1$ leads to the expression for $X$ which includes the subdifferential of the indicator function of interval $[0, 1]$, $\partial\chi_{[0,1]}(c)$. Formally, we may supplement the formula for $\widetilde{W}$,

$$\begin{aligned} \widetilde{W}_\chi(\boldsymbol{E}, c) &= \frac{1}{2}(\boldsymbol{E} - c\boldsymbol{D}) \cdot \mathbb{A}[\boldsymbol{E} - c\boldsymbol{D}] + ((1-c)\varpi_1 + c\varpi_2) + \frac{1}{2}Bc(1-c) \\ &\quad + \chi_{[0,1]}(c). \end{aligned} \tag{4.44}$$

In the light of the definition of the indicator function $\chi_{[0,1]}$, cf. (2.4), and its subdifferential,

$$\partial\chi_{[0,1]}(c) = \begin{cases} (-\infty, 0], & c = 0, \\ \{0\}, & c \in (0,1), \\ [0, +\infty), & c = 1, \end{cases} \tag{4.45}$$

we have the following expression for the driving force,

$$X = \boldsymbol{T} \cdot \boldsymbol{D} - \Delta\varpi - \frac{1}{2} B(1-2c) - r(c), \tag{4.46}$$

where the number $r(c)$, $r(c) \in \partial\chi_{[0,1]}(c)$, may be interpreted as a reaction to violation of the constraint that $c \in [0,1]$ (Lagrange's multiplier).

With $X$ defined by the extended formula (4.46) the nonnegativness conditions (4.41) are now satisfied also on the boundary of [0,1], i.e. $c = 0$, or $c = 1$, for any values of stress $\boldsymbol{T}$ and variable $p$. Normally, the constraint $\chi_{[0,1]}(c)$ is not included in an expression for free energy, with the exception of FREMOND [38]. In our further considerations the admissible changes of $c$ are controlled by the set of constraints $K$, cf. (4.48), which in terms of the numerical LCP algorithm (4.59), to be defined in section 4.2.4, lead to two vectors $\boldsymbol{r}^1$, $\boldsymbol{r}^0$. ❑

Inequality (4.43) implicitly defines the evolution law of $c$, thereby the kinetics of the strain induced by the phase transformation. Usually, the evolution law for the volume fraction variable is written in the form of an equation for the active phase transformation process which is the pivotal concern in the metalurgical literature. However, from the standpoint of computational mechanics one of the main difficulties lies in the determination of the domain in a body where the forward and reverse phase transformations do take place, i.e. where the evolution law(s) of $c$ with $\dot{c} \neq 0$ is in force, and the domain where the response is elastic and a different constitutive law with $\dot{c} = 0$ holds. The variational inequality encompasses both the "active" and the "passive" evolution of $c$, playing the role of a switch. It may be remarked that the above formulation of the phase transformation criteria is similar to that of the loading/unloading conditions in the flow theory of plasticity [89]. Yet, one of the main differences is due to the constraint $c \in [0,1]$ and that imposed on the plastic multiplier $\lambda$ which is bounded only from below and whose rate must be non-negative, i.e. $\lambda \geq 0$, with $\dot{\lambda} \geq 0$.

From the computational reasons, it is natural to express the functions (4.41) in terms of displacements through the strain tensor. This leads to the new phase transformation functions

$$
\begin{aligned}
G^{+}(\boldsymbol{E},c,p) &\equiv -\boldsymbol{D}\cdot\mathbb{A}[\boldsymbol{E}]+(\boldsymbol{D}\cdot\mathbb{A}[\boldsymbol{D}]-B)\,c+\kappa^{+}(c,p)+\Delta\varpi+B/2\\
G^{-}(\boldsymbol{E},c,p) &\equiv \boldsymbol{D}\cdot\mathbb{A}[\boldsymbol{E}]-(\boldsymbol{D}\cdot\mathbb{A}[\boldsymbol{D}]-B)\,c-\kappa^{-}(c,p)-\Delta\varpi-B/2
\end{aligned}
\tag{4.47}
$$

The discussed above formulation constitutes a natural advantageous basis for the numerical treatment of the problem. Toward this end, the finite dimensional counterpart of the variational inequality (4.43) in terms of the phase transformation functions (4.47) is obtained by the finite element method, and its evolution in time is solved as a sequence of linear complementarity problems.

### Weak formulation

For boundary value problems of practical significance it is necessary to solve the evolution problem (4.43) in a weak form with respect to the space variable, and incrementally in time. To this end, the relations (4.47) will be expressed in displacements through the strain tensor and imposed to be valid for the body $\Omega$ as a whole. Doing this, from (4.36) we arrive at a reduced form of the global Clausius-Duhem inequality [50]. We apply the implicit time integration scheme, imposing the phase transformation conditions (4.47) and the elastic equilibrium equations (4.40) at selected times $t_n \in [0,T]$, with $n = 1,2,\dots$, and $T < \infty$. This amounts to treating the evolution problem as the piecewise monotone one. In terms of the monotone path rule formulated in section 4.1.3, the decisive quantity is now the rate $\dot{\boldsymbol{T}}\cdot\boldsymbol{D}$ instead of the rate of stress $\dot{\sigma}$ (scalar) only.

Using the notations $\boldsymbol{u}_n \equiv \boldsymbol{u}(\cdot,t_n)$, $c_n \equiv c(\cdot,t_n)$ for the displacement vector and the volume fraction at time $t = t_n$ and the symbol $\Delta$ for finite increments, we define

$$
\begin{aligned}
\Delta\boldsymbol{u}_n &\equiv \boldsymbol{u}_n - \boldsymbol{u}_{n-1}\\
\Delta c_n &\equiv c_n - c_{n-1}
\end{aligned}
$$

Further, we split the function $\Delta\boldsymbol{c}_n$ into its positive and negative part, cf. (4.42), obtaining the decomposition

$$
\Delta c_n = \Delta c_n^{+} - \Delta c_n^{-}.
$$

Let $V(t_n)$ designate the set of kinematically admissible (increments of) displacements of the body $\Omega$ at time $t = t_n$,

$$
V(t_n) = \left\{\boldsymbol{v}\in H^1(\Omega,\mathcal{R}^d)|\ \boldsymbol{v}(\boldsymbol{x}) = \boldsymbol{w}(\boldsymbol{x},t_n)\ \text{ for a.e. }\ \boldsymbol{x}\in\Gamma_u\right\}
$$

where $H^1(\Omega, \mathcal{R}^d)$ is a usual Hilbert space of vector-valued functions defined on $\Omega$, i.e. the set of function which together with their first derivatives are square-integrable. By $\Gamma_u$ we denote a part of the boundary $\Gamma$ of region $\Omega$ where displacements $\boldsymbol{w}$ are prescribed (at time $t_n$). The sets $K_+(c_{n-1})$ and $K_-(c_{n-1})$ that impose constraints on the finite, positive $\Delta c_n^+$ and negative $\Delta c_n^-$ parts of increments of volume fraction take the form

$$
\begin{aligned}
K(z) &= \big\{ w \in L^2(\Omega) : \ 0 \le z + w \le 1, \, z \in Z \big\} \\
K_+(z) &= \big\{ w \in L^2(\Omega) : \ w \ge 0, \, z + w \le 1, \, z \in Z \big\} \\
K_-(z) &= \big\{ w \in L^2(\Omega) : \ w \ge 0, \, z - w \ge 0, \, z \in Z \big\} \qquad (4.48) \\
Z &= \big\{ z \in L^2(\Omega) : \ 0 \le z \le 1 \big\}
\end{aligned}
$$

where $L^2(\Omega)$ is the space of square-integrable functions.

Before giving a weak formulation of the boundary value problem we define the following bilinear and linear forms which correspond to relations (4.47) and (4.40),

$$
\begin{aligned}
a(\boldsymbol{w}, \boldsymbol{v}) &= \int_\Omega \mathbb{A}[\nabla \boldsymbol{w}] \cdot \nabla \boldsymbol{v} \, d\boldsymbol{x} \\
g(w, \boldsymbol{v}) &= \int_\Omega w \mathbb{A}[\boldsymbol{D}] \cdot \nabla \boldsymbol{v} \, d\boldsymbol{x} \qquad (4.49) \\
h(w, v) &= \int_\Omega (\boldsymbol{D} \cdot \mathbb{A}[\boldsymbol{D}] + L - B) w v \, d\boldsymbol{x}
\end{aligned}
$$

$$
\begin{aligned}
f_{n,n-1}(\boldsymbol{v}) &= \int_\Omega \Delta \boldsymbol{f}_n \cdot \boldsymbol{v} \, d\boldsymbol{x} + (\text{terms on}\, \Gamma)_{n,n-1} \\
b^{\pm}_{n-1}(c_{n-1}, w) &= \int_\Omega [B/2 + (\varpi_2 - \varpi_1) + L(c_{n-1} - p_{n-1})^{\pm}] w \, d\boldsymbol{x} \qquad (4.50) \\
&\quad \mp g(w, \boldsymbol{u}_{n-1}) \pm h(c_{n-1}, w).
\end{aligned}
$$

With these notations we can define a typical time step $t_{n-1} \Longrightarrow t_n$ of the incremental boundary value problem for the phase transformation process under consideration as the variational inequality.

$$\boxed{\begin{array}{l} \text{Find } (\Delta\boldsymbol{u}_n, \Delta c_n) \in V(t_n) \times K(c_{n-1}) \text{ such that} \\[1ex] \begin{array}{rcl} a(\Delta\boldsymbol{u}_n, \boldsymbol{v}) - g(\Delta c_n, \boldsymbol{v}) & = & f_{n,n-1}(\boldsymbol{v}) \\ \mp g(z_\pm - \Delta c_n^\pm, \Delta\boldsymbol{u}_n) \pm h(\Delta c_n, z_\pm - \Delta c_n^\pm) & \geq & \mp b_{n-1}^\pm(c_{n-1}, z_\pm - \Delta c_n^\pm) \end{array} \\[1ex] \text{for all } (\boldsymbol{v}, z_\pm) \in V(t_n) \times K_\pm(c_{n-1}). \end{array}} \tag{4.51}$$

Having solved (4.51) for increments $\Delta\boldsymbol{u}_n$ and $\Delta c_n$, we can easily update the discrete memory $p_{n-1}$ to $p_n$ at the current time $t = t_n$ by controlling the values of the driving force $X$, cf. the function $\mathcal{P}$ of (4.18) and discussion in Section 4.1.5 for the 1D case.

The first equation of the system (4.51) is a weak form of the equilibrium condition (4.40), whilst $(4.51)_2$ represents two variational inequalities which are a weak form of the phase transformation rules (4.38) in virtue of the equivalence (4.43). The system (4.51) can conveniently be discretized in space by the finite element method and is solved finally as a standard form of the linear complementarity problem, after some rearrangements due to the restricted variations of the variables $\Delta c_n^+$, $\Delta c_n^-$ and the fact that changes $\Delta\boldsymbol{u}_n$ of the displacement vector are not restricted in sign.

### 4.2.3 Existence and uniqueness

In this section we follow the line of reasoning presented in Section 3.1.3. Although both problems (3.44) and (4.51) have a lot in common, they are different as far as the constraint set $K$ is concerned. In (3.44), $K$ is a positive cone with vertex at the origin in $L^2(\Omega)$, whereas in (4.51) the corresponding set $K$ defined in $(4.48)_1$ is bounded. We shall show that a bilinear form $A$ associated with the variational inequality (4.51) is continuous and coercive on the product space $\mathcal{V} \sim \mathcal{V}_n \equiv V_n \times \Lambda$ with $\Lambda = L^2(\Omega)$, where $\mathcal{V}$ corresponds to homogeneous boundary conditions on $\Gamma_{u_n}$ (the latter are non-zero in the displacement-driven experiment). The set of constraints is now $\mathcal{K}_{n,n-1} \equiv V_n \times K_{n-1}$. For the test elements in $\mathcal{V}$ we will drop the index of time level,

$$u \equiv (\boldsymbol{u}, c), \qquad v \equiv (\boldsymbol{v}, z), \qquad u, v \in \mathcal{V},$$

but we keep the subscripts where it might cause some confusion, so we designate:

$$\Delta u_n \equiv (\Delta\boldsymbol{u}_n, \Delta c_n), \quad \langle\, l_{n,n-1},\, v\,\rangle \equiv f_{n,n-1}(\boldsymbol{v}) - b_{n-1}^+(z) + b_{n-1}^-(z), \tag{4.52}$$

where the linear forms $f_{n,n-1}(\boldsymbol{v})$, $b^{+}_{n-1}(z)$, $b^{-}_{n-1}(z)$ are defined in (4.50), and $l_{n,n-1}$ is an element of the topological dual of $V_n$, i.e., $l_{n,n-1} \in \mathcal{V}^{*}_{n}$.

Let us introduce the bilinear form $A : \mathcal{V} \times \mathcal{V} \longrightarrow \mathcal{R}$ by

$$A(u,\, v) \equiv a(\boldsymbol{u},\, \boldsymbol{v}) - g(c,\, \boldsymbol{v}) - g(z,\, \boldsymbol{u}) + h(c,\, z). \tag{4.53}$$

wherein the forms $a, g, h$ are defined in (4.49).

With the above notations (4.52) and (4.53) we can rewrite the problem (4.51) as the variational inequality:

Find $\Delta u_n \in \mathcal{K}_{n,n-1}$ such that

$$A(\Delta u_n, v - \Delta u_n) \geq \langle\, l_{n,n-1},\, v - \Delta u_n \,\rangle \quad \text{for all } v \in \mathcal{K}_{n,n-1}, \tag{4.54}$$

wherein

$$\begin{aligned} A(\Delta u,\, v - \Delta u) \;\; \equiv \;\; & a(\Delta \boldsymbol{u},\, \boldsymbol{v} - \Delta \boldsymbol{u}) - g(\Delta c,\, \boldsymbol{v} - \Delta \boldsymbol{u}) - g(z - \Delta c,\, \Delta \boldsymbol{u}) + \\ & h(\Delta c,\, z - \Delta c). \end{aligned}$$

The bilinear form $A$ is characterized by the following two lemmas.

**Lemma 4.3.** *The bilinear form $A$ is continuous on $\mathcal{V}$, that is, there exists a positive constant $k$ such that*

$$|A(u,\, v)| \leq k \, \|u\|_{\mathcal{V}} \, \|v\|_{\mathcal{V}} \quad \textit{for all } \; u,\, v \in \mathcal{V}. \tag{4.55}$$

**Proof.** The continuity of $A$ follows from the continuity of the bilinear forms $a, g$ and $h$, since it is easy to show that there exist positive constants $k_1$, $k_2$, $k_4$ such that

$$\begin{aligned} |a(\boldsymbol{u},\, \boldsymbol{v})| &\leq k_1 \, \|\boldsymbol{u}\|_V \, \|\boldsymbol{v}\|_V, \\ |g(z,\, \boldsymbol{v})| &\leq k_2 \, \|z\|_\Lambda \, \|\boldsymbol{v}\|_V, \\ |h(z, w)| &\leq k_4 \, \|z\|_\Lambda \, \|w\|_\Lambda, \end{aligned}$$

hence

$$\begin{aligned} |A(u,\, v)| \;\; &\leq \;\; k_1 \|\boldsymbol{u}\|_V \, \|\boldsymbol{v}\|_V + k_2 \|c\|_\Lambda \, \|\boldsymbol{v}\|_V + k_2 \|z\|_\Lambda \, \|\boldsymbol{u}\|_V + k_4 \|c\|_\Lambda \, \|z\|_\Lambda \\ &\leq \;\; \frac{1}{2} k \, (\|\boldsymbol{u}\|_V + \|c\|_\Lambda) \, (\|\boldsymbol{v}\|_V + \|z\|_\Lambda) = k \, \|u\|_{\mathcal{V}} \, \|v\|_{\mathcal{V}} \end{aligned} \tag{4.56}$$

with $k = 2 \max\{k_1,\, k_2,\, k_4\}$ and where inequality $\alpha + \beta \leq \sqrt{2} \left(\alpha^2 + \beta^2\right)^{1/2}$ was used. ❏

**Lemma 4.4.** *Let $H_p = \inf_\Omega(L - B)$ be strictly positive, $H_p > 0$. The bilinear form $A$ is coercive on $\mathcal{V}$, that is, there exists a constant $k_0 > 0$ such that*

$$A(v,\, v) \geq k_0 \, \|v\|^2_{\mathcal{V}} \quad \textit{for all } v \in \mathcal{V}. \tag{4.57}$$

**Proof.** We have, cf. (3.68),

$$\begin{aligned} A(v,\, v) &= \int_\Omega \left\{ (\boldsymbol{E}(\boldsymbol{v}) - z\boldsymbol{D}) \cdot \mathbb{A}[\boldsymbol{E}(\boldsymbol{v}) - z\boldsymbol{D}] + H_p z^2 \right\} \, \mathrm{d}x \\ &\geq \int_\Omega k_A \beta \boldsymbol{E}(\boldsymbol{v}) \cdot \boldsymbol{E}(\boldsymbol{v}) \, \mathrm{d}x + \int_\Omega \left( H_p - \frac{k_A \beta k_D}{1-\beta} \right) z^2 \, \mathrm{d}x, \end{aligned} \tag{4.58}$$

where $k_A$ is given in (3.6), $k_D = \sup_\Omega(\boldsymbol{D} \cdot \boldsymbol{D})$, and $\beta \in (0,1)$. Using Korn's inequality (3.66) and choosing $\beta = \frac{H_p}{(H_p + 2k_A k_D)}$ we arrive at the assertion (4.55),

$$A(v,\, v) \geq k_0 \, \left( \|\boldsymbol{v}\|^2_V + \|z\|^2_\Lambda \right) = k_0 \, \|v\|^2_{\mathcal{V}} \,,$$

with

$$k_0 = \min\left\{ \frac{k_A H_p k_K}{H_p + 2k_A k_D}, \frac{1}{2} H_p \right\}.$$

❏

The obtained results are gathered in the following theorem on the existence and uniqueness of solutions to (4.54), i.e., to the incremental problem (4.51).

**Theorem 4.5.** *Under the assumptions made on the data, there exists a unique solution of the problem (4.54). The solution depends continuously on data $l_{n,n-1} \in \mathcal{V}^*_n$.*

**Proof.** The assertion follows from Theorem 2.2. ❏

### 4.2.4 Linear complementarity problems

Let $\varphi_i(x)\,(1 \leq i \leq N)$ and $\psi_j(x)\,(1 \leq j \leq M)$ be the finite element bases we use for the displacement $\boldsymbol{u}$ and phase fraction $c$ in $H^1(\Omega)$ and $L^2(\Omega)$. In particular, the field of displacement $\boldsymbol{u}$ can be approximated by a piecewise quadratic polynomial, whereas for the function of phase fraction $c$ (and $p$) a piecewise linear approximation can be utilized. We remark that using of piecewise linear basis functions $\psi_j$ leads to the internal approximation of the sets $K_\pm$ in (4.48).

The finite dimensional counterpart of the weak formulation (4.51) may be expressed as the following linear complementarity problem:

$$\boxed{\begin{gathered} \boldsymbol{A}^\star \boldsymbol{x}_n + \boldsymbol{y}_n = \boldsymbol{b}_{n,n-1} \\ \boldsymbol{x}'_n \geq \boldsymbol{0},\ \boldsymbol{y}^1_n = \boldsymbol{0},\ \boldsymbol{y}_n \geq \boldsymbol{0},\ \boldsymbol{x}_n \cdot \boldsymbol{y}_n = 0 \end{gathered}} \tag{4.59}$$

in which $\boldsymbol{A}^\star$ is a square matrix, $\boldsymbol{x}_n$ is a vector of unknowns (nodal values of the finite element approximations), $\boldsymbol{y}_n$ denotes a vector of slack variables, and the vector $\boldsymbol{b}_{n,n-1}$ is known at time $t_n$. By $\boldsymbol{x}'_n$ we denote the elements of the vector $\boldsymbol{x}_n$, excluding the subvector $\boldsymbol{x}^1_n \equiv \Delta \boldsymbol{u}_n$ which is sign-unrestricted. The above matrix and vectors have the following structure

$$\boldsymbol{A}^\star = \begin{bmatrix} -\boldsymbol{K} & \boldsymbol{G}^{\mathrm{T}} & -\boldsymbol{G}^{\mathrm{T}} & \boldsymbol{0} & \boldsymbol{0} \\ \boldsymbol{G} & -\boldsymbol{H} & \boldsymbol{H} & -\boldsymbol{I} & \boldsymbol{0} \\ -\boldsymbol{G} & \boldsymbol{H} & -\boldsymbol{H} & \boldsymbol{0} & -\boldsymbol{I} \\ \boldsymbol{0} & \boldsymbol{I} & \boldsymbol{0} & \boldsymbol{0} & \boldsymbol{0} \\ \boldsymbol{0} & \boldsymbol{0} & \boldsymbol{I} & \boldsymbol{0} & \boldsymbol{0} \end{bmatrix}, \tag{4.60}$$

$$\boldsymbol{x}_n = \begin{Bmatrix} \Delta \boldsymbol{u}_n \\ \Delta \boldsymbol{c}^+_n \\ \Delta \boldsymbol{c}^-_n \\ \boldsymbol{r}^1_n \\ \boldsymbol{r}^0_n \end{Bmatrix}, \qquad \boldsymbol{b}_{n,n-1} = \begin{Bmatrix} \boldsymbol{f}^u_{n,n-1} \\ \boldsymbol{b}^{c+}_{n-1} \\ \boldsymbol{b}^{c^-}_{n-1} \\ \boldsymbol{1} - \boldsymbol{c}_{n-1} \\ \boldsymbol{c}_{n-1} \end{Bmatrix}.$$

Matrices $\boldsymbol{K}, \boldsymbol{G}$ and $\boldsymbol{H}$ are generated by the bilinear forms (4.49),

$$\begin{aligned} \boldsymbol{K} &= [K_{ij}] = [a(\varphi_i, \varphi_j)]\,, \quad \dim \boldsymbol{K} = N \times N, \\ \boldsymbol{G} &= [G_{ij}] = [g(\psi_i, \varphi_j)]\,, \quad \dim \boldsymbol{G} = M \times N, \\ \boldsymbol{H} &= [H_{ij}] = [h(\psi_i, \psi_j)]\,, \quad \dim \boldsymbol{H} = M \times M, \end{aligned}$$

and $\boldsymbol{I}$ is the $M \times M$ identity matrix corresponding to the vectors $\Delta \boldsymbol{c}^+_n$, $\Delta \boldsymbol{c}^-_n$ and their conjugates $\boldsymbol{r}^1_n$, $\boldsymbol{r}^0_n$. The latter are Lagrange's multipliers which are induced by the constraint imposed on the volume fraction that $c \in [0,\, 1]$, cf. remark 1. Vectors $\boldsymbol{b}^u_{n,n-1}$, $\boldsymbol{b}^{c^+}_{n-1}$ and $\boldsymbol{b}^{c^-}_{n-1}$ are generated by the linear forms (4.50). Matrices $\boldsymbol{K}$ and $\boldsymbol{H}$ are symmetric and positive definite.

### 4.2.5 Numerical examples

To illustrate some of the effects covered by the proposed model we have simulated numerically the basic, uniaxial tensile test on two-phase material strips, as a plane stress displacement-driven problem. Two examples are considered. Moreover, in Example 1 two cases were calculated with the same material parameters and boundary conditions, the difference is only in the proportion of *length* $a$ : *width* $b$, being 3:1 in Case 1 and 6:1 in Case 2. Example 2 differs from Example 1 in the following: (i) the middle point of the right-hand side of the strip, which has the coordinates $(x, y) = (a, b/2)$, is allowed to move transversely, (ii) the transformation strain tensor $\boldsymbol{D}$ is (slightly) different, (iii) the proportion of sides is 8:1 and, (iv) the cross-sectional area of the strip in not constant. Example 2 is motivated by the laboratory experiments of ICHINOSE *et al.* [61]. Due to lack of a complete set of material data at this time, we have used the following material parameters corresponding to a CuZnAl single crystal [59]: Young's modulus $E = 10000.00$ MPa, $B = 1.20$ J/m$^3$, $L = 1.01B$, Poisson's ratio $\nu = 0.30$, and the difference in energies at the stress free state $\Delta\varpi = \varpi_2 - \varpi_1 = 3.756$ J/m$^3$.

For the field of displacements $\boldsymbol{u}(\cdot, t) \equiv (u(\cdot, t),\, v(\cdot, t))$, in the coordinate axes $xy$, we have used a 6-node triangle finite element with quadratic shape functions (linear strain triangle), whilst for the volume fraction $c(\cdot, t)$ a 3-node linear triangle. The three possible layouts of one "cell" of the mesh are displayed in Fig. 22.

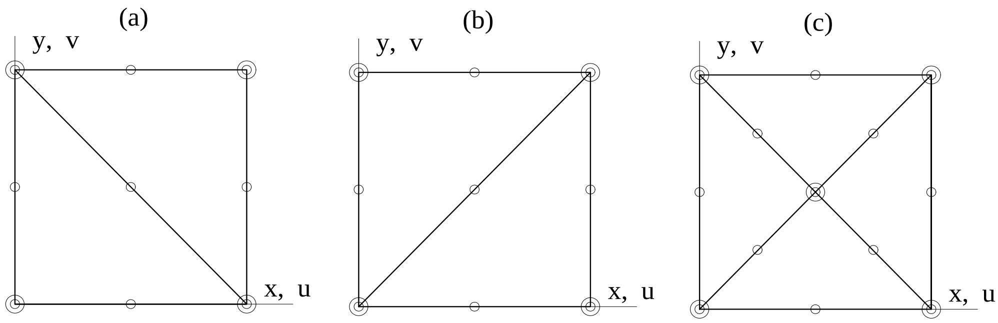


Figure 22: Types of finite element meshes: $\circ$ = node of the mesh of displacements $(u,\, v)$, $\bigcirc$ = node of the mesh of volume fraction $c$

For the solution of the resulting linear complementarity problems we used the direct algorithm in Example 1, and the iterative two-step algorithm (SSORP plus PCG) in Example 2, cf. Section 2.3.

**Example 1**

The strip and the imposed boundary conditions (4.61) are schematically displayed in Fig. 23. We used the uniform mesh of type shown in Fig. 22c with $(6 \times 18) \times 4$ finite elements. The following boundary conditions were taken:

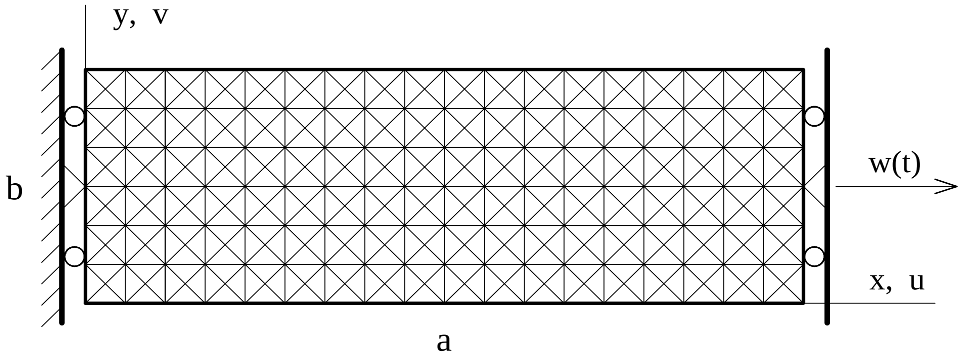


Figure 23: The strip made of a material with two preferred states, of length $a$ and width $b$ with $a : b = 12 : 4$, under uniaxial tension $w(t)$

$$\text{on the left-hand side of the strip} \quad \begin{cases} u(0,y) = 0 & 0 \leq y \leq b, \\ v(0,b/2) = 0, & \end{cases}$$

$$\text{on the right-hand side of the strip} \quad \begin{cases} u(a,y) = w(t) & 0 \leq y \leq b, \\ v(a,b/2) = 0. & \end{cases} \tag{4.61}$$

We used the transformation strain tensors $\boldsymbol{D}_1 = \mathbf{0}$ and $\boldsymbol{D}_2 = \boldsymbol{D}$ with

$$\boldsymbol{D} = \begin{bmatrix} 0.045 & 0.020 \\ 0.020 & 0.045 \end{bmatrix},$$

which corresponds to one variant of a CuAlNi alloy [9].

The loading program $w(t)$ is a bilinear hat function, increasing from zero to the scaled maximum value at a time $t = t'$, $w(t')/a = 0.050833$, and then decreasing to zero. With the same material data we have calculated the strip for two proportions of its length to width: case 1 with $a : b = 12$ mm : 4 mm, and case 2 with $a : b = 24$ mm : 4 mm, and the same thickness of 0.4 mm. In its initial state the strip was in the austenite phase, and $c(\boldsymbol{x}, t_0) = p(\boldsymbol{x}, t_0) = 0$, $\boldsymbol{x} \in \Omega = [0,a] \times [0,b]$. The characteristic major hysteresis loop is shown in Fig. 24a. Displayed is the relation between the force $F$ at the side $(x = a, 0 \leq y \leq b)$, divided by the initial cross-sectional area $A_0$ of the strip, versus the scaled elongation $w(t)/a$. On the graph two pairs (A,A') and (B,B') of states corresponding to the same scaled elongation but with different histories are marked. Fig. 24b and c, and Fig. 26 reveal that the extension of the two-phase strip induces inhomogeneous fields whose paths of evolution do not coincide during the loading and unloading stages, even for this simple uniaxial loading program. Observe also that the initially straight axis ($0 \leq x \leq a, y = b/2$) of the strip does not remain straight in the $xy$-plane in the course of the process, see Fig. 25c for the transverse component $v$ of the displacement vector $\boldsymbol{u}$. It has turned out rather as quite a surprise that **during** the final stage of **elongation** (not releasing !), at about 4.25 % of overall strain (point B in Fig. 24) **unloading appears**, starting from around the boundaries $x = 0$ and $x = a$ and moving to the middle of the strip.

Finally, it is worthwhile to mention that the proposed formulation allows us to determine the solution of this initially homogeneous problem without introducing any disturbance to the system in order to initiate the phase transformation.

**Example 2**

This example is motivated by the laboratory tests of ICHINOSE, FUNATSU & OTSUKA [61], see Fig. 27. The calculated strip and the imposed boundary conditions (4.62) are schematically displayed in Fig. 28a. Allowing the right-hand side of the strip to move transversely, we have applied the following boundary conditions:

$$\begin{aligned}
&\text{on the left-hand side of the strip} \quad \left\{ \begin{array}{ll} u(0,y) = 0 & 0 \leq y \leq b, \\ v(0,b/2) = 0, & \end{array} \right. \\
&\text{on the right-hand side of the strip} \quad \left\{ \; u(a,y) = w(t) \quad 0 \leq y \leq b. \right.
\end{aligned} \tag{4.62}$$

The loading program $w(t)$ is a linear function increasing from zero to the scaled maximum value of $w(t_E)/a = 0.05159$ corresponding to point E in Fig. 28b. Further, we assumed that the thickness of the strip changes linearly along the $x$-axis with characteristic values of 1.00 mm in the middle ($x = 12.00$ mm) and of 0.99 mm at the ends ($x = 0.00$ and $x = 20.00$), while being constant along the $y$-direction. The variable thickness introduced makes the problem nonhomogeneous, and is to reflect in some sense the influence of temperature induced in the course of the austenite-martensite phase transformation, see the development of the temperature and phase transformation fronts in Fig. 17 and cf. [160]. The transformation strain tensor adopted is now

$$\boldsymbol{D} = \left[ \begin{array}{cc} 0.04 & 0.06 \\ 0.06 & 0.04 \end{array} \right].$$

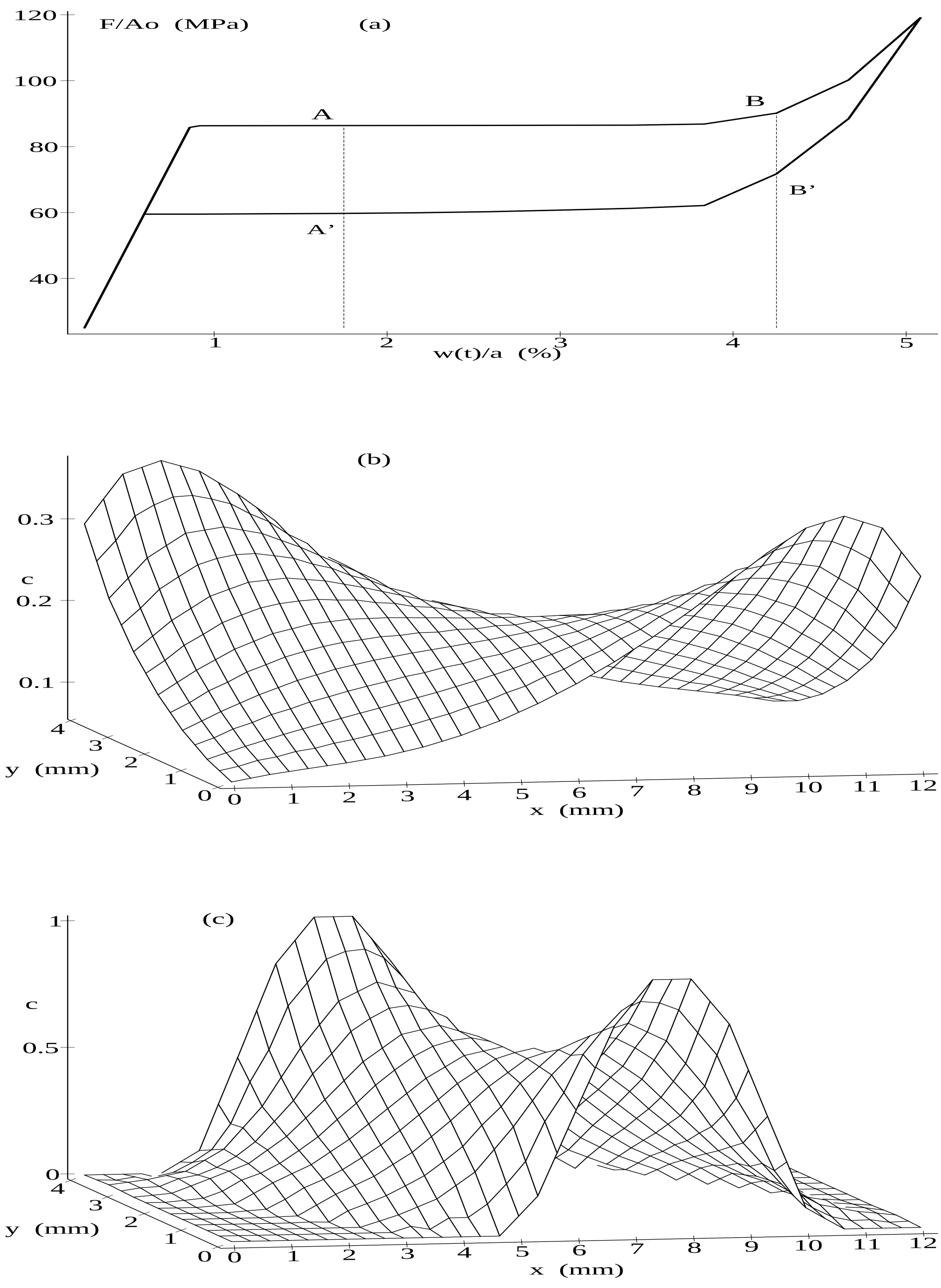


Figure 24: Example 1. The $12 \times 4$ strip under uniaxial extension program $w(t)$. (a) Major hysteresis loop in the scaled force–elongation space $(F/A_0)$ — $(w(t)/a)$, (b) and (c) Distribution of volume fraction $c$ at the corresponding states A and A'

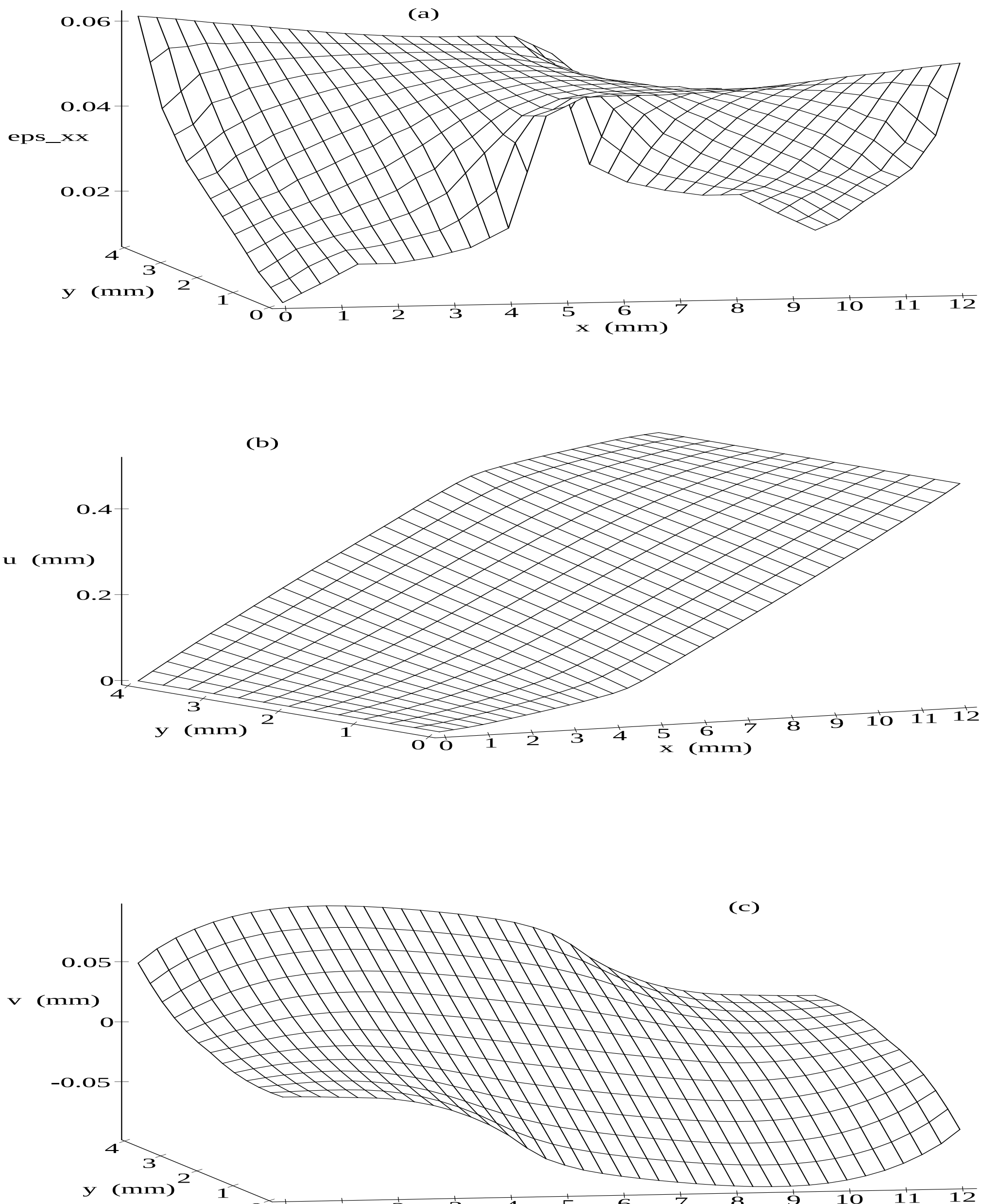


Figure 25: Example 1, case 1. Distributions of strain $\epsilon_{xx}$, (a), and the corresponding displacement $u$ along the elongation, (b), and transverse displacement $v$, (c), at the state B in Fig. 24

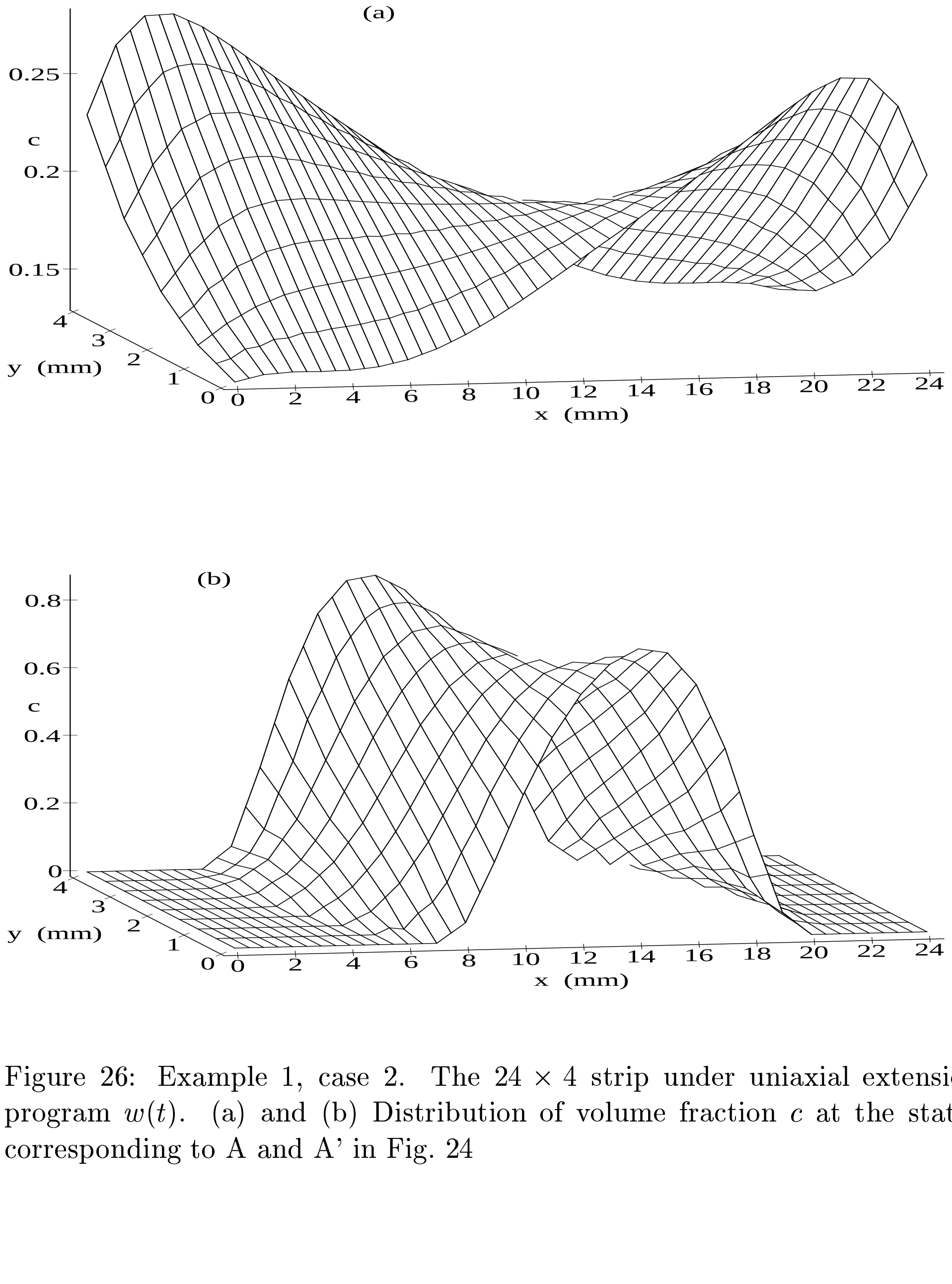


Figure 26: Example 1, case 2. The $24 \times 4$ strip under uniaxial extension program $w(t)$. (a) and (b) Distribution of volume fraction $c$ at the states corresponding to A and A' in Fig. 24

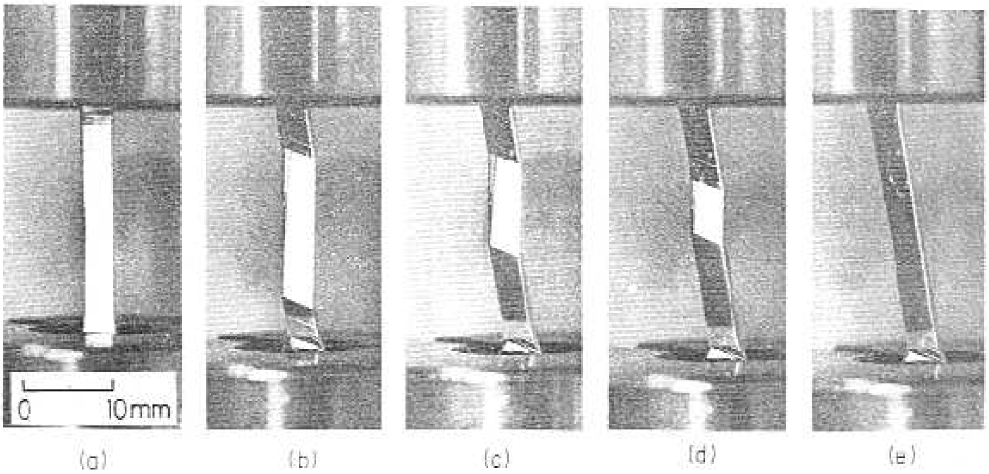


Figure 27: Example 2. A series of macrographs (a) – (e) taken in the experiments by ICHINOSE, FUNATSU & OTSUKA [61]. The propagation of phase transformation fronts (black region) induced by elongation of the specimen can be seen. Observe the resulting transverse movement of the lower grip

The strip was divided into $(12 \times 100) \times 2$ finite elements of the mesh type shown in Fig. 22b, which results in 5025 nodes of displacement field and 1313 nodes of volume fraction, so the number of unknowns of the problem was 12 676. The calculations of the deformation process were performed with the initial mesh of the undeformed strip, while Fig. 28b shows just by means of the mesh the characteristic deformation stages of the strip. In its initial state the strip was in the pure austenite phase, and elastically deformed the strip remains in this state at point A of Fig. 28b. Then the phase transformation starts at the left and right ends of the strip, leading finally to the state E of pure martensite in the whole strip. In the intermediate stages of the process the phase transformation fronts move from the ends to the middle, cf. states B, C, and D in Figs. 28b and 29. During the process there are moving regions of the strip in which the material is in the pure austenite phase ($c = 0$) or martensite phase ($c = 1$), and the transition zone where there is a mixture of both phases ($0 < c < 1$). Since the total strain consists of elastic strain and phase transformation strain, the normal component $E_{xx}$ is non-zero also in the middle part of the strip at state C where $c = 0$, see Fig. 29b (the distribution of $c$ at state C is similar to that of $E_{xx}$). Note that even though the average strain at point D, $w/a = 0.04011$, is greater than the transformation strain component $D_{xx} = 0.04$, the phase transformation has not taken place in the whole strip at this level of elongation. The reason is the two-dimensional stress-strain state of the material.

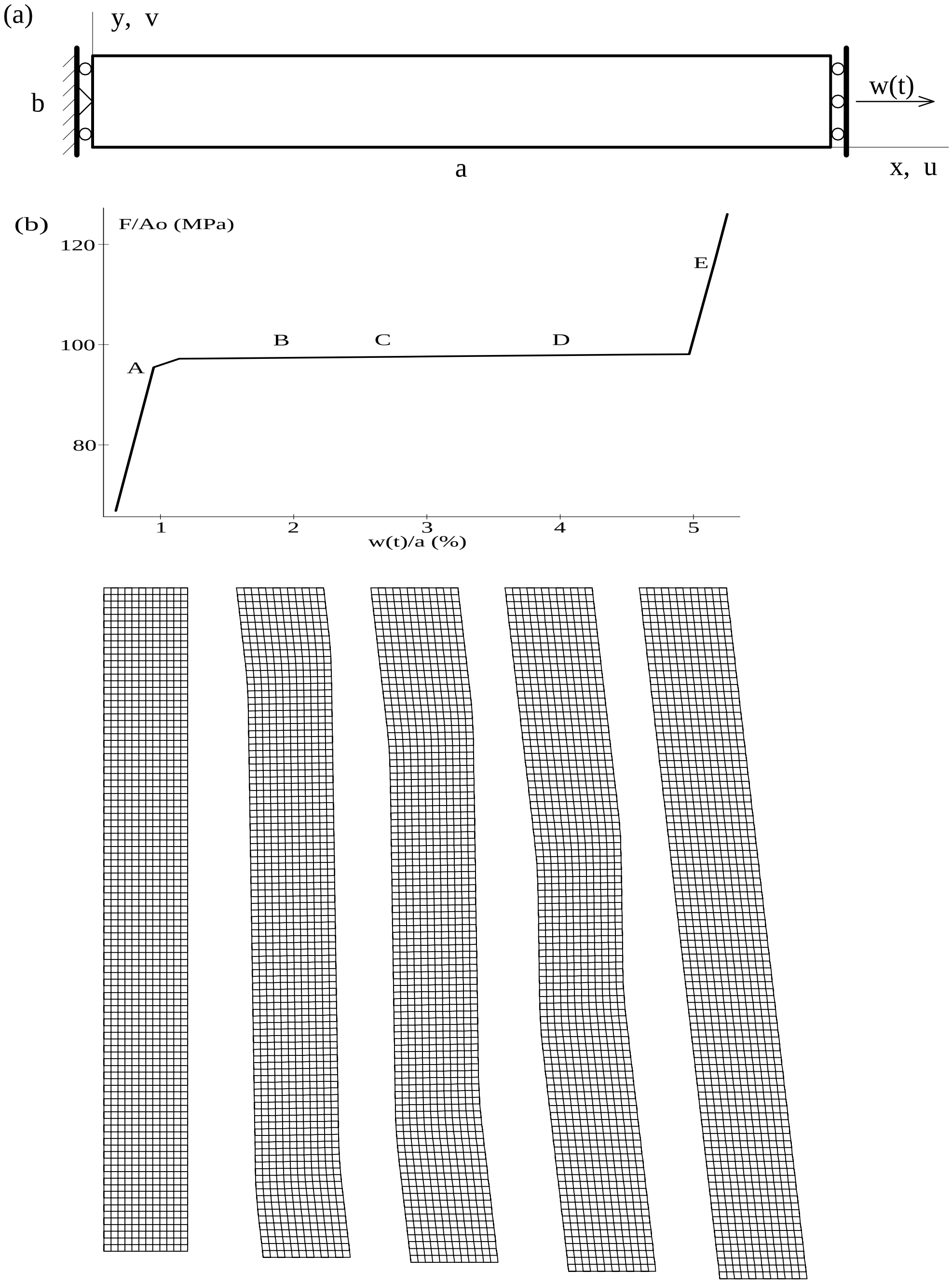


Figure 28: Example 2. (a) The strip of length $a = 20.00$ mm, width $b = 2.50$ mm, under uniaxial tension $w(t)$ and imposed boundary conditions. (b) The diagram of scaled force $(F/A_0)$ vs. scaled elongation $(w(t)/a)$, and the shape of the deformed strip at selected states: A = (0.950, 95.479), B = (1.907, 97.370), C = (2.672, 97.557), D = (4.011, 97.885), E = (5.159, 116.454)

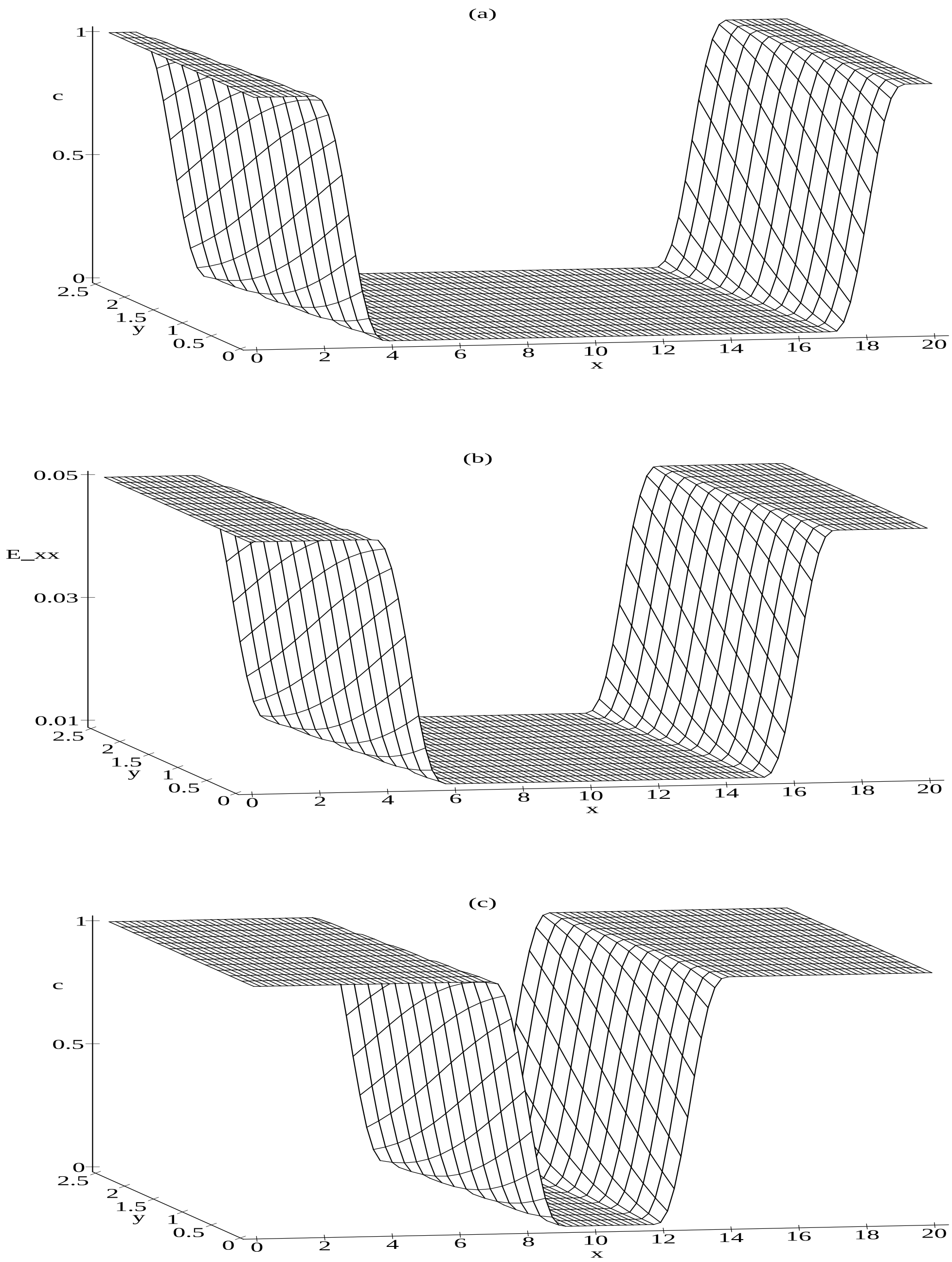


Figure 29: The distribution of volume fraction $c$ at state B, (a), and state D, (c), and that of strain $E_{xx}$ at state C, (b), of Fig. 28b

## 4.3 The multi-well problem

Our aim here is to extend the variational inequality approach of Section 4.2 to the case of multi-phase mixture. As before, we present a variational inequality formulation of the phase transformation problem and show that under suitable hypotheses there exists a unique solution to the problem. Directly relative aspects have been studied in [75, 10, 39, 114].

### 4.3.1 Variational inequality formulation

In this section we are concerned with the quasi-static evolution of a shape memory elastic solid undergoing martensitic phase transformations. We will build on the concepts presented in the previous section. We admit here the material to appear in $N+1$ preferred strain states: the parent phase (austenite), indexed with $i = N+1 \equiv a$, and the $N$-variants of martensite, [9]. Again, we postulate the Helmholtz free energy $W_i$, $i = 1, 2, \ldots, N+1$ in the form

$$W_i(\boldsymbol{E}, \theta) = \frac{1}{2}(\boldsymbol{E} - \boldsymbol{D}_i) \cdot \mathbb{A}_i(\boldsymbol{E} - \boldsymbol{D}_i) + \varpi_i(\theta),$$

with the same elasticity tensor $\mathbb{A}_i = \mathbb{A}$ for each phase (variant). $\boldsymbol{D}_i \in Sym$ is the transformation strain (domain) in $i$-th phase (with $\boldsymbol{D}_a = \boldsymbol{0}$). The tensor $\boldsymbol{D}_i$ corresponds to the *point of convexity* related to the unloaded state, in the terminology of James [64]. The function $\varpi_i(\theta)$ is defined in (4.3). Thus, in a material point $\boldsymbol{x} \in \Omega$, the free energy is a multi-well function which is piecewise quadratic

$$W(\boldsymbol{E}) = \min_{1 \le i \le N+1} \{W_i(\boldsymbol{E})\}.$$

Denoting by $c_i$ the volume fraction of $i$-th phase we will define the quasiconvexified (or, relaxed at fixed volume fractions) free energy of the mixture, cf. [75], as the following expression

$$\widetilde{W}(\boldsymbol{E}, \boldsymbol{c}) = \frac{1}{2}(\boldsymbol{E} - \boldsymbol{D}(\boldsymbol{c})) \cdot \mathbb{A}[\boldsymbol{E} - \boldsymbol{D}(\boldsymbol{c})] + \sum_{i=1}^{N+1} c_i \varpi_i + \frac{1}{2} \sum_{i=1}^{N+1} \sum_{j=1}^{N+1} c_i c_j B_{ij}. \quad (4.63)$$

where the effective transformation strain $\boldsymbol{D}(\boldsymbol{c})$ is the convex combination,

$$\boldsymbol{D}(\boldsymbol{c}) \equiv \sum_{i=1}^{N+1} c_i \boldsymbol{D}_i, \quad \text{with } c_i \ge 0, \ \sum_{i=1}^{N+1} c_i = 1, \quad (4.64)$$

that is an element of the convex hull spanned by the set of transformation strains $\boldsymbol{D}_i$, $\boldsymbol{D}(\boldsymbol{c}) \in \operatorname{conv}\{\boldsymbol{D}_1, \boldsymbol{D}_2, \ldots, \boldsymbol{D}_{N+1}\}$. Moreover $B_{ij}$ are material constants, being entries of the symmetric matrix $\boldsymbol{B}$ with zero diagonal elements.

Following the procedure discussed before, we arrive at the reduced form of the dissipation inequality

$$\mathcal{D} = -\frac{\partial \widetilde{W}}{\partial \boldsymbol{c}} \cdot \dot{\boldsymbol{c}} \equiv \boldsymbol{X} \cdot \dot{\boldsymbol{c}} = \sum_{m=1}^{N} X_m \, \dot{c}_m \geq 0. \tag{4.65}$$

where the driving force for phase transformations, $\boldsymbol{X}$, is an $N$-tuple quantity with components

$$X_m = \boldsymbol{D}_m \cdot \mathbb{A}[\boldsymbol{E}] - \sum_{i=1}^{N} \left( \boldsymbol{D}_m \cdot \mathbb{A}[\boldsymbol{D}_i] + B^{\star}_{mi} \right) c_i - (\varpi_m - \varpi_a) - B_{am}. \tag{4.66}$$

In virtue of the mechanically obvious constraint $(4.64)_3$ we can express the volume fraction of austenite $c_a$, $a = N+1$, in terms of $c_m$, $1 \leq m \leq N$, which leads effectively to the $N \times N$ matrix of material parameters, $\boldsymbol{B}^{\star}$, with the components

$$B^{\star}_{mi} = B_{mi} - B_{ai} - B_{am}.$$

In the case of multi-phase mixture, for each $m$-th variant of martensite we define the phase transformation functions,

$$F^{+}_{m} = \kappa^{+}_{m} - X_m \geq 0, \qquad F^{-}_{m} = X_m - \kappa^{-}_{m} \geq 0 \qquad \text{for} \quad 1 \leq m \leq N, \tag{4.67}$$

the threshold functions

$$\begin{aligned} \kappa^{+}_{m} &= \max\left\{ L_m \left( c_m - p_m \right), 0 \right\} \geq 0, \\ \kappa^{-}_{m} &= \min\left\{ L_m \left( c_m - p_m \right), 0 \right\} \leq 0, \end{aligned} \tag{4.68}$$

and split the rate of volume fraction $\dot{c}_m$ into the positive and the negative part

$$\dot{c}^{+}_{m} = \max\left\{ \dot{c}_m, 0 \right\} \geq 0, \qquad \dot{c}^{-}_{m} = \max\left\{ -\dot{c}_m, 0 \right\} \geq 0. \tag{4.69}$$

Now, instead of one material constant $L$ in the case of two-phase systems, we have an $N$-tuple of the material constants $L_m > 0$, which have a meaning of the energy dissipated during the forward and reverse transformation of the unit volume of $m$-th variant of martensite. By $p_m$ we denote the memory variable corresponding to the $m$-th variant of martensite, which in particular may take only two values: 0 and 1.

Accounting for the dissipation inequality (4.65) we stipulate the following phase transformation criteria (PTC) for the multi-phase mixture, requiring for each component $X_m$ $(1 \leq m \leq N)$ of the driving force that

$$\boxed{\begin{array}{llll} \text{if} & X_m(\boldsymbol{c}) = \kappa_m^+(c_m) & \text{then} & \dot{c}_m \geq 0 \\ \text{if} & X_m(\boldsymbol{c}) = \kappa_m^-(c_m) & \text{then} & \dot{c}_m \leq 0 \\ \text{if} & \kappa_m^-(c_m) < X_m(\boldsymbol{c}) < \kappa_m^+(c_m) & \text{then} & \dot{c}_m = 0 \end{array}} \tag{4.70}$$

which can be expressed as the following system of variational inequalities,

$$c_m \geq 0, \ \sum_{m=1}^{N} c_m \leq 1, \qquad \sum_{m=1}^{N} F_m^{\pm}(\boldsymbol{c}) \cdot (y_m^{\pm} - \dot{c}_m^{\pm}) \geq 0 \quad \text{for all } y_m^{\pm} \geq 0. \tag{4.71}$$

Thus, according to the PTC (4.70) among all variants of martensite those are activated whose driving forces are equal to their thresholds. Moreover, at subsequent stages of the PT process various phases can be simultaneously induced or 'consumed'. The stresses play here the decisive role, introducing the 'order' into the mixture of phases. Note that the expression (4.66), cf. also (4.37), accounts for the observation of PATEL & COHEN cited on page 14, incorporating in a natural way the direction properties both of the stress tensor $\boldsymbol{T}$ and the phase transformation tensors $\boldsymbol{D}_m$.

For completeness we recall the equilibrium equations,

$$\operatorname{div} \mathbb{A}[\boldsymbol{E}(\boldsymbol{u}) - \boldsymbol{D}(\boldsymbol{c})] + \boldsymbol{f} = \boldsymbol{0}. \tag{4.72}$$

**Weak formulation**

As before, we consider finite increments

$$\Delta \boldsymbol{u}_n \equiv \boldsymbol{u}_n - \boldsymbol{u}_{n-1}$$
$$\Delta \boldsymbol{c}_n \equiv \boldsymbol{c}_n - \boldsymbol{c}_{n-1}$$

and decompose the vector function $\Delta \boldsymbol{c}_n$ into its positive and negative part,

$$\Delta \boldsymbol{c}_n = \Delta \boldsymbol{c}_n^+ - \Delta \boldsymbol{c}_n^- .$$

The conditions $(4.71)_{1,2}$ dictate the following constraint sets on the increments of volume fraction, $\Delta \boldsymbol{c}_n$, $\Delta \boldsymbol{c}_n^+$, and $\Delta \boldsymbol{c}_n^-$,

$$\begin{aligned} K(\boldsymbol{z}) &= \left\{ \boldsymbol{w} \in L^2(\Omega, \mathcal{R}^N) \mid |w_i| \leq 1, \, 0 \leq \textstyle\sum_{i=1}^N (z_i + w_i) \leq 1, \, \boldsymbol{z} \in Z \right\} \\ K_+(\boldsymbol{z}) &= \left\{ \boldsymbol{w} \in L^2(\Omega, \mathcal{R}^N) \mid w_i \geq 0, \, \textstyle\sum_{i=1}^N (z_i + w_i) \leq 1, \, \boldsymbol{z} \in Z \right\} \\ K_-(\boldsymbol{z}) &= \left\{ \boldsymbol{w} \in L^2(\Omega, \mathcal{R}^N) \mid w_i \geq 0, \, z_i - w_i \geq 0, \, \boldsymbol{z} \in Z \right\} \\ Z &= \left\{ \boldsymbol{z} \in L^2(\Omega, \mathcal{R}^N) \mid z_i \geq 0, \, \textstyle\sum_{i=1}^N z_i \leq 1 \right\} . \end{aligned} \tag{4.73}$$

Now we are in a position to formulate a typical time-step of the incremental boundary value problem defined by (4.72) and (4.71) as the variational inequality.

Find $(\Delta\boldsymbol{u}_n, \Delta\boldsymbol{c}_n) \in V(t_n) \times K(\boldsymbol{c}_{n-1})$ such that

$$\begin{array}{rcl} a(\Delta\boldsymbol{u}_n, \boldsymbol{v}) - g(\Delta\boldsymbol{c}_n, \boldsymbol{v}) & = & f_{n,n-1}(\boldsymbol{v}) \\ \mp g(\boldsymbol{z}_\pm - \Delta\boldsymbol{c}_n^\pm, \Delta\boldsymbol{u}_n) \pm h(\Delta\boldsymbol{c}_n, \boldsymbol{z}_\pm - \Delta\boldsymbol{c}_n^\pm) & \geq & \mp b_{n-1}^\pm(\boldsymbol{z}_\pm - \Delta\boldsymbol{c}_n^\pm) \end{array}$$

for all $\boldsymbol{v} \in V(t_n)$, $\boldsymbol{z}_\pm \in K_\pm(\boldsymbol{c}_{n-1})$.

(4.74)

The forms $a$ and $f_{n,n-1}$ are as before in $(4.49)_1$ and $(4.50)_1$, while the others

$$g(\boldsymbol{w}, \boldsymbol{v}) = \sum_{m=1}^{N} \int_\Omega w_m \mathbb{A}[\boldsymbol{D}_m] \cdot \nabla\boldsymbol{v} \, \mathrm{d}x \tag{4.75}$$

$$h(\boldsymbol{w}, \boldsymbol{v}) = \sum_{m=1}^{N} \sum_{i=1}^{N} \int_\Omega (\boldsymbol{D}_m \cdot \mathbb{A}[\boldsymbol{D}_i] + B_{mi}^\star + \delta_{mi} L_m) w_m v_i \, \mathrm{d}x \tag{4.76}$$

$$\begin{aligned} b_{n-1}^\pm(\boldsymbol{w}) = {} & \sum_{m=1}^{N} \int_\Omega [B_{am} + (\varpi_m - \varpi_a) + L_m (c_{m,n-1} - p_{m,n-1})^\pm] w_m \, \mathrm{d}x \\ & \mp g(\boldsymbol{w}, \boldsymbol{u}_{n-1}) \pm h(\boldsymbol{c}_{n-1}, \boldsymbol{w}). \end{aligned} \tag{4.77}$$

### 4.3.2 Existence and uniqueness

In this section we follow the line of reasoning presented in Sections 3.1.3 and 4.2. We shall show that a bilinear form $A$ corresponding to the variational inequality (4.74) is continuous and coercive on the product space $\mathcal{V} \sim \mathcal{V}_n \equiv V_n \times \Lambda$ with $\Lambda = L^2(\Omega, \mathcal{R}^N)$, under some assumptions to be presented here. The norm on $\mathcal{V}$ is assigned in (3.49). Again, let $\mathcal{K}_{n,n-1} \equiv V_n \times K_{n-1}$ with $K_{n-1}$ of (4.73) stand for the convex set of constraints, $\mathcal{K}_{n,n-1} \subset \mathcal{V}_n$. The elements $u$, $v \in \mathcal{V}$ represent here the pairs

$$u \equiv (\boldsymbol{u}, \boldsymbol{c}), \qquad v \equiv (\boldsymbol{v}, \boldsymbol{z}).$$

Further, for simplicity in notation we set:

$$\Delta u_n \equiv (\Delta\boldsymbol{u}_n, \boldsymbol{c}_n), \qquad \langle\, l_{n,n-1},\, v\,\rangle \equiv f_{n,n-1}(\boldsymbol{v}) - b_{n-1}^+(\boldsymbol{z}) + b_{n-1}^-(\boldsymbol{z}). \tag{4.78}$$

As previously, the bilinear form $A : \mathcal{V} \times \mathcal{V} \longrightarrow \mathcal{R}$ is defined by

$$A(u,\, v) \equiv a(\boldsymbol{u},\, \boldsymbol{v}) - g(\boldsymbol{c},\, \boldsymbol{v}) - g(\boldsymbol{z},\, \boldsymbol{u}) + h(\boldsymbol{c},\, \boldsymbol{z}). \tag{4.79}$$

Now, the problem (4.74) can be rewritten as the variational inequality:

Find $\Delta u_n \in \mathcal{K}_{n,n-1}$ such that

$$A(\Delta u_n, v - \Delta u_n) \geq \langle\, l_{n,n-1},\, v - \Delta u_n \,\rangle \quad \text{for all } v \in \mathcal{K}_{n,n-1}. \tag{4.80}$$

The critical role in the question of uniqueness will be played by the symmetric matrix $\boldsymbol{B}^L$ whose elements depend upon the material properties $B^\star_{ij}$ and $L_i$,

$$B^L_{ij} = B^\star_{ij} + \delta_{ij} L_i, \quad 1 \leq i, j \leq N. \tag{4.81}$$

We assume that $\boldsymbol{B}^L$ is positive definite, i.e. there exists a constant $H_p > 0$ such that

$$\boldsymbol{y} \cdot \boldsymbol{B}^L \boldsymbol{y} \geq H_p\, |\boldsymbol{y}|^2 \quad \text{for all}\, \boldsymbol{y} \in \mathcal{R}^N. \tag{4.82}$$

Furthermore, it is natural to assume that the transformation strain of each martensitic variant are bounded,

$$\max_{i,j} \|(\boldsymbol{D}_m)_{ij}\|_\infty \leq \gamma, \qquad \gamma < \infty, \quad 1 \leq m \leq N. \tag{4.83}$$

Hence for the average phase transformation strain tensor $\boldsymbol{D}(\boldsymbol{z})$ we have the estimation,

$$\boldsymbol{D}(\boldsymbol{z}) \cdot \boldsymbol{D}(\boldsymbol{z}) \leq k_D\, |\boldsymbol{z}|^2 \qquad k_D < \infty. \tag{4.84}$$

The required properties of the bilinear form $A$ are formulated as the following lemmas.

**Lemma 4.6.** *The bilinear form $A$ is continuous on $\mathcal{V}$, that is, there exists a positive constant $k$ such that*

$$|A(u,\, v)| \leq k\, \|u\|_{\mathcal{V}}\, \|v\|_{\mathcal{V}} \quad \textit{for all } u, v \in \mathcal{V}. \tag{4.85}$$

**Proof.** The proof goes along the lines of the proof of Theorem 4.3. ❑

**Lemma 4.7.** *Let $\boldsymbol{B}^L$ be positive definite. The bilinear form $A$ is coercive on $\mathcal{V}$, i.e., there exists a constant $k_0 > 0$ such that*

$$A(v,\, v) \geq k_0\, \|v\|^2_{\mathcal{V}} \quad \textit{for all } v \in \mathcal{V}. \tag{4.86}$$

**Proof.** Let $\beta = H_p/(H_p + 2k_A k_D)$. We have,

$$
\begin{aligned}
A(v,\, v) &= \int_\Omega \left\{ [\boldsymbol{E}(\boldsymbol{v}) - \boldsymbol{D}(\boldsymbol{z})]\cdot\mathbb{A}[\boldsymbol{E}(\boldsymbol{v}) - \boldsymbol{D}(\boldsymbol{z})] + \boldsymbol{z}\cdot\boldsymbol{B}^L\boldsymbol{z} \right\}\ \mathrm{d}x \\
&\geq \int_\Omega \left\{ k_A[\boldsymbol{E}(\boldsymbol{v}) - \boldsymbol{D}(\boldsymbol{z})]\cdot[\boldsymbol{E}(\boldsymbol{v}) - \boldsymbol{D}(\boldsymbol{z})] + \boldsymbol{z}\cdot\boldsymbol{B}^L\boldsymbol{z} \right\}\ \mathrm{d}x \\
&\geq \int_\Omega \left\{ k_A\beta\,|\boldsymbol{E}(\boldsymbol{v})|^2 - \frac{k_A\beta}{1-\beta}\,|\boldsymbol{D}(\boldsymbol{z})|^2 + H_p|\boldsymbol{z}|^2 \right\}\ \mathrm{d}x + \\
&\quad \int_\Omega k_A \left| \sqrt{1-\beta}\,\boldsymbol{E}(\boldsymbol{v}) - \frac{1}{\sqrt{1-\beta}}\boldsymbol{D}(\boldsymbol{z}) \right|^2\ \mathrm{d}x \\
&\geq \int_\Omega k_A\beta\,|\boldsymbol{E}(\boldsymbol{v})|^2\ \mathrm{d}x + \int_\Omega \left( H_p - \frac{k_A\beta k_D}{1-\beta} \right) |\boldsymbol{z}|^2\ \mathrm{d}x \\
&\geq k_0\, \left( \|\boldsymbol{v}\|_V^2 + \|\boldsymbol{z}\|_\Lambda^2 \right) = k_0\ \|v\|_{\mathcal{V}}^2\,,
\end{aligned}
\tag{4.87}
$$

with
$$
k_0 = \min\left\{ \frac{k_A H_p k_K}{H_p + 2k_A k_D},\, \frac{1}{2}H_p \right\}.
$$

❏

The following theorem on existence and uniqueness holds.

**Theorem 4.8.** *Let the elasticity tensor $\mathbb{A} \in LinLin$ satisfy conditions (3.6), matrix $\boldsymbol{B}^L$ be positive definite, and transformation strain tensors $\boldsymbol{D}_m$ satisfy condition (4.84). There exists a unique solution of the problem (4.80). The solution depends continuously on data $l_{n,n-1} \in \mathcal{V}_n^*$.*

**Proof.** The proof follows from Theorem 2.2. ❏

## 4.4 Concluding remarks

Summing up this chapter we stress the following. The proposed variational inequlity approach to the PT process seems to be the advantagous tool both in the qualitative analysis on existence and uniqueness of its solutions, as well as in the numerical treatment of the problem. The obtained results in Sections 4.1 and 4.2 demonstrate the extraordinary response of the PT systems. In particular, the numerical results of Example 2 in Section 4.2 confirm the dominant shear character of the martensitic PT, and are in good qualitative agreement with the experimental findings of Ichinose *et al.* [61]. On the other hand, Examples 1 and 2 there show how different may be the deformation mode of the strip if boundary conditions are changed and/or some inhomogeneity is present, the occurence to be expected from the analysis in Section 4.1. Some additional, general remarks are given in the next section.

# 5 Closure

## 5.1 Final conclusions

Even nowadays when the experimental facilities allow for the investigation of microstructures and the computational power of computers is quite impressive, we are still unable to calculate an engineering construction by treating it as a conglomerate of atoms (if this would make any practical sense in any case). Of course, to get an understanding of the mechanism of deformation processes and to tailor the special properties and microstructure of the material, laboratory tests and crystallographic calculations related to some fine scale are necessary. On the other hand, in order to be capable of handling the IBVP encountered in engineering practice we finally need possibly simple models which should, however, properly reflect the characteristic features of material behaviour. These are usually averaged continuum models which describe the material behaviour on the higher (meso or macro) scale. The averaging procedures corresponding to the relaxation or homogenization of the microscale relations have become recently the subject of intensive mathematical research in which the refined notion of generalized curves of YOUNG [194] and various subtle concepts of convergence, e.g. $H$-convergence and $\Gamma$-convergence, are used. In the field of continuum mechanics, the phenomenological models of deformation processes have been devised in which the microstructural rearrangements are taken into account by means of a set of internal variables with their evolution laws. We emphasize here the interplay between mathematics and mechanics. While mathematics can substantiate the existing averaged models of mechanics and put them in a wide panorama of mathematical concepts, mechanics suggests the physical interpretation of the averaging quantities of interest (e.g. our volume fractions $\boldsymbol{c}$) and in addition to that, and what is of critical importance, mechanics supplies the evolution laws for internal variables upon the basis of physical arguments. In this connection we recall that the models of plastic flow (with additional effects of viscosity and slackening) in Chapter 3 have a macroscopic character. Also, the starting point of the suggested model for martensitic PT, cf. (4.74), is the expression for the homogenized, macroscopic free energy of a multi-phase mixture (4.63), which in this work is treated as granted. The detailed, strictly mathematical homogenization of the microscopic relations for the mechanical problems examined in this account would lead us aside of our present aims, as it is in fact a difficult delicate problem in itself.

The analysis presented in the present work borrows a lot from the results obtained by other researches, but in some respects it is different from the preceding models. First of all, we have tried to develop a fairly complete approach which resolves the interrelated tasks listed in Section 1.3: from a physical phenomenon through mathematical analysis to verification of model's prediction against laboratory tests. On the mathematical side, the main novelty of this approach consists of the unifying variational inequality formulation of the yield, phase transformation, and slackening criteria which allows for the global projection in the numerical solution of the associated IBVP. The VI formulation constitutes the necessary optimality conditions for the deformation process, which become sufficient for the existence of unique solutions if certain requirements of positive energy dissipation are accounted for. The latter is measured in (4.70) by threshold functions $\kappa_m^{\pm}$. Moreover, the formulation directly leads to the computational algorithms of general character (LCP, SSORP, PCG). On the mechanical side, the proposed models of plastic flow and martensitic PT have proved to be capable of capturing the complex material behaviours considered.

Summing up the discussions in the previous chapters we wish to highlight the following:

- We have shown that the loading/unloading conditions of plastic flow, the criteria of martensitic PT and the slackening (locking) conditions are equivalent to a variational inequality. In particular, it turns out that the loading/unloading criteria assure the consistency condition, cf. Proposition 3.1.

- For the material models considered we have established the conditions of existence of unique solutions to the corresponding incremental boundary value problem.

- We developed numerous computer codes which solve the finite dimensional counterpart of the proposed VI formulations, resulting from the finite element approximation. For solving the resulting LCP two methods are devised: a direct procedure and an iterative algorithm. Various numerical experiments were carried out, the results of which were compared with available experimental observations.

- The variational inequality formulation of the model problem of plastic flow, Section 3.1, can be extended strightforwardly to the non-smooth multi-surface plasticity or the gradient dependent plasticity [120]. On non-convex yield surfaces the reader may consult [89] where further references are given and Dvorak *et al.* [28].

- A new model for the slackened-viscoelastic-plastic response is advanced. The obtained numerical results with this model reveal that the history of the deformation process has the critical impact on the present state of structural systems.

- The homogenized energy of the phase-mixture and the conditions imposed by the second principle of thermodynamics lead to the mathematically well-posed, stable models of martensitic PT which describe the material behaviour at a macroscopic level.

- The phase transformation criteria (4.70) define implicitly the evolution law of volume fractions $\boldsymbol{c}$, thereby the kinetics of the PT process.

- As a major finding of the 1D simulations we have obtained that the local material behaviour (stress vs. strain) is different from that observed at the level of global quantities (force vs. displacement). The strain-temperature coupling makes the martensisitic PT deformation process rate-dependent. Also, the numerical results obtained for the tension test on austenite-martensite strips show that two corresponding states on the force-elongation diagram are connected with different inhomogeneous states in the bulk of the sample. The influence of the phase transformation strain and boundary conditions on the propagation of transformation fronts and the deformation mode of the specimen is observed. The results of numerical simulation of PT on a two-component strip are in good agreement with the experimental findings [61], cf. Figs. 27 and 28.

- The proposed VI formulation of the PT process, seems to be, *inter alia*, a very promising approach in dealing with similar hysteretic boundary value problems.

## 5.2 Directions for further work

The problems treated in this work are difficult in many aspects and we are still far from their complete solution, but we believe that the present work is the good basis for further work in many, different directions. Among the many points which deserve further attention we will mention the following.

- We assumed the same elasticity properties for all phases (variants), but it seems possible to extend the VI formulation to the case of different phase moduli by making $\mathbb{A}$ dependent upon the volume fractions, i.e. $\mathbb{A} = \mathbb{A}(\boldsymbol{c})$ (effective elasticity tensor), cf. HASHIN & SHTRIKMAN [53], MILTON [115] and others.

- The interaction of the effects of phase transformation, plasticity and temperature is important. Yet, it may not be trivial to "seperate" these phenomena, both in the laboratory tests and mathematical modelling.

- The extension of the presented formulations to the range of large strains is desirable, although there are still some controversial aspects both in plasticity theory and in martensitic PT, e.g. cf. [162, 103, 7, 9, 39].

- We believe that the proposed unifying formulations for plastic flow and martensitic phase transformations will be a useful starting point in the sensitivity analysis of shape optimization and optimal control problems, as discussed among others by SZEFER [178], SOKOLOWSKI & ZOLESIO [165], and HASLINGER & NEITTAANMAKI [54]. Of great practical interest is here the optimal design of skeletal structures by optimization of positions of structural joints, e.g. cf. GARSTECKI [40]. It will be useful to extend the model of Section 3.2 to such an optimization problem, additionally accounting for the constraints on the generalized stresses (via the yield condition) and generalized strains (e.g. rotation at a joint). Optimal location of actuators for active control of flexible structures is a related domain where our approach could be utilized.

- Both the problems of plasticity and of martensitic PT are free boundary problems which describe localization processes (of strains, temperature), so the application of adaptive mesh strategies and parallel computing will be profitable.

We hope that in the future we shall have the opportunity to attack some of the issues listed above.

# List of Figures

## References


[1] R. ABEYARATNE, S.-J. KIM, and J. KNOWLES. A one-dimensional continuum model for shape memory alloys. *Int. J. Solids Structures*, 31:2229–2249, 1994.

[2] R. ABEYARATNE and J. KNOWLES. Non-elliptic elastic materials and the modeling of elastic-plastic behavior for finite deformation. *J. Mech. Phys. Solids*, 35:343–365, 1987.

[3] E. ACERBI and N. FUSCO. Semicontinuity problems in the calculus of variations. *Arch. Rational Mech. Anal.*, 86:125–145, 1984.

[4] J. ARGYRIS, I. DOLTSINIS, and V. da SILVA. Constitutive modelling and computation of non-linear viscoelastic solids. Part I: Reological models and numerical integration techniques. *Comput. Meth. Appl. Mech. Engng.*, 88:135–163, 1991.

[5] J. BALL, C. CHU, and R. JAMES. Hysteresis during stress-induced variant rearrangement. *J. de Physique IV, Coll. C8, suppl. J. de Physique III*, 5:(C8–245)–(C8–251), 1995.

[6] J. BALL and R. JAMES. Fine phase mixtures as minimizers of energy. *Arch. Rational Mech. Anal.*, 100(1):13–52, 1987.

[7] J. BALL and R. JAMES. Proposed experimental tests of a theory of fine microstructure and two-well problem. *Phil. Trans. R. Soc. Lond.*, 338A:389–450, 1992.

[8] M. BERVEILLER, E. PATOR, and M. BUISSON. Thermomechanical constitutive equations for shape memory alloys. *J. de Physique IV, Coll. C4, suppl. J. de Physique III*, 1:C4–387—C4–396, 1991.

[9] K. BHATTACHARYA. Comparison of the geometrically nonlinear and linear theories of martensitic transformation. *Continuum Mech. and Themodyn.*, 5:205–242, 1993.

[10] K. BHATTACHARYA and R. KOHN. Symmetry, texture and the recoverable strain of shape-memory polycrystals. *Acta mater.*, 44(2):529–542, 1996.

[11] Z. BO and D. C. LAGOUDAS. Thermomechanical modeling of polycrystalline SMAs under cyclic loading, Part IV: Modelling of minor hysteresis loops. *Int. J. Engng. Sci.*, 1997. (submitted).

[12] Z. BOJARSKI and H. MORAWIEC. *Metals with shape memory* (Polish). PWN, Warszawa, 1989.

[13] A. BORKOWSKI. *Analysis of Skeletal Structural Systems in the Elastic and Elastic-Plastic Ranges*. PWN-Elsevier, Warszawa, 1988.

[14] R. D. BORST, J. PAMIN, and L. SLUYS. Gradient plasticity for localization problems in quasi-brittle and frictional materials. pages 509–533, 1995.

[15] J. BOYD and D. LAGOUDAS. A thermomechanical constitutive model for shape memory materials. Part I. The monoclithic shape memory alloy. *Int. J. Plasticity*, 12:805–842, 1996.

[16] D. BRANDON and R. ROGERS. Constitutive laws for pseudo-elastic materials. *J. Intell. Mater. Syst. Struct.*, 3:255–267, 1992.

[17] M. BROKATE and J. THEEL. Some numerical simulations of pseudoelastic hysteresis in shape memory alloys. *Continuum Mech. Thermodyn.*, 5:265–280, 1993.

[18] C. CARSTENSEN and P. PLECHÁČ. Numerical solution of the scalar double-well problem allowing microstructure, 1995. (Preprint).

[19] M. CHIPOT and D. KINDERLEHRER. Equilibrium configuration of crystals. *Arch. Rational Mech. Anal.*, 103:237–277, 1988.

[20] P. CIARLET. *Mathematical Elasticity*, volume Vol. I: Three-dimensional Elasticity. North-Holland, Amsterdam, 1988.

[21] B. COLEMAN and E. GURTIN. Thermodynamics with internal state variables. *Arch. Rat. Mech. Anal.*, 47(2):597–613, 1967.

[22] L. CORRADI and G. MAIER. A matrix theory of elastic-locking structures. *Meccanica*, 4:298–313, 1969.

[23] R. COTTLE, J.-S. PANG, and R. STONE. *The Linear Complementarity Problem.* Academic Press, Inc., Boston, 1992.

[24] F. DEMENGEL and P.-M. SUQUET. On locking materials. *Acta Applicandea Mathematicae*, 6:185–211, 1986.

[25] L. DEMKOWICZ and M. ŚWIERCZEK. An adaptive finite element method for a class of variational inequalities. In W. Kosiński *et al.*, editor, *Proc. Italian-Polish Symposium of Continuum Mechanics*, pages 1–18, Bologna, July 1987.

[26] D. DRUCKER. A definition of stable inelastic material. *Transaction of the ASME J. Appl. Mechanics*, 26(1):101–106, March 1959.

[27] G. DUVAUT and J.-L. LIONS. *Inequalities in Mechanics and Physics.* Springer-Verlag, Berlin, 1976.

[28] G. DVORAK, D. LAGOUDAS, and C.-M. HUANG. Fatigue damage and shake-down in metal matrix composite laminates. *Mech. Comp. Mater. Struct.*, 1:171–202, 1994.

[29] D. EDELEN. Primitive thermodynamics: A new look at the Clausius-Duhem inequality. *Int. J. Engng Sci.*, 12:121–141, 1974.

[30] I. EKELAND and R. TEMAM. *Convex Analysis and Variational Problems.* North-Holland, Amsterdam, 1976.

[31] J. ERICKSEN. Equilibrium of bars. *J. Elasticity*, 5(3-4):191–201, 1975.

[32] J. ERICKSEN. Continuous martensitic transitions in thermoelastic solids. *J. Thermal Stresses*, 4:107–119, 1981.

[33] F. FALK. One-dimensional model of shape memory alloys. *Arch. Mech.*, 35:63–84, 1983.

[34] B. FEDELICH and G. ZANZOTTO. One-dimensional quasistatic nonisothermal evolution of shape-memory material inside the hysteresis loop. *Continuum Mech. Thermodyn.*, 3:251–276, 1991.

[35] F. FISCHER. A micromechanical model for transformation plasticity in steels. *Acta metall. mater.*, 38(8):1535–1546, 1990.

[36] F. FISCHER, M. BERVEILLER, K. TANAKA, and E. OBERAIGNER. Continuum mechanical aspects of phase transformations in solids. *Arch. Appl. Mech.*, 64:54–85, 1994.

[37] I. FONSECA and S. MÜLLER. Relaxation of quasiconvex functionals in $\mathrm{BV}(\omega, \mathbb{R}^p)$ for integrands $f(x, u, \nabla u)$. *Arch. Rational Mech. Anal.*, 123:1–49, 1993.

[38] M. FREMOND. *Shape memory alloy. A thermomechanical macroscopic study*, volume 351 of *CISM*, chapter 1, pages 1–67. Springer, Wien, New York, 1996.

[39] E. FRIED and M. E. GURTIN. Semi-quadratic variational problems for multiphase equilibria. *Quart. Appl. Math.*, 1:73–84, 1996.

[40] A. GARSTECKI. Optimal design of joints in elastic structures. *Acta Mechanica*, 75:63–76, 1988.

[41] A. GAWĘCKI. Elastic-plastic beams and frames with unilateral boundary conditions. *J. Struct. Mech.*, 14:53–76, 1986.

[42] A. GAWĘCKI. *Elastic-Plastic Skeletal Structures with Clearances* (Polish), volume 185 of *Transactions of PUT*. PUT Press, Poznań, 1987.

[43] A. GAWĘCKI. Elasto-plasticity of slackened systems. *Arch. Mech.*, 44:363–390, 1992.

[44] A. GAWĘCKI and B. JANIŃSKA. Computer analysis of slackened elastic-plastic beams under non-proportional loads. *Computer Assisted Mech. Engng. Sci.*, 2:25–40, 1995.

[45] A. GAWĘCKI and M. KUCZMA. Elastic-plastic unilateral contact problem for slackened systems. *Journal of Computational and Applied Mathematics*, 63:313–323, 1995.

[46] A. GAWĘCKI, M. KUCZMA, and P. KRÜGER. Analysis of slackened skeletal systems by mathematical programming. *Computers and Structures*, 69:639–654, 1998.

[47] P. GERMAIN, Q. NGUYEN, and P. SUQUET. Continuum thermodynamics. *Transactions of the ASME J. Appl. Mechanics*, 50:1010–1020, 1983.

[48] F. GIANNESSI and G. MAIER. Complementaity systems and optimization problems in structural engineering. *Eng. Opt.*, 18:43–66, 1991.

[49] R. GLOWINSKI, J. LIONS, and TREMOLIERES. *Analyse numérique des inéquations variationnelles.* Dunod, Paris, 1976.

[50] A. E. GREEN and N. LAWS. On a global entropy production inequality. *Quart. J. Mech. Appl. Math.*, 25:1–11, 1972.

[51] M. E. GURTIN. *An Introduction to Continum Mechanics.* Academic Press, New York, 1981.

[52] B. HALPHEN and Q. NGUYEN. Sur les matériaux standards généralisés. *J. Méc.*, 14(1):39–63, 1975.

[53] Z. HASHIN and S. SHTRIKMAN. A variational approach to the theory of the elastic behaviour of multiphase materials. *J. Mech. Phys. Solids*, 11:127–140, 1963.

[54] J. HASLINGER and P. NEITTAANMAKI. *Finite Element Approximation for Optimal Shape, Material and Topology Design.* J. Wiley & Sons, Chichester, 1996.

[55] P. HAUPT. On the mathematical modelling of material behavior in continuum mechanics. *Acta Mechanica*, 100:129–154, 1993.

[56] R. HILL. *The Mathematical Theory of Plasticity.* Clarendon Press, Oxford, 1950.

[57] R. HILL. Uniqueness criteria and extremum principles is self-adjoint problems of continuum mechanics. *J. Mech. Phys. Solids*, 10:185–194, 1962.

[58] I. HLAVÁČEK, J. ROSENBERG, A. BEAGLES, and J. WHITEMAN. Variational inequality formulation in strain space and finite element solution of an elasto-plastic problem with hardening. *Comput. Meth. Appl. Mech. Engrg.*, 94:93–112, 1992.

[59] Y. HUO and I. MÜLLER. Nonequlibrium thermodynamics of pseudoelasticity. *Continuum Mech. and Thermodyn.*, 5:163–204, 1993.

[60] K. HUTTER. The fundations of thermodynamics, its basic postulates and implications. A review of modern thermodynamics. *Acta Mechanica*, 27:1–54, 1977.

[61] S. ICHINOSE, Y. FUNATSU, and K. OTSUKA. Type II deformation twinning in $\gamma_1'$ martensite in a Cu-Al-Ni alloy. *Acta metall.*, 33(9):1613–1620, 1985.

[62] A. A. ILYUSHIN. On the postulate of plasticity (in russian). *Prikl. Mat. Mech.*, 25:503–507, 1961.

[63] R. JAMES. Co-existent phases in one-dimensional static theory of elastic bars. *Arch. Rational Mech. Anal.*, 72:99–140, 1979.

[64] R. JAMES. Displacive phase transformations in solids. *J. Mech. Phys. Solids*, 34(4):359–394, 1986.

[65] L. JIANG. On an elastic-plastic problem. *Jour. Diff. Eqns.*, 51:97–115, 1984.

[66] C. JOHNSON. Existence theorems for plasticity problems. *J. Math. Pures Appl.*, 55:431–444, 1976.

[67] L. KACHANOV. *Fundamentals of the Theory of Plasticity.* Mir Publishers, Moscow, 1974.

[68] J. KESTIN and J. RICE. Paradoxes in the application of thermodynamics to strained solids. In E.B. Stuart *et al.*, editor, *A Critical Review of Thermodynamics*, pages 275–298. Mono Book Corp., Baltimore, 1970.

[69] A. G. KHACHATURYAN. *Theory of structural transformations in solids.* John Wiley & Sons, New York, 1983.

[70] N. KIKUCHI and J. T. ODEN. *Contact Problems in Elasticity: A Study of Variational Inequalities and Finite Elements Methods.* SIAM, Philadelphia, PA, 1988.

[71] S. KIM and J. ODEN. Generalized potentials in finite elastoplasticity (Part I). *Internat. J. Engrg. Sci.*, 22:1235–1257, 1984.

[72] D. KINDERLEHRER and G. STAMPACCHIA. *An Introduction to Variational Inequalities and Their Applications.* Academic Press, New York *et al.*, 1980.

[73] M. KLEIBER. *Finite Element Method in Nonlinear Continuum Mechanics* (in Polish). PWN Publishers, Warszawa–Poznan, 1985.

[74] R. KOHN. The relationship between linear and nonlinear variational models of coherent phase transitions. In *Proceedings ofSeventh Army Conference on Applied Mathematics and Computing*, page 26 p., West Point, June 1989.

[75] R. KOHN. The relaxation of a double-well energy. *Continuum Mech. Thermodyn.*, 3:193–236, 1991.

[76] W. KOITER. Stress-strain relations, uniqueness and variational theorems for elasto-plastic materials with a singular yield surface. *Quart. Appl. Math.*, 11:350–354, 1953.

[77] M. KOČVARA and J. ZOWE. An iterative two-step algorithm for linear complementarity problems. *Numer. Math.*, 68:95–106, 1994.

[78] M. A. KRASNOSIELSKI and A. V. POKROWSKI. *Systems with Hysteresis.* Springer-Verlag, Berlin, 1989.

[79] M. KUCZMA. *The Problem of Unilateral Contact of Beams and Plates on Viscoelastic Foundations* (Polish), volume 255 of *Transactions of PUT.* PUT Press, Poznań, 1991. (based on PhD Thesis).

[80] M. KUCZMA. A multi-well problem for phase transformations. In *Proc. of Tenth Conference on Mathematics of Finite Elements and Applications.* Elsevier, 1999. (in press).

[81] M. KUCZMA. A viscoelastic-plastic model for skeletal structural systems with clearances. *Comp. Assist. Mech. Engng. Sci.*, 6(1):83–106, 1999.

[82] M. KUCZMA and L. DEMKOWICZ. An adaptive algorithm for the unilateral contact problem of viscoelastic beams and plates on viscoelastic foundations. *Comput. Meth. Appl. Mech. Engrg.*, 101:183–196, 1992.

[83] M. KUCZMA, V. LEVITAS, A. MIELKE, and E. STEIN. Nonisothermal hysteresis loops in pseudoelasticity. In *Proc. XIII Conference on Computer Methods in Mechanics*, pages 711–718, Poznan, 1997.

[84] M. KUCZMA and A. MIELKE. Variational approach to pseudoelastic behaviour. *ZAMM*, 77, Suppl. 1,:S175–S176, 1997.

[85] M. KUCZMA and A. MIELKE. Influence of hardening and inhomogeneity on internal loops in pseudoelasticity. *ZAMM*, 1998. (accepted).

[86] M. KUCZMA, A. MIELKE, and E. STEIN. Modelling of hysteresis in two phase systems. *Arch. Mech.*, 1999. (in press).

[87] M. KUCZMA and J. RAKOWSKI. The interaction problem of a plate on a unilateral foundation. In *Proc. Third Internat. Workshop on the Design and Evaluation of Concrete Pavements*, pages 93–102, Krumbach, Austria, September 1994. CROW and PIARC.

[88] M. KUCZMA, J. RAKOWSKI, and P. LITEWKA. Elastoplastic analysis of plates on unilateral foundations. *ZAMM*, 76:(S2)583–584, 1996.

[89] M. KUCZMA and E. STEIN. On nonconvex problems in the theory of plasticity. *Arch. Mech.*, 46(4):505–529, 1994.

[90] M. KUCZMA and J. WHITEMAN. Variational inequality formulation for flow theory plasticity. *Int. J. Engng Sci.*, 33:1153–1169, 1995.

[91] J. LEBLOND. Mathematical modelling of transformation plasticity in steels – II: coupling with strain hardening phenomena. *Int. J. Plast.*, 5:573–591, 1989.

[92] J. LEBLOND, J. DEVAUX, and J. DEVAUX. Mathematical modelling of transformation plasticity in steels – I: case of ideal-plastic phases. *Int. J. Plast.*, 5:551–572, 1989.

[93] J. LEMAITRE and J.-L. CHABOCHE. *Mechanics of Solid Materials.* Cambridge University Press, Cambridge, 1990.

[94] P. LEO, T. SHIELD, and O. BRUNO. Transient heat transfer effects on the pseudoelastic behavior of shape-memory wires. *Acta metall. mater.*, 41:2477–2485, 1993.

[95] A. LEVITAS, V. I. IDESMAN and E. STEIN. Finite element simulation of martensitic phase transformations in elastoplastic materials. *Int. J. Solids Structures*, 35:855–887, 1998.

[96] V. LEVITAS. *Thermomechanics of Phase Transitions and Inelastic Deformations of Microinhomogeneous Materials* (Russian). Naukova Dumka, Kiev, 1992.

[97] V. I. LEVITAS. The postulate of realizability: Formulation and applications to post-bifurcation bahavior and phase transitions in elastoplastic materials. Part I and II. *Int. J. Engng. Sci.*, 33:921–971, 1995.

[98] V. I. LEVITAS and E. STEIN. Simple micromechanical model of thermoelastic martensitic transformations. *Mech. Res. Commun.*, 24:309–318, 1997.

[99] V. I. LEVITAS, E. STEIN, and M. LENGNICK. On a unified approach to the description of phase transition and strain localization. *Arch. Appl. Mech.*, 66:242–254, 1996.

[100] C. LEXCELLENT, C. LICHT, and B. GUO. Stress rate effect on the pseudoelastic behaviour CuZnAl single crystals. *J. de Physique IV, Coll. 8, suppl. J. de Physique III*, 5:(C8–883)–(C8–888), 1995.

[101] J. LIONS and G. STAMPACCHIA. Variational inequalities. *Comm. Pure Appl. Math.*, XX:493–519, 1967.

[102] T. ŁODYGOWSKI and P. PERZYNA. Numerical modelling of localized fracture of inelastic solids in dynamic loading processes. *Int. J. Numer. Methods Engng*, 40:4137–4158, 1997.

[103] J. LUBLINER. *Plasticity Theory.* Macmillan Publishing Company, New York, 1990.

[104] G. MAIER. A matrix structural theory of piecewise linear elastoplasticity with interacting yield surfaces. *Meccanica*, 5(7):54–65, 1970.

[105] G. MAIER. Piecewise linearization of yield criteria in structural plasticity. *SM Archives*, 1:239–281, 1976.

[106] J. MANDEL. Generalisation de la theorie de plasticite de W.T. Koiter. *Int. J. Solids Struct.*, 1:273–295, 1965.

[107] F. MARKETZ and F. FISCHER. Micromechanical modelling of stress-assisted martensitic transformation. *Modelling Simul. Mater. Sci. Eng.*, 2:1017–1046, 1994.

[108] J. E. MARSDEN and T. J. R. HUGHES. *Mathematical Foundation of Elasticity.* Prentice-Hall, Inc., Englewood Cliffs, 1983.

[109] H. MATTHIES. Existence theorems in thermo-plasticity. *J. Méc.*, 18:695–712, 1979.

[110] G. MAUGIN. *The Thermomechanics of Plasticity and Fructure.* Cambridge University Press, Cambridge, 1992.

[111] R. MICHAŁOWSKI and Z. MRÓZ. Associated and non-associated sliding rules in contact friction problems. *Arch. Mech.*, 30:259–276, 1978.

[112] C. MIEHE. *Kanonische Modelle multiplikativer Elasto-Plastizität. Thermodynamische Formulierung und numerische Implementation.*, volume F 93/1. IBNM Universität Hannover, Germany, November 1993.

[113] A. MIELKE. Flow properties for Young-measure solutions of semilinear hyperbolic problems. IfAM-Preprint A4, Institute for Applied Mathematics, University of Hannover, September 1997.

[114] A. MIELKE, F. THEIL, and V. LEVITAS. Mathematical formulation of quasistatic phase transformations with friction using an extremum principle. IfAM-Preprint A8, Institute for Applied Mathematics, University of Hannover, September 1998.

[115] G. MILTON. On characterizing the set of possible effective tensors of composites: the variational method and the translation method. *Comm. Pure Appl. Math.*, XLIII:63–125, 1990.

[116] J. MOREAU. On unilateral constrains, friction and plasticity. In G. Capriz and G. Stampacchia, editors, *New Variational Techniques in Mathematical Physics*, pages 171–322, Roma, 1974. Edizioni Cremonese.

[117] J. MOREAU. Evolution problem associated with a moving convex set in a Hilbert space. *J. Diff. Equat.*, 26:347–374, 1977.

[118] Z. MRÓZ. On forms of constitutive laws for elastic-plastic solids. *Arch. Mech.*, 18:1–34, 1966.

[119] Z. MRÓZ and B. RANIECKI. Variational principles in uncoupled thermoplasticity. *Int. J. Engng Sci.*, 11:1133–1141, 1973.

[120] H.-B. MÜHLHAUS and E. AIFANTIS. A variational principle for gradient plasticity. *Int. J. Solids Structures*, 28:845–857, 1991.

[121] I. MÜLLER. On the entropy inequality. *Arch. Rational Mech. Anal.*, 26:118–141, 1967.

[122] I. MÜLLER and H. XU. On the pseudoelastic hysteresis. *Acta metall. mater.*, 39:263–271, 1991.

[123] W. MUSCHIK. Thermodynamical theories survay and comparison. *J. Appl. Sci.*, 4:190–200, 1986.

[124] P. M. NAGHDI and S. MURCH. On the mechanical behavior of viscoelastic/plastic solids. *J. Appl. Mech.*, 30:321–328, 1963.

[125] P. M. NAGHDI and J. A. TRAPP. The significance of formulating plasticity theory with reference to loading surface in strain space. *Int. J. Engng Sci.*, 13:785–797, 1975.

[126] Z. NANIEWICZ and P. PANAGIOTOPOULOS. *Mathematical Theory of Hemivariational Inequalities Problems and Applications.* Marcel Dekker, Inc., New York, 1995.

[127] S. NEMAT-NASSER and M. HORI. *Micromechanics: Overall properties of heterogeneous materials.* North-Holland, Amasterdam, 1993.

[128] J. NEČAS and I. HLAVÁČEK. *Mathematical Theory of Elasto Plastic Bodies: An Introduction.* Elsevier, Amsterdam, 1981.

[129] Q. NGUYEN. On the elastic plastic initial-boundary value problem and its numerical integration. *Internat. J. Num. Meth. Engrg.*, 11:817–832, 1977.

[130] M. NIEZGÓDKA and J. SPREKELS. Convergent numerical approximations of the thermomechanical phase transitions in shape memory alloys. *Numer. Math.*, 58:759–778, 1991.

[131] Z. NISHIYAMA. *Martensitic Transformation.* Academic Press, New York, 1978.

[132] J. ODEN. *Qualitative Methods in Nonlinear Mechanics.* Prentice-Hall, Englewood Cliffs, NJ, 1986.

[133] G. OLSON and M. COHEN. Kinetics of strain-induced martensitic nucleation. *Mettal. Transactions A*, 6A:791–795, April 1975.

[134] G. OLSON and W. OWEN, editors. *Martensite. A tribute to Morris Cohen.* ASM International, 1992.

[135] W. OLSZAK, P. PERZYNA, and A. SAWCZUK, editors. *Theory of Plasticity* (Polish). PWN–Polish Scientific Publishers, Warszawa, 1965.

[136] J. ORKISZ. Concept of analysis of residual stresses based on enhanced data obtained from destructive measurement techniques. In *Proc. XIth Conf. Computer Methods in Mechanics*, pages 667–674, Kielce-Cedzyna, 1993.

[137] J. ORTIN and A. PLANES. Thermodynamics and hysteresis behaviour of thermoelastic martensitic transformations. *J. de Physique IV, Coll. C4, suppl. J. de Physique III*, 1:(C4–13)—(C4–23), 1991.

[138] M. ORTIZ and E. POPOV. Accuracy and stability of integration algorithms for elastoplstic constitutive relations. *Internat. J. Numer. Meth. Engrg.*, 21:1561–1576, 1985.

[139] J. PATEL and M. COHEN. Criterion for the action of applied stress in the martensitic transformation. *Acta Metall.*, 1:531–538, 1953.

[140] E. PATOR, A. EBERHARD, and M. BERVEILLER. Thermomechanical behaviour of shape memory alloys. *Arch. Mech.*, 40:775–794, 1988.

[141] J. PERKINS, editor. *Shape Memory Effects in Alloys.* Plenum Press, New York and London, 1975.

[142] P. PERZYNA. The constitutive equations for rate sensitive plastic materials. *Quartl. Appl. Math.*, 20:321–332, 1963.

[143] H. PETRYK. On the second-order work in plasticity. *Arch. Mech.*, 43(2-3):377–397, 1991.

[144] A. PIPKIN. Elastic materials with two prefferred states. *Quart. J. Mech Appl. Math.*, 44:1–15, 1991.

[145] A. PONTER and F. LECKIE. The application of energy theorems to bodies with creep in the plastic range. *J. Appl. Mech.*, 37:753–758, 1970.

[146] W. PRAGER. On ideal locking materials. *Trans. Soc. Rheol.*, 1:169–175, 1957.

[147] B. RANIECKI. Uniqueness criteria in solids with non-associated plastic flow laws at finte deformations. *Bull. Acad. Pol. Sc., Ser. sc. tech.*, 28:391–399, 1979.

[148] B. RANIECKI. *Thermomechanics of Pseudoelasticity of Shape Memory Materials* (Polish), volume 1 of *Current Trends in the Mechanics of Materials* (ed. W.K. Nowacki), chapter 2, pages 55–140. IPPT PAN, Warsaw, 1996.

[149] B. RANIECKI and O. BRUHNS. Bounds to bifurcation stresses in solids wiyh non-associated plastic flow law at finite strain. *J. Mech. Phys. Solids*, 29(2):153–172, 1981.

[150] B. RANIECKI and C. LEXCELLENT. Thermodynamics of isotropic pseudoelasticity in shape memory alloys. *Eur. J. Mech., A/Solids*, 17(2):185–205, 1998.

[151] B. RANIECKI, C. LEXCELLENT, and K. TANAKA. Thermodynamic models of pseudoelastic behaviour of shape memory alloys. *Arch. Mech.*, 44(3):261–284, 1992.

[152] B. RANIECKI and K. TANAKA. On the thermodynamic driving force for coherent phase transformations. *Int. J. Engng Sci.*, 32(12):1845–1858, 1994.

[153] B. REDDY. Existence of solutions to quasistatic problems in plasticity. In C. Bandle *et al.*, editor, *Progress in Partial Differential Equations: Calculus of Variations, Applications*, pages 299–311. IUTAM, Longman, 1992. Pitman Research Notes in Mathematics 267.

[154] B. REDDY and T. GRIFFIN. Variational principles and convergence of finite element approximations of a holonomic elastic-plastic problem. *Numer. Math.*, 52:101–117, 1988.

[155] J. RICE. On the structure of stress-strain relations for time-dependent plastic deformation metals. *J. Appl. Mech.*, pages 728–737, 1970.

[156] J. RICE. Inelastic constitutive relations for solids: An internal-variable theory and its application to metal plasticity. *J. Mech. Phys. Solids*, 19:433–455, 1971.

[157] R. ROCKAFELLAR. *Convex Analysis.* Princeton University Press, Princeton, New Jersey, 1970.

[158] R. ROGERS. Some remarks on nonlocal interactions and hysteresis in phase transitions. *Continuum Mech. Thermodyn.*, 8:65–73, 1996.

[159] T. SCHROEDER and C. WAYMAN. Pseudoelastic effects in Cu-Zn single crystals. *Acta Metallurgica*, 27:405–417, 1979.

[160] J. SHAW and S. KIRIAKIDES. On the nucleation and propagation of phase transformation fronts in a NiTi alloy. *Acta mater.*, 45(2):683–700, 1997.

[161] S. SHAW, M. WARBY, J. WHITMAN, C. DAWSON, and M. WHEELER. Numerical techniques for the treatment of quasistatic viscoelastic stress problems in linear isotropic solids. *Computer Meth. Appl. Mech. Engrg.*, 118(3-4):211–237, 1993.

[162] J. SIMO and T. HUGHES. *Computational Inelasticity.* Springer, New York, 1998.

[163] J. SIMO and R. TAYLOR. Consistent tangent operators for rate-independent elastoplasticity. *Comput. Methods Appl. Mech. Engng.*, 48:101–118, 1985.

[164] J. SKRZYPEK. *Plasticity and Creep. Theory, Examples and Problems.* CRC Press, Boca Raton, 1993.

[165] J. SOKOLOWSKI and J.-P. ZOLESIO. *Introduction to Shape Optimization. Shape Sensitivity Analysis.* Springer-Verlag, Berlin, 1992.

[166] J. SPIELFELD and E. HORNBOGEN. The influence of dislocation arrangements in austenite on the course of diffusionless transformation in Cu-based shape memory alloys. *J. de Physique IV, Coll. C8, suppl. J. de Physique III*, 5, 1995.

[167] E. STEIN and F.-J. BARTHOLD. *Elastizitätstheorie.* IBNM, Universität Hannover, Hannover, 1991.

[168] E. STEIN, V. LEVITAS, and M. KUCZMA. A nonconvex problem for solids with phase transformations. *ZAMM*, 76:(S5) 583–584, 1996.

[169] E. STEIN, G. ZHANG, and R. MAHNKEN. Shake-down analysis for perfect plasticity and kinematic hardening materials. In E. Stein, editor, *Progress in Computational Analysis of Inelastic Structures*, pages 175–244, Wien, New York, 1993. Springer-Verlag.

[170] P. STEINMANN and K. WILLAM. Finite elements for capturing localized failure. *Archive of Appl. Mech.*, 61:259–275, 1991.

[171] D. STÖCKEL, E. HORNBOGEN, F. RITTER, and P. TAUTZENBERGER. *Legierungen mit Formged achtnis.* expert verlag, Ehningen bei Böblingen, 1988.

[172] H. STRANG, H. MATTHIES, and R. TEMAM. Mathematical and computational methods in plasticity. In S. Nemat-Nasser, editor, *Variational Methods in the Mechanics of Solids*, pages 20–28, Oxford, 1980. Pergamon.

[173] Q. SUN and K. HWAN. Micromechanical modelling for the constitutive behavior of polycrystalline shape memory alloys. Parts I & II. *J. Mech. Phys. Solids*, 41:1–17, 19–33, 1993.

[174] P.-M. SUQUET. Existence and regularity of solutions in plasticity problems. In S. Nemat-Nasser, editor, *Variational Methods in the Mechanics of Solids*, pages 304–309, Oxford, 1980. Pergamon.

[175] P.-M. SUQUET. Discontinuities and plasticity. In J. Moreau and P. Panagiotopoulos, editors, *Nonsmooth Mechanics and Applications*, pages 279–340, Wien, New York, 1988. Springer-Verlag.

[176] R. ŚWITKA and B. HUSIAR. Discrete analysis of reological models (Polish). *Mech. Teoret. Stosow.*, 22:209–233, 1984.

[177] G. SZEFER. Variational principles in the computer methods of mechanics (Polish). In *Proc. V Conference on the Computer Methods in the Mechanics of Structures*, pages 65–83, Wrocław, 1981.

[178] G. SZEFER. Analysis of sensitivity and the optimization of dynamic systems with distributed parameters. *Mechanika*, 1(4):5–36, 1982(3).

[179] G. SZEFER, D. JASIŃSKA, and W. SALOMON. Concept of a singular surface in contact mechanics. *Arch. Mech.*, 46:581–603, 1994.

[180] K. TANAKA, F. NISHIMURA, and H. TOBUSHI. Thenomenological analysis on subloops in shape memory alloys due to incomplete transformations. *J. Intell. Mater. Syst. Struct.*, 5:487–493, 1994.

[181] J. TELEGA. Variational principles for rate boundary-value problems in non-associated plasticity. *Advances in Mechanics*, 10(2):3–95, 1987.

[182] J. TELEGA. *Variational Methods and Convex Analysis in Contact Problems and Homogenization* (Polish). IPPT PAN, Warsaw, 1990.

[183] R. TEMAM. *Mathematical Problems in Plasticity.* Trans-Inter-Scientia, Tonbridge, 1985.

[184] C. TRUESDELL. *Rational thermodynamics.* Springer, Berlin, 1984.

[185] C. Van de PANNE. *Methods for Linear and Quadratic Programming.* North-Holland, Amsterdam, 1975.

[186] A. VISINTIN. Mathematical models of hysteresis. In J.J. Moreau *et al.*, editor, *Topics in Nonsmooth Mechanics*, pages 295–326. Birkhäser, Basel, 1988.

[187] P. ŠITTNER, V. NOVÁK, and N. ZÁRUBOVÁ. Martensitic trnaformations in [001] CuAlZnMn single crystals. *Acta mater.*, 46:1265–1281, 1998.

[188] V. ŠVERÁK. Rank-one convexity does not imply quasiconvexity. *Proc. R. Soc. Edinburgh*, 120:185–189, 1992.

[189] Z. WASZCZYSZYN. Computational methods and plasticity. Technical Report LR-583, TU Delft, 1989.

[190] K. WILMANSKI. Model of stress-strain hysteresis loops in shape memory alloys. *Int. J. Engng Sci.*, 31(8):1121–1138, 1993.

[191] P. WOLLANTS, J. ROOS, and L. DELAEY. Thermally- and stress-induced thermoelastic martensitic transformations in the reference frame of equilibrium thermodynamics. *Progress in Materials Science*, 37:227–288, 1993.

[192] C. WOŹNIAK. *Constraints in the Mechanics of Deformable Bodies* (Polish). Ossolineum, Wrocław, 1988.

[193] P. WRIGGERS, C. MIEHE, M. KLEIBER, and J. SIMO. On the coupled thermomechanical treatment of necking problems via finite element methods. *Int. J. Numer. Meth. Engng.*, 33:869–883, 1992.

[194] L. YOUNG. *Calculus of Variations and Optimal Control Theory.* W.B. Saunders Comp., Philadelphia, 1969.

[195] E. ZEIDLER. *Nonlinear Functional Analysis and its Applications. Monotone Operators*, volume 2. Springer-Verlag, New York, 1990.

[196] O. ZIENKIEWICZ and R. TAYLOR. *The Finite Element Method*, volume 1 & 2. Mc-Graw-Hill, London, 1989.

[197] A. ZIÓŁKOWSKI. *Pseudoelasticity Problems of Materials with Shape-Memory* (Polish). PhD thesis, IPPT PAN, Warsaw, 1995.

[198] M. ŻYCZKOWSKI. *Combined Loadings in the Theory of Plasticity.* PWN–Polish Scientific Publishers, Warszawa, 1981.

**Mieczyslaw Sylwester Kuczma**

# ZASTOSOWANIE NIERÓWNOŚCI WARIACYJNYCH W MECHANICE PLASTYCZNEGO PŁYNIĘCIA I MARTENZYTYCZNYCH PRZEMIAN FAZOWYCH


## Streszczenie

Praca dotyczy matematycznego modelowania i numerycznego rozwiązywania zagadnień nierównościowym dla dwóch klas zachowania się materiałów: plastycznego płynięcia i wywołanych naprężeniem termosprężystych martenzytycznych przemian fazowych. Odpowiadające zagadnienia początkowo-brzegowe dla tych deformacyjnych procesów z histerezą sformułowano w jednolitej postaci ewolucyjnej nierówności wariacyjnej, która obejmuje warunki równowagi statycznej i kryteria obciążenia/odciążenia i poluzowania, lub kryteria zachodzenia przemian fazowych. Przy przyjęciu odpowiednich hipotez, udowodniono istnienie i jednoznaczność rozwiązań dla tych globalnych sformułowań. Zaproponowano dwa algorytmy numeryczne i opracowano kilka programów komputerowych. Algorytmy te okazały się efektywne w rozwiązywaniu złożonych, konkretnych zadań brzegowych. Otrzymane rezultaty symulacji numerycznej dla zaproponowanych modeli materiału ukazują interesujące własności lepkosprężysto-plastycznych układów konstrukcyjnych, a dla procesów przemian fazowych są niezwykłe, jednak zgodne z wynikami obserwacji laboratoryjnych.


**Słowa kluczowe:** nierówności wariacyjne, liniowe zadania komplementarne (LZK), metoda elementów skończonych, algorytmy numeryczne bezpośredni i iteracyjny (SSORP plus PCG) do LZK, lepkosprężystoplastyczność, poluzowanie, martenzytyczne przemiany fazowe, stopy z pamięcią kształtu.